

Photo-induced Chern Insulating States in Semi-Dirac Systems



By
Shakeel Ahmad

Supervised by
Dr. Kashif Sabeeh

Department of Physics
QUAID-I-AZAM UNIVERSITY, ISLAMABAD,
PAKISTAN

Photo-induced Chern Insulating States in Semi-Dirac Systems

By

Shakeel Ahmad

A thesis submitted in partial fulfilment for
the
degree of Master of Philosophy

in the

Department of Physics
QUAID-I-AZAM UNIVERSITY, ISLAMABAD,
PAKISTAN

February 2020

Certificate

This thesis is submitted **Shakeel Ahmad s/o Abdussattar**,
Reg. No. 02181711001, is accepted in its present form
by Department of Physics, Quaid-I-Azam University, Islamabad,
Pakistan. It satisfies the thesis requirements for the degree
of Master of Philosophy in Physics.



Supervisor

Dr. Kashif Sabeeh

Professor

Department of Physics

Chairman

Dr. Nawazish Ali Khan

Professor

Department of Physics

*This thesis is dedicated to my
parents, teachers, and siblings for
their endless love, support, and encouragement.*

Abstract

Two-dimensional semi-Dirac materials have quadratic dispersion relation along one direction and linear dispersion relation, similar to low energy graphene dispersion, along the other orthogonal direction. We study the topological phase transition in such two dimensional systems. The semi-Dirac Hamiltonian has two gapless Dirac nodes in the presence of time-reversal symmetry and mirror symmetry. We show that by impinging light on the surface of a semi-Dirac material, gap opens because of time-reversal symmetry breaking and turning the system into a Chern insulator. Firstly, we show that the intensity of circularly polarized light can be used as a knob to induce topological states with non-zero Chern number in gapless semi-Dirac system. Secondly, for a gapped semi-Dirac system, by fixing the intensity and a frequency of the incident light, we induce topological transition as a function of polarization of the incident light.

Contents

1	Introduction	3
1.1	Gauge Transformations	4
1.1.1	Gauge Freedom in Classical Electromagnetism	5
1.1.2	Electromagnetic Gauge Freedom in Quantum Mechanics	6
1.2	Berry Phase	8
1.2.1	Properties of Berry Phase	11
1.2.2	Two-Level Hamiltonian:	12
1.3	Topological Band Theory	15
1.4	Berry Curvature of Two-Level System in 2D k-Space	19
1.5	Time-Reversal Symmetry (TRS)	20
1.5.1	TRS in Classical Mechanics	20
1.5.2	TRS in Quantum Mechanics	21
1.5.3	TRS of Schrödinger Equation	22
1.5.4	Kramers Degeneracy	24
1.5.5	Symmetry Restrictions on Berry Phase	25
2	Su-Schrieffer-Heeger(SSH) Model	27
2.1	Polarization In 1D	27
2.2	The SSH Model	29
2.2.1	Domain Wall States and the J-Rebbi Model	36
3	Haldane Model	38
3.1	Model Hamiltonian	39
3.1.1	Berry Curvature and Chern number Calculation	43
4	Floquet Theory and Semi-Dirac Hamiltonian	45
4.1	Floquet Theorem	45
4.1.1	Floquet Hamiltonian in differential Form	48
4.1.2	The Non-Stroboscopic Floquet Hamiltonian and the Kick Operator	49
4.1.3	Relation between the Kick Operator and the P-Operator	49
4.1.4	Inverse Frequency Expansion for the Floquet Hamiltonian	51
4.2	Semi-Dirac Hamiltonian	52

4.3	Floquet Theory	59
4.3.1	Chern number calculation for gape-less Semi-Dirac system	62
4.3.2	Chern Insulating States in Gapped Semi-Dirac System	63
4.3.3	Chern number calculation for gapped Semi-Dirac system	66
A	Gauge Transformation in Quantum Mechanics	68
B	Floquet Theory	70
C	Gapped semi-Dirac Hamiltonian	76

Chapter 1

Introduction

In condensed matter physics, we are interested in understanding how order emerges when a large number of simple constituents, such as ions, magnetic moments or electrons interact with each other. For example, in crystalline solids and magnets, the order is described through the symmetry breaking: in crystal, ions are arranged periodically, thereby breaking continuous translational symmetry; in typical magnets, the rotational symmetry of spins is broken.

In the 1980s, an important discovery was made by physicists that electrons confined in two dimensions and subjected to a strong magnetic field manifest the quantum version of the classical Hall effect, and these are known as the integer quantum Hall systems. In the integer quantum Hall effect, lattice background and electron-electron interactions do not play any significant role; however, there exist systems where electron-electron interactions play an important role called fractional quantum Hall systems. These systems exhibit a novel type of order called topological order. The consequences of this topological order are dissipation-less transport, emergent particles having fractional charge and statistics, and quantized Hall conductivity.

The Landau-Ginzburg theory explained successfully the phase transitions on the basis of symmetry breaking, like transition from liquid to solid due to breaking of continuous translational symmetry. However, in the recent past, new phase has been discovered which cannot be distinguished on the basis of symmetry-breaking theory. So, the symmetry-breaking concept is not enough to characterize different phases, and we need to define a topological invariant to distinguish them. For example, in a topological insulator which has a conducting boundary, the metallic boundaries stem from invariants of topology, which remain unchanged until a material remains insulating. In a topological insulator, we associate a topological invariant with the electron's wave function that can not change as long as the material remains insulating [1].

The main objective of my thesis is to study how Chern insulating states

arise in semi-Dirac materials. The Integer quantum Hall effect is the first example of a Chern insulator. It was first experimentally observed by K. von Klitzing, G. Dorda, and M. Pepper that the Hall conductivity

$$\sigma_{xy} = \frac{e^2}{2\pi\hbar}n,$$

took precise integer values. Although we are familiar with quantization of different observables for microscopic systems, but this was something novel and also astonishing; it is the quantization of an emergent macroscopic property in a dirty sample having large number of particles and its explanation required a new perspective. It turn out that this something new is that topology can play a an important role quantum many body systems [2]. In fact, the Hall conductivity σ_{xy} is quantized because of topological invariance of the Chern number. The Chern number is defined in terms of the Berry curvature calculated for Bloch states, and it defines invariant of topology in 2D.

In this chapter, I discuss the topics that build foundation for Chern insulators. First of all, I explore the concepts related to gauge transformations. In the Schrödinger equation, we can remove electromagnetic gauge fields by introducing a particular phase factor with the state function. However, if we change a parameter in a Hamiltonian adiabatically, another phase factor arises called Berry phase or geometric phase. This phase is arbitrary on an open path in the parametric space, but well-defined in a closed path and can not be removed by any gauge transformation. As an example, I calculate the Berry phase of two level system, which underpins the basic understanding of the Berry phase.

Secondly, I introduce the topological band theory. In the topological band theory, we consider non-zero Berry phase, as a result the Berry phase of electrons in two dimensional Bloch states is equal to 2π times an integer called the Chern number of a band.

Lastly, I discuss Time-Reversal Symmetry (TRS), and how the time-reversal symmetry restricts the Berry phase. For a two dimensional lattice, the Berry phase is an odd function in crystal momentum space if a system has TRS. As a result, the Chern number is always zero for this case. So, to get a non-zero Chern number, we need to break TRS of a Hamiltonian.

1.1 Gauge Transformations

In classical electrodynamics, the potentials (V, \mathbf{A}) are not directly measurable, and the physical quantities are the electric and magnetic fields. These fields satisfy Maxwell's equations. We can define new potentials in such a way that the fields do not change: it is called the "Gauge Freedom".

In quantum mechanics, the potentials play a more significant role; because they enter the Hamiltonians of charged particles. Although the theory is still

gauge invariant, the potentials affect the dynamics of charged particles in a region where fields are zero, but potentials are non-zero.

1.1.1 Gauge Freedom in Classical Electromagnetism

The electric charge density $\rho(\mathbf{x}, t)$ and electric current density $\mathbf{J}(\mathbf{x}, t)$ are sources of electromagnetic fields $\mathbf{E}(\mathbf{x}, t)$ and $\mathbf{B}(\mathbf{x}, t)$, and these fields satisfy following Maxwell's equations [3],

$$\nabla \cdot \mathbf{E}(\mathbf{x}, t) = \frac{\rho(\mathbf{x}, t)}{\epsilon_0}, \quad \nabla \cdot \mathbf{B}(\mathbf{x}, t) = 0, \quad (1.1)$$

$$\nabla \times \mathbf{E}(\mathbf{x}, t) = -\frac{\partial \mathbf{B}(\mathbf{x}, t)}{\partial t}, \quad \nabla \times \mathbf{B}(\mathbf{x}, t) = \mu_0 \mathbf{J}(\mathbf{x}, t) + \mu_0 \epsilon_0 \frac{\partial \mathbf{E}(\mathbf{x}, t)}{\partial t}. \quad (1.2)$$

The magnetic field $\mathbf{B}(\mathbf{x}, t)$ is divergenceless because there is no magnetic monopole. Therefore, we can write the magnetic field in terms of curl of the electromagnetic vector potential $\mathbf{A}_{em}(\mathbf{x}, t)$,

$$\mathbf{B}(\mathbf{x}, t) = \nabla \times \mathbf{A}_{em}(\mathbf{x}, t), \quad (1.3)$$

putting equation (1.3) in the first equation of equation (1.2),

$$\begin{aligned} \nabla \times \mathbf{E}(\mathbf{x}, t) &= -\frac{\partial}{\partial t}(\nabla \times \mathbf{A}_{em}(\mathbf{x}, t)), \\ \nabla \times \left(\mathbf{E}(\mathbf{x}, t) + \frac{\partial \mathbf{A}_{em}(\mathbf{x}, t)}{\partial t} \right) &= 0, \end{aligned}$$

the quantity in the parenthesis of the above equation can be expressed as the gradient of a scalar function; because gradient of a function is always curl-less.

$$\begin{aligned} \mathbf{E}(\mathbf{x}, t) + \frac{\partial \mathbf{A}_{em}(\mathbf{x}, t)}{\partial t} &\equiv -\nabla V(\mathbf{x}, t), \\ \Rightarrow \boxed{\mathbf{E}(\mathbf{x}, t) = -\nabla V(\mathbf{x}, t) - \frac{\partial \mathbf{A}_{em}(\mathbf{x}, t)}{\partial t}}, & \quad (1.4) \end{aligned}$$

where $V(\mathbf{x}, t)$ is a scalar potential. We have a freedom to define new potentials $(V'(\mathbf{x}, t), \mathbf{A}'_{em}(\mathbf{x}, t))$ in terms of $(V(\mathbf{x}, t), \mathbf{A}_{em}(\mathbf{x}, t))$ in such a way such that $\mathbf{E}(\mathbf{x}, t)$ and $\mathbf{B}(\mathbf{x}, t)$ remain invariant. This freedom is called ‘‘Gauge Freedom,’’

$$\mathbf{A}'_{em}(\mathbf{x}, t) = \mathbf{A}_{em}(\mathbf{x}, t) + \nabla \eta(\mathbf{x}, t), \quad V'(\mathbf{x}, t) = V(\mathbf{x}, t) - \frac{\partial \eta(\mathbf{x}, t)}{\partial t},$$

where $\eta(\mathbf{x}, t)$ is an arbitrary scalar function. Putting in equation (1.3) and (1.4)

$$\begin{aligned} \mathbf{B}'(\mathbf{x}, t) &= \nabla \times \mathbf{A}'_{em}(\mathbf{x}, t), \\ &= \nabla \times (\mathbf{A}_{em}(\mathbf{x}, t) + \nabla \eta(\mathbf{x}, t)), \\ &= \nabla \times \mathbf{A}_{em}(\mathbf{x}, t), \end{aligned}$$

which shows

$$\boxed{\mathbf{B}'(\mathbf{x}, t) = \mathbf{B}(\mathbf{x}, t),}$$

and

$$\begin{aligned} E'(\mathbf{x}, t) &= -\nabla V'(\mathbf{x}, t) - \frac{\partial \mathbf{A}'_{em}(\mathbf{x}, t)}{\partial t}, \\ &= -\nabla \left(V(\mathbf{x}, t) - \frac{\partial \eta(\mathbf{x}, t)}{\partial t} \right) - \frac{\partial}{\partial t} (\mathbf{A}_{em}(\mathbf{x}, t) + \nabla \eta(\mathbf{x}, t)), \\ &= -\nabla V(\mathbf{x}, t) - \frac{\partial \mathbf{A}_{em}(\mathbf{x}, t)}{\partial t} - \frac{\partial}{\partial t} (\nabla \eta(\mathbf{x}, t) - \nabla \eta(\mathbf{x}, t)), \\ &= E(\mathbf{x}, t). \end{aligned}$$

Hence

$$\boxed{E'(\mathbf{x}, t) = E(\mathbf{x}, t).}$$

This shows that both $\mathbf{E}(\mathbf{x}, t)$ and $\mathbf{B}(\mathbf{x}, t)$ remain invariant by choosing this specific gauge transformation. It is worthwhile to mention that integral of the electromagnetic vector potential \mathbf{A}_{em} on a closed path in real space is gauge invariant [4]. In the following section, we discuss how electromagnetic gauge transformations work in quantum mechanics.

1.1.2 Electromagnetic Gauge Freedom in Quantum Mechanics

The Hamiltonian of a spin-less charged particle, having charge q and mass m , in the presence of the potentials, \mathbf{A}_{em} and V , is written as follows

$$\hat{H}(\mathbf{x}, t) = \frac{1}{2m} (\hat{\mathbf{p}} - q\mathbf{A}_{em}(\mathbf{x}, t))^2 + qV(\mathbf{x}, t). \quad (1.5)$$

The evolution of the state $|\psi_s\rangle$ of the system in the Schrödinger picture is given as,

$$\begin{aligned} i\hbar \frac{\partial |\psi_s(\mathbf{x}, t)\rangle}{\partial t} &= \hat{H}(\mathbf{x}, t) |\psi_s(\mathbf{x}, t)\rangle, \\ &= \left[\frac{1}{2m} (\hat{\mathbf{p}} - q\mathbf{A}_{em}(\mathbf{x}, t))^2 + qV(\mathbf{x}, t) \right] |\psi_s(\mathbf{x}, t)\rangle, \end{aligned} \quad (1.6)$$

by using the electromagnetic gauge freedom

$$\mathbf{A}'_{em}(\mathbf{x}, t) = \mathbf{A}_{em}(\mathbf{x}, t) + \nabla \eta(\mathbf{x}, t), \quad V'(\mathbf{x}, t) = V(\mathbf{x}, t) - \frac{\partial \eta(\mathbf{x}, t)}{\partial t},$$

where $\eta(\mathbf{x}, t)$ is an arbitrary scalar function. The Hamiltonian becomes

$$\hat{H}'(\mathbf{x}, t) = \frac{1}{2m} (\hat{\mathbf{p}} - q\mathbf{A}'_{em}(\mathbf{x}, t))^2 + qV'(\mathbf{x}, t).$$

$\hat{H}'(\mathbf{x}, t)$ satisfies the evolution equation (1.6), but with a new transformed state

$$|\psi'_s(\mathbf{x}, t)\rangle = e^{iq\eta(\mathbf{x}, t)/\hbar} |\psi_s(\mathbf{x}, t)\rangle. \quad (1.7)$$

Proof:

From appendix A

$$\begin{aligned} (\hat{\mathbf{p}} - q\mathbf{A}'_{em}(\mathbf{x}, t))^2 |\psi'_s(\mathbf{x}, t)\rangle &= e^{iq\eta(\mathbf{x}, t)/\hbar} \left[(-i\hbar\nabla - q\mathbf{A}_{em}(\mathbf{x}, t))^2 \right. \\ &\quad \left. \times |\psi_s(\mathbf{x}, t)\rangle \right], \end{aligned} \quad (1.8)$$

operation of the transformed Hamiltonian on the proposed state in equation (1.7) gives

$$\begin{aligned} \hat{H}'(\mathbf{x}, t) |\psi'_s(\mathbf{x}, t)\rangle &= \left[\frac{1}{2m} (\hat{\mathbf{p}} - q\mathbf{A}'_{em}(\mathbf{x}, t))^2 + qV(\mathbf{x}, t) \right. \\ &\quad \left. - q\frac{\partial\eta(\mathbf{x}, t)}{\partial t} \right] |\psi'_s(\mathbf{x}, t)\rangle, \\ &= e^{iq\eta(\mathbf{x}, t)/\hbar} \left[(-i\hbar\nabla - q\mathbf{A}_{em}(\mathbf{x}, t))^2 + qV(\mathbf{x}, t) \right. \\ &\quad \left. - q\frac{\partial\eta(\mathbf{x}, t)}{\partial t} \right] |\psi_s(\mathbf{x}, t)\rangle, \quad (1.9) \\ &= e^{iq\eta(\mathbf{x}, t)/\hbar} \left[i\hbar\frac{\partial}{\partial t} - q\frac{\partial\eta(\mathbf{x}, t)}{\partial t} \right] |\psi_s(\mathbf{x}, t)\rangle, \\ &= i\hbar\frac{\partial}{\partial t} \left(e^{iq\eta(\mathbf{x}, t)/\hbar} |\psi_s(\mathbf{x}, t)\rangle \right), \\ &= i\hbar\frac{\partial |\psi'_s(\mathbf{x}, t)\rangle}{\partial t}, \\ &\Rightarrow \boxed{\hat{H}'(\mathbf{x}, t) |\psi'_s(\mathbf{x}, t)\rangle = i\hbar\frac{\partial |\psi'_s(\mathbf{x}, t)\rangle}{\partial t}}. \quad (1.10) \end{aligned}$$

This shows that we can remove the effect of the gauge field by introducing a phase factor with the wave function. So, the state function itself changes, but probability density does not change. Similarly, we can remove the vector potential in Hamiltonian (1.5) by introducing another phase called ‘‘Aharonov-Bohm Phase’’, which depends on the line integral of the vector potential in real space. The Aharonov-Bohm phase is one of the examples of the Berry phase or geometric phase, and it is well-defined in a closed path [4]. In the next subsection, we formally introduce the Berry phase.

1.2 Berry Phase

A general time independent Hamiltonian satisfies the following eigenvalue equation

$$\hat{H} |\phi_m\rangle = E_m |\phi_m\rangle,$$

and at any later time the system remains in m th eigenstate. Evolution of the eigenstate is simply picking up a phase factor,

$$|\phi_m(t)\rangle = |\phi_m(0)\rangle e^{-iE_m t}.$$

However, if the Hamiltonian is time dependent, both eigenstates and eigenvalues will be time dependent,

$$\hat{H}(t) |\phi_m(t)\rangle = E_m(t) |\phi_m(t)\rangle. \quad (1.11)$$

A general state, which is a linear superposition of all eigenstates [4], is a solution of the time dependent Schrödinger equation,

$$i\hbar \frac{\partial}{\partial t} |\psi_s(t)\rangle = \hat{H}(t) |\psi_s(t)\rangle. \quad (1.12)$$

The general state can be described as

$$|\psi_s(t)\rangle = \sum_m a_m(t) e^{i\beta_m(t)} |\phi_m(t)\rangle, \quad (1.13)$$

where coefficients $a_m(t)$ are related to probability amplitude of finding the system in eigenstate $|\phi_m(t)\rangle$ at time t and

$$\beta_m(t) \equiv -\frac{1}{\hbar} \int_0^t E_m(t') dt',$$

is a generalized phase factor in the case when E_m is time-dependent.

Substituting equation (1.13) in (1.12), we obtain

$$i\hbar \frac{\partial}{\partial t} \left[\sum_m a_m(t) e^{i\beta_m(t)} |\phi_m(t)\rangle \right] = \hat{H}(t) \left[\sum_m a_m(t) e^{i\beta_m(t)} |\phi_m(t)\rangle \right], \quad (1.14)$$

$$\begin{aligned} i\hbar \sum_m \left[\dot{a}_m(t) |\phi_m(t)\rangle + a_m(t) \left| \dot{\phi}_m(t) \right\rangle + i\dot{\beta}_m(t) a_m(t) |\phi_m(t)\rangle \right] e^{i\beta_m(t)} \\ = \sum_m a_m(t) e^{i\beta_m(t)} \hat{H}(t) |\phi_m(t)\rangle, \end{aligned}$$

$$\begin{aligned}
i\hbar \sum_m \dot{a}_m(t) |\phi_m(t)\rangle e^{i\beta_m(t)} + \sum_m a_m(t) \left| \dot{\phi}_m(t) \right\rangle \\
= \sum_m a_m(t) e^{i\beta_m(t)} \hat{H}(t) |\phi_m(t)\rangle \\
- \sum_m a_m(t) E_m(t) |\phi_m(t)\rangle e^{i\beta_m(t)}, \\
\sum_m \dot{a}_m(t) e^{i\beta_m(t)} |\phi_m(t)\rangle = - \sum_m a_m(t) e^{i\beta_m(t)} \left| \dot{\phi}_m(t) \right\rangle, \quad (1.15)
\end{aligned}$$

multiplying both sides of equation (1.15) with $\sum_{m'} \langle \phi_{m'}(t) |$,

$$\begin{aligned}
\sum_{m'} \sum_m \dot{a}_m(t) e^{i\beta_m(t)} \langle \phi_{m'}(t) | \phi_m(t) \rangle &= - \sum_{m'} \sum_m a_m(t) e^{i\beta_m(t)} \langle \phi_{m'}(t) | \dot{\phi}_m(t) \rangle, \\
\sum_{m'} \sum_m \dot{a}_m(t) e^{i\beta_m(t)} \delta_{m,m'} &= - \sum_{m'} \sum_m a_m(t) e^{i\beta_m(t)} \langle \phi_{m'}(t) | \dot{\phi}_m(t) \rangle, \\
\dot{a}_{m'}(t) e^{i\beta_{m'}(t)} &= - \sum_m a_m(t) e^{i\beta_m(t)} \langle \phi_{m'}(t) | \dot{\phi}_m(t) \rangle, \\
\dot{a}_{m'}(t) &= - \sum_m a_m(t) e^{i[\beta_m(t) - \beta_{m'}(t)]} \\
&\quad \times \langle \phi_{m'}(t) | \dot{\phi}_m(t) \rangle. \quad (1.16)
\end{aligned}$$

Differentiating equation (1.11) w.r.t time,

$$\begin{aligned}
\frac{\partial}{\partial t} \left(\hat{H} |\phi_m(t)\rangle \right) &= \frac{\partial}{\partial t} (E_m(t) |\phi_m(t)\rangle), \\
\dot{\hat{H}} |\phi_m(t)\rangle + \hat{H} \left| \dot{\phi}_m(t) \right\rangle &= \dot{E}_m(t) |\phi_m(t)\rangle + E_m(t) \left| \dot{\phi}_m(t) \right\rangle.
\end{aligned}$$

Multiplying the above equation with $\langle \phi_{m'}(t) |$ on both sides

$$\begin{aligned}
\langle \phi_{m'}(t) | \dot{\hat{H}} |\phi_m(t)\rangle + \langle \phi_{m'}(t) | \hat{H} \left| \dot{\phi}_m(t) \right\rangle &= \dot{E}_m(t) \langle \phi_{m'}(t) | \phi_m(t) \rangle \\
&\quad + E_m(t) \langle \phi_{m'}(t) | \dot{\phi}_m(t) \rangle \\
\langle \phi_{m'}(t) | \dot{\hat{H}} |\phi_m(t)\rangle + E_{m'}(t) \langle \phi_{m'}(t) | \dot{\phi}_m(t) \rangle &= \dot{E}_m(t) \delta_{m,m'} \\
&\quad + E_m(t) \langle \phi_{m'}(t) | \dot{\phi}_m(t) \rangle.
\end{aligned}$$

If $m \neq m'$, the above equation implies

$$\langle \phi_{m'}(t) | \dot{\hat{H}} |\phi_m(t)\rangle = [E_m(t) - E_{m'}(t)] \langle \phi_{m'}(t) | \dot{\phi}_m(t) \rangle, \quad (1.17)$$

putting equation (1.17) in equation (1.16),

$$\dot{a}_{m'}(t) = -a_{m'} \langle \phi_{m'}(t) | \dot{\phi}_{m'}(t) \rangle - \sum_m a_m(t) e^{i[\beta_m(t) - \beta_{m'}(t)]} \frac{\langle \phi_{m'}(t) | \dot{\hat{H}} |\phi_m(t)\rangle}{E_m - E_{m'}},$$

the second term of the above equation contains a term, $\langle \phi_n(t) | \dot{\hat{H}} | \phi_m(t) \rangle$, which depends on the rate of change of the Hamiltonian. When the Hamiltonian is slowly changing with time, we can ignore this term. This approximation is called “adiabatic approximation”,

$$\Rightarrow \boxed{\dot{a}_{m'}(t) \approx -a_{m'}(t) \langle \phi_{m'}(t) | \dot{\phi}_{m'}(t) \rangle}. \quad (1.18)$$

Equation (1.18) is a 1st order linear differential equation, and its solution is,

$$\begin{aligned} a_{m'}(t) &= a_{m'}(0) \exp \left\{ i^2 \int_0^t \langle \phi_{m'}(t') | \dot{\phi}_{m'}(t') \rangle dt' \right\}, \\ &= a_{m'}(0) \exp \{ i \gamma_{m'}(t) \}, \end{aligned} \quad (1.19)$$

where

$$\begin{aligned} \gamma_{m'}(t) &\equiv i \int_0^t \langle \phi_{m'}(t') | \dot{\phi}_{m'}(t') \rangle dt', \\ &= i \int_0^t \left\langle \phi_{m'}(t') \left| \frac{\partial}{\partial t'} \phi_{m'}(t') \right. \right\rangle dt', \end{aligned} \quad (1.20)$$

finally, putting the value of $a_{m'}(t)$ from equation (1.19) to equation (1.13),

$$\boxed{|\psi(t)\rangle = \sum_m e^{i\gamma_m(t)} e^{i\beta_m(t)} |\phi_m(t)\rangle}. \quad (1.21)$$

Thus, in the case of adiabatic evolution, the system remains in the m th eigenstate by picking an extra phase factor. This new phase is called the Berry phase or geometric phase. Let $|\phi_m\rangle$ be time-dependent because some parameters $\mathbf{\Lambda}(t)$ are changing in the Hamiltonian, these parameters have explicit time dependence

$$\hat{H} = \hat{H}(\Lambda_1(t), \Lambda_2(t), \Lambda_3(t), \Lambda_4(t), \Lambda_5(t) \dots, \Lambda_N(t)),$$

then the state will depend on these parameters

$$|\phi_m\rangle = |\phi_m(\Lambda_1(t), \Lambda_2(t), \Lambda_3(t), \Lambda_4(t), \Lambda_5(t) \dots, \Lambda_N(t))\rangle,$$

taking partial derivative w.r.t time,

$$\frac{\partial \phi_m}{\partial t} = \frac{\partial \phi_m}{\partial \Lambda_1} \frac{\partial \Lambda_1}{\partial t} + \frac{\partial \phi_m}{\partial \Lambda_2} \frac{\partial \Lambda_2}{\partial t} + \frac{\partial \phi_m}{\partial \Lambda_3} \frac{\partial \Lambda_3}{\partial t} + \frac{\partial \phi_m}{\partial \Lambda_4} \frac{\partial \Lambda_4}{\partial t} + \dots + \frac{\partial \phi_m}{\partial \Lambda_N} \frac{\partial \Lambda_N}{\partial t},$$

it can be written in the form

$$\frac{\partial \phi_m}{\partial t} = \nabla_{\mathbf{\Lambda}} \phi_m \cdot \frac{d\mathbf{\Lambda}}{dt},$$

where

$$\nabla_{\Lambda} \equiv \hat{\mathbf{s}}_1 \frac{\partial}{\partial \Lambda_1} + \hat{\mathbf{s}}_2 \frac{\partial}{\partial \Lambda_2} + \hat{\mathbf{s}}_3 \frac{\partial}{\partial \Lambda_3} + \hat{\mathbf{s}}_4 \frac{\partial}{\partial \Lambda_4} + \dots + \hat{\mathbf{s}}_N \frac{\partial}{\partial \Lambda_N},$$

is a generalized gradient operator and $\hat{\mathbf{s}}_1, \hat{\mathbf{s}}_2, \hat{\mathbf{s}}_3, \hat{\mathbf{s}}_4, \dots, \hat{\mathbf{s}}_N$ are unit vectors along $\Lambda_1(t), \Lambda_2(t), \Lambda_3(t), \Lambda_4(t), \dots, \Lambda_N(t)$, respectively. Equation (1.20) becomes

$$\gamma_m(t) = i \int_{\Lambda_i}^{\Lambda_f} \langle \phi_m | \nabla_{\Lambda} \phi_m \rangle \cdot d\Lambda.$$

If the Hamiltonian returns to its original form after time T , then geometric phase implies

$$\gamma_m(T) = i \oint \langle \phi_m | \nabla_{\Lambda} \phi_m \rangle \cdot d\Lambda = \oint \mathbf{A} \cdot d\Lambda,$$

where $\mathbf{A} = i \langle \phi_m | \nabla_{\Lambda} \phi_m \rangle$ is called Berry connection.

For instance, if a Hamiltonian depends on \mathbf{k} and is periodic with respect to \mathbf{k}

$$\hat{H} = \hat{H}(\mathbf{k}(t)),$$

its Berry phase is

$$\boxed{\gamma_m(T) = i \oint \langle \phi_m(\mathbf{k}) | \nabla_{\mathbf{k}} \phi_m(\mathbf{k}) \rangle \cdot d\mathbf{k}.} \quad (1.22)$$

1.2.1 Properties of Berry Phase

- If the parametric space is one dimensional and the Hamiltonian is periodic in time having time-period T then the Berry phase vanishes.
- Along a closed path in parametric space (which is atleast 2-dimensional), the Berry phase is **gauge invariant**.

Proof:

The Berry phase for an open path is

$$\begin{aligned} \gamma_m(t) &= i \int_{\Lambda_i}^{\Lambda_f} \langle \phi_m(\Lambda) | \nabla_{\Lambda} \phi_m(\Lambda) \rangle \cdot d\Lambda, \\ &= \int_{\Lambda_i}^{\Lambda_f} \mathbf{A} \cdot d\Lambda, \end{aligned} \quad (1.23)$$

where $\mathbf{A}(\Lambda)$ is the Berry connection. If we redefine new instantaneous state as

$$|\phi_m(\Lambda)\rangle \rightarrow |\phi'_m(\Lambda)\rangle = e^{-i\xi(\Lambda)} |\phi_m(\Lambda)\rangle,$$

where $\xi(\mathbf{\Lambda})$ is an arbitrary function. The new Berry connection is

$$\begin{aligned}
\mathbf{A}'(\mathbf{\Lambda}) &= i \langle \phi'_m(\mathbf{\Lambda}) | \nabla_{\mathbf{\Lambda}} \phi'_m(\mathbf{\Lambda}) \rangle, \\
&= i \langle \phi_m(\mathbf{\Lambda}) e^{-i\xi(\mathbf{\Lambda})} | \nabla_{\mathbf{\Lambda}} e^{-i\xi(\mathbf{\Lambda})} \phi_m(\mathbf{\Lambda}) \rangle, \\
&= i \langle \phi_m(\mathbf{\Lambda}) e^{-i\xi(\mathbf{\Lambda})} | \left(-i \nabla_{\mathbf{\Lambda}} \xi(\mathbf{\Lambda}) e^{-i\xi(\mathbf{\Lambda})} + e^{-i\xi(\mathbf{\Lambda})} \nabla_{\mathbf{\Lambda}} \right) \phi_m(\mathbf{\Lambda}) \rangle, \\
&= e^{-i\xi(\mathbf{\Lambda})} e^{i\xi(\mathbf{\Lambda})} \nabla_{\mathbf{\Lambda}} \xi(\mathbf{\Lambda}) \langle \phi_m(\mathbf{\Lambda}) | \phi_m(\mathbf{\Lambda}) \rangle \\
&\quad + e^{-i\xi(\mathbf{\Lambda})} e^{i\xi(\mathbf{\Lambda})} i \langle \phi_m(\mathbf{\Lambda}) | \nabla_{\mathbf{\Lambda}} \phi_m(\mathbf{\Lambda}) \rangle,
\end{aligned}$$

first term of above equation is $\langle \phi_m(\mathbf{\Lambda}) | \phi_m(\mathbf{\Lambda}) \rangle = \mathbb{1}$; because eigenvectors are normalized,

$$\boxed{\mathbf{A}'(\mathbf{\Lambda}) = \mathbf{A}(\mathbf{\Lambda}) + \nabla_{\mathbf{\Lambda}} \xi(\mathbf{\Lambda})}, \quad (1.24)$$

equation (1.24) shows that the Berry connection is gauge dependent and transforms like electromagnetic vector potential, as defined in subsection (1.1.1). The Berry phase transforms as follows:

$$\begin{aligned}
\gamma'_m(t) &= \int_{\mathbf{\Lambda}_i}^{\mathbf{\Lambda}_f} \mathbf{A}'(\mathbf{\Lambda}) \cdot d\mathbf{\Lambda}, \\
&= \int_{\mathbf{\Lambda}_i}^{\mathbf{\Lambda}_f} (\mathbf{A}(\mathbf{\Lambda}) + \nabla_{\mathbf{\Lambda}} \xi(\mathbf{\Lambda})) \cdot d\mathbf{\Lambda}, \\
&= \gamma_m(t) + \int_{\mathbf{\Lambda}_i}^{\mathbf{\Lambda}_f} \nabla_{\mathbf{\Lambda}} \xi(\mathbf{\Lambda}) \cdot d\mathbf{\Lambda}, \\
\Rightarrow \gamma'_m(t) &= \gamma_m(t) + \xi(\mathbf{\Lambda}_f) - \xi(\mathbf{\Lambda}_i). \quad (1.25)
\end{aligned}$$

Equation (1.25) shows that although the geometrical phase is arbitrary in any open path in parametric space, it is completely well-defined on a closed path. On a closed path $\xi(\mathbf{\Lambda}_f) = \xi(\mathbf{\Lambda}_i)$, as a result,

$$\boxed{\gamma'_m(t) = \gamma_m(t)},$$

on any closed path. As an example, I calculate the Berry phase of two level system in the next subsection.

1.2.2 Two-Level Hamiltonian:

In quantum mechanics, a two-level system is a system having two independent states, and a two dimensional Hilbert space describes this system. Examples of the two-level system are a spin half particle in a magnetic field, qubit algebra for quantum computing, and neutrino oscillations, etc. Furthermore, in condensed matter systems, graphene Hamiltonian, semi-Dirac Hamiltonian, and the Su-Schrieffer-Heeger (SSH) model, etc., are examples of two-level systems.

For a general two-level system, the Hamiltonian can be written in terms of Pauli matrices $\boldsymbol{\sigma}$ as

$$\hat{H}(\mathbf{k}) = \mathbf{d}(\mathbf{k}) \cdot \boldsymbol{\sigma} + E(\mathbf{k})\mathbb{1}. \quad (1.26)$$

We can neglect the second term in the Hamiltonian; because it does not affect eigenvectors

$$\begin{aligned} \hat{H}(\mathbf{k}) &= d_x\sigma_x + d_y\sigma_y + d_z\sigma_z, \\ &= \begin{pmatrix} d_z & d_x - id_y \\ d_x + id_y & -d_z \end{pmatrix}. \end{aligned} \quad (1.27)$$

Energy Spectrum:

$$\begin{aligned} \hat{H}^2 &= (d_i\sigma_i)(d_j\sigma_j), \\ &= (d_id_j)(\sigma_i\sigma_j), \\ &= (d_id_j)(\delta_{ij} + i\epsilon_{ijk}\sigma_k), \\ &= \mathbf{d} \cdot \mathbf{d}, \\ \Rightarrow & \boxed{E(\mathbf{k}) = \pm\sqrt{\mathbf{d} \cdot \mathbf{d}} = \pm|\mathbf{d}(\mathbf{k})|.} \end{aligned} \quad (1.28)$$

Eigenvectors:

For eigenvectors, it is convenient to transform the Hamiltonian into spherical polar co-ordinates

$$\begin{aligned} d_x(\mathbf{k}) &= |\mathbf{d}(\mathbf{k})| \sin\theta \cos\phi, & d_y(\mathbf{k}) &= |\mathbf{d}(\mathbf{k})| \sin\theta \sin\phi, \\ d_z(\mathbf{k}) &= |\mathbf{d}(\mathbf{k})| \cos\theta, \end{aligned}$$

putting these in equation (1.26)

$$\hat{H}(\mathbf{k}) = |\mathbf{d}(\mathbf{k})| \begin{pmatrix} \cos\theta & \sin\theta e^{-i\phi} \\ \sin\theta e^{i\phi} & -\cos\theta \end{pmatrix}. \quad (1.29)$$

For eigenvectors

$$\hat{H}(\mathbf{k}) |\chi\rangle = E |\chi\rangle, \quad |\chi\rangle = \begin{pmatrix} a \\ b \end{pmatrix},$$

substituting

$$|\mathbf{d}(\mathbf{k})| \begin{pmatrix} \cos\theta & \sin\theta e^{-i\phi} \\ \sin\theta e^{i\phi} & -\cos\theta \end{pmatrix} \begin{pmatrix} a \\ b \end{pmatrix} = \pm|\mathbf{d}(\mathbf{k})| \begin{pmatrix} a \\ b \end{pmatrix},$$

it implies

$$\begin{aligned} (\cos\theta)a + \sin\theta e^{-i\phi}b &= \pm a, \\ \sin\theta e^{i\phi}a - (\cos\theta)b &= \pm b, \end{aligned}$$

solving the above equations for positive and negative energy bands, $E = \pm|\mathbf{d}(\mathbf{k})|$, we get

$$|\chi_+\rangle = \begin{pmatrix} \cos \frac{\theta}{2} e^{-i\phi} \\ \sin \frac{\theta}{2} \end{pmatrix}, \quad |\chi_-\rangle = \begin{pmatrix} \cos \frac{\theta}{2} e^{i\phi} \\ \sin \frac{\theta}{2} \end{pmatrix}.$$

Berry Phase Calculation:

If we change the parameter \mathbf{k} in the Hamiltonian adiabatically without band gap closing, we can calculate the the Berry phase. By using the definition of the Berry phase from equation (1.22)

$$\gamma_+ = i \oint \langle \chi_+ | \nabla \chi_+ \rangle \cdot d\mathbf{k},$$

we convert line integral on a closed path into a surface integral by using Stokes' theorem

$$\gamma_+ = \int (\nabla \times \mathbf{A}) \cdot d^2\mathbf{k},$$

where

$$\mathbf{A} = i \langle \chi_+ | \nabla \chi_+ \rangle. \quad (1.30)$$

Using gradient operator in spherical polar co-ordinates

$$\nabla \chi_+ = \frac{\partial \chi_+}{\partial d} \hat{\mathbf{r}} + \frac{1}{d} \frac{\partial \chi_+}{\partial \theta} \hat{\boldsymbol{\theta}} + \frac{1}{d \sin \theta} \frac{\partial \chi_+}{\partial \phi} \hat{\boldsymbol{\phi}},$$

putting the value of χ_+ in the above equation and taking partial derivative w.r.t θ and ϕ ,

$$\nabla \chi_+ = \frac{1}{2d} \begin{pmatrix} -\sin \frac{\theta}{2} e^{-i\phi} \\ \cos \frac{\theta}{2} \end{pmatrix} \hat{\boldsymbol{\theta}} - \frac{i}{d \sin \theta} \begin{pmatrix} \cos \frac{\theta}{2} e^{-i\phi} \\ 0 \end{pmatrix} \hat{\boldsymbol{\phi}},$$

putting this result in equation (1.29) and taking inner product

$$\begin{aligned} \mathbf{A} &= \frac{i}{2d} \begin{pmatrix} \cos \frac{\theta}{2} e^{i\phi} & \sin \frac{\theta}{2} \end{pmatrix} \begin{pmatrix} -\sin \frac{\theta}{2} e^{-i\phi} \\ \cos \frac{\theta}{2} \end{pmatrix} \hat{\boldsymbol{\theta}} \\ &\quad - \frac{i^2}{d \sin \theta} \begin{pmatrix} \cos \frac{\theta}{2} e^{i\phi} & \sin \frac{\theta}{2} \end{pmatrix} \begin{pmatrix} \cos \frac{\theta}{2} e^{-i\phi} \\ 0 \end{pmatrix} \hat{\boldsymbol{\phi}}, \\ &= \frac{1}{d \sin \theta} \cos^2 \left(\frac{\theta}{2} \right) \hat{\boldsymbol{\phi}}, \end{aligned} \quad (1.31)$$

for the Berry curvature we need to calculate curl of \mathbf{A} ,

$$\begin{aligned}\nabla \times \mathbf{A} &= \frac{1}{d \sin \theta} \frac{\partial}{\partial \theta} \left(\sin \theta \frac{\cos^2(\theta/2)}{d \sin \theta} \right) \hat{\mathbf{r}}, \\ &= -\frac{1}{2d^2} \hat{\mathbf{r}}.\end{aligned}$$

Finally, the Berry phase becomes

$$\gamma_+ = \int -\frac{1}{2d^2} \hat{\mathbf{r}} \cdot \hat{\mathbf{r}} d\Omega = -\frac{1}{2} \int d\Omega = \frac{-1}{2} \Omega,$$

where Ω is solid angle swept by $\hat{d}(\mathbf{k})$

$$\begin{aligned}\Rightarrow \quad \gamma_+ &= \frac{-1}{2} \Omega, \\ &= \frac{-1}{2} \left(\text{Solid angle traced by } \hat{d}(\mathbf{k}) \right).\end{aligned}\tag{1.32}$$

Similarly, for the negative energy band, the Berry phase is $1/2\Omega$.

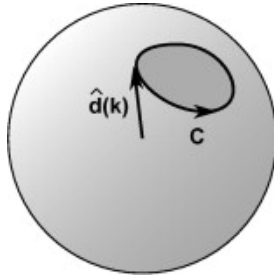


Figure 1.1: The Berry phase is one half times the solid angle traced by $\hat{d}(\mathbf{k})$.

In the subsequent section, I discuss topological band theory, which builds the foundation for studying solids with non-trivial topological properties. In this theory, the electronic wave function has non-zero Berry phase; it addresses the question of how the non-zero Berry phase affects the dynamics of electrons on a lattice.

1.3 Topological Band Theory

In a crystalline solid, an electron feels a periodic potential due to ions. If we ignore interactions among electrons, Hamiltonian of single electron can be written as

$$\hat{H}(\mathbf{x}) = \frac{\hat{\mathbf{p}}^2}{2m} + V(\mathbf{x}),\tag{1.33}$$

where potential due to ions $V(\mathbf{x})$ has discrete translational symmetry of Bravais lattice with lattice vector \mathbf{R}

$$V(\mathbf{R} + \mathbf{x}) = V(\mathbf{x}),$$

and due to this

$$\hat{H}(\mathbf{x} + \mathbf{R}) = \hat{H}(\mathbf{x}).$$

We exploit the discrete translational symmetry of lattice to calculate eigenstates $|\phi_j(\mathbf{x}, \mathbf{k})\rangle$ of Hamiltonian (1.33). To do this, we define a discrete translational $\hat{T}_{\mathbf{R}}$ operator

$$\hat{T}_{\mathbf{R}} |\phi_j(\mathbf{x}, \mathbf{k})\rangle \equiv |\phi_j(\mathbf{x} + \mathbf{R}, \mathbf{k})\rangle,$$

and $|\phi_j(\mathbf{x}, \mathbf{k})\rangle$ satisfies the energy eigenvalue equation

$$\hat{H}(\mathbf{x}) |\phi_j(\mathbf{x}, \mathbf{k})\rangle = \hat{H}(\mathbf{x}) |\phi_j(\mathbf{x}, \mathbf{k})\rangle,$$

operating $\hat{T}_{\mathbf{R}}$ on both sides of the above equation and by using $\hat{T}_{\mathbf{R}}\hat{H}(\mathbf{x}) = \hat{H}(\mathbf{x} + \mathbf{R})\hat{T}_{\mathbf{R}}$

$$\begin{aligned} \hat{T}_{\mathbf{R}}\hat{H}(\mathbf{x}) |\phi_j(\mathbf{x}, \mathbf{k})\rangle &= \hat{H}(\mathbf{x} + \mathbf{R})\hat{T}_{\mathbf{R}} |\phi_j(\mathbf{x}, \mathbf{k})\rangle, \\ \hat{T}_{\mathbf{R}}\hat{H}(\mathbf{x}) |\phi_j(\mathbf{x}, \mathbf{k})\rangle &= \hat{H}(\mathbf{x})\hat{T}_{\mathbf{R}} |\phi_j(\mathbf{x}, \mathbf{k})\rangle, \end{aligned}$$

where we have used $\hat{H}(\mathbf{x} + \mathbf{R}) = \hat{H}(\mathbf{x})$ in the above equation

$$\Rightarrow \left(\hat{T}_{\mathbf{R}}\hat{H}(\mathbf{x}) - \hat{H}(\mathbf{x})\hat{T}_{\mathbf{R}} \right) |\phi_j(\mathbf{x}, \mathbf{k})\rangle = 0,$$

it implies

$$\left[\hat{T}_{\mathbf{R}}, \hat{H}(\mathbf{x}) \right] = 0,$$

so, it means that both $\hat{T}_{\mathbf{R}}$ and $\hat{H}(\mathbf{x})$ share common eigenstates

$$\begin{aligned} \hat{H}(\mathbf{x}) |\phi_j(\mathbf{x}, \mathbf{k})\rangle &= E_j(\mathbf{k}) |\phi_j(\mathbf{x}, \mathbf{k})\rangle, \\ \hat{T}_{\mathbf{R}} |\phi_j(\mathbf{x}, \mathbf{k})\rangle &= \lambda_{\mathbf{R}} |\phi_j(\mathbf{x}, \mathbf{k})\rangle. \end{aligned}$$

The translational operator has to satisfy following properties:

- Because each lattice site is identical and has discrete translational symmetry equal to Bravais lattice vector \mathbf{R} , so operation of translational operator should not change probability density

$$||\phi_j(\mathbf{x}, \mathbf{k})\rangle|^2 = ||\phi_j(\mathbf{x} + \mathbf{R}, \mathbf{k})\rangle|^2. \quad (1.34)$$

From the eigenvalue equation

$$\begin{aligned} \left| \hat{T}_{\mathbf{R}} |\phi_j(\mathbf{x}, \mathbf{k})\rangle \right|^2 &= |\lambda_{\mathbf{R}} |\phi_j(\mathbf{x}, \mathbf{k})\rangle|^2, \\ ||\phi_j(\mathbf{x} + \mathbf{R}, \mathbf{k})\rangle|^2 &= |\lambda_{\mathbf{R}}|^2 ||\phi_j(\mathbf{x}, \mathbf{k})\rangle|^2, \end{aligned} \quad (1.35)$$

comparing equation (1.35) with (1.34)

$$\Rightarrow |\lambda_{\mathbf{R}}|^2 = 1. \quad (1.36)$$

- Two or more successive translations should be equal to sum of all individual translations

$$\hat{T}_{\mathbf{R}}\hat{T}_{\mathbf{R}} = \hat{T}_{\mathbf{R}+\mathbf{R}}.$$

Let us operate twice

$$\begin{aligned}\hat{T}_{\mathbf{R}}\hat{T}_{\mathbf{R}}|\phi_j(\mathbf{x}, \mathbf{k})\rangle &= \lambda_{\mathbf{R}}\lambda_{\mathbf{R}}|\phi_j(\mathbf{x}, \mathbf{k})\rangle, \\ \hat{T}_{\mathbf{R}+\mathbf{R}}|\phi_j(\mathbf{x}, \mathbf{k})\rangle &= \lambda_{\mathbf{R}+\mathbf{R}}|\phi_j(\mathbf{x}, \mathbf{k})\rangle,\end{aligned}\tag{1.37}$$

above equations imply

$$\lambda_{\mathbf{R}}\lambda_{\mathbf{R}} = \lambda_{\mathbf{R}+\mathbf{R}},\tag{1.38}$$

to satisfy equation (1.36) and (1.38), $\lambda_{\mathbf{R}}$ should be equal to $e^{i\mathbf{k}\cdot\mathbf{R}}$

$$\hat{T}_{\mathbf{R}}|\phi_j(\mathbf{x}, \mathbf{k})\rangle = e^{i\mathbf{k}\cdot\mathbf{R}}|\phi_j(\mathbf{x}, \mathbf{k})\rangle.\tag{1.39}$$

Let

$$|\phi_j(\mathbf{x}, \mathbf{k})\rangle = e^{i\mathbf{k}\cdot\mathbf{x}}|\phi_j(\mathbf{x}, \mathbf{k})\rangle,$$

this eigenfunction should satisfy the property defined in equation (1.39)

$$\begin{aligned}\hat{T}_{\mathbf{R}}|\phi_j(\mathbf{x}, \mathbf{k})\rangle &= e^{i\mathbf{k}\cdot(\mathbf{x}+\mathbf{R})}|\phi_j(\mathbf{x} + \mathbf{R}, \mathbf{k})\rangle, \\ &= e^{i\mathbf{k}\cdot\mathbf{x}}e^{i\mathbf{k}\cdot\mathbf{R}}|\phi_j(\mathbf{x} + \mathbf{R}, \mathbf{k})\rangle,\end{aligned}\tag{1.40}$$

if $|\phi_j(\mathbf{x}, \mathbf{k})\rangle$ is periodic in real space

$$\begin{aligned}|\phi_j(\mathbf{x} + \mathbf{R}, \mathbf{k})\rangle &= |\phi_j(\mathbf{x}, \mathbf{k})\rangle, \\ \Rightarrow \hat{T}_{\mathbf{R}}|\phi_j(\mathbf{x}, \mathbf{k})\rangle &= e^{i\mathbf{k}\cdot\mathbf{R}}|\phi_j(\mathbf{x}, \mathbf{k})\rangle,\end{aligned}$$

then the proposed eigenfunction satisfies equation (1.39). These eigenstates are called ‘‘Bloch states’’, where subscript j is the band index. The energy eigenvalue equation states

$$\begin{aligned}\hat{H}|\phi_j(\mathbf{x}, \mathbf{k})\rangle &= E_j|\phi_j(\mathbf{x}, \mathbf{k})\rangle, \\ \hat{H}e^{i\mathbf{k}\cdot\mathbf{x}}|\phi_j(\mathbf{x}, \mathbf{k})\rangle &= E_je^{i\mathbf{k}\cdot\mathbf{x}}|\phi_j(\mathbf{x}, \mathbf{k})\rangle, \\ e^{-i\mathbf{k}\cdot\mathbf{x}}\hat{H}e^{i\mathbf{k}\cdot\mathbf{x}}|\phi_j(\mathbf{x}, \mathbf{k})\rangle &= E_j|\phi_j(\mathbf{x}, \mathbf{k})\rangle, \\ \hat{H}(\mathbf{k})|\phi_j(\mathbf{x}, \mathbf{k})\rangle &= E_j(\mathbf{k})|\phi_j(\mathbf{x}, \mathbf{k})\rangle,\end{aligned}\tag{1.41}$$

where

$$\begin{aligned}\hat{H}(\mathbf{k}) &\equiv e^{-i\mathbf{k}\cdot\mathbf{x}}\hat{H}e^{i\mathbf{k}\cdot\mathbf{x}} \\ &= e^{-i\mathbf{k}\cdot\mathbf{x}}\left(\frac{\hat{\mathbf{p}}^2}{2m} + V(\mathbf{x})\right)e^{i\mathbf{k}\cdot\mathbf{x}}, \\ \hat{H}(\mathbf{k}) &= \frac{1}{2m}(\mathbf{p} + \hbar\mathbf{k})^2 + V(\mathbf{x}).\end{aligned}$$

$\hat{H}(\mathbf{k})$ is called Bloch Hamiltonian. Substituting the value of $\hat{H}(\mathbf{k})$ in equation (1.41)

$$\left[\frac{1}{2m}(\mathbf{p} + \hbar\mathbf{k})^2 + V(\mathbf{x}) \right] |\phi_j(\mathbf{x}, \mathbf{k})\rangle = E_j(\mathbf{k}) |\phi_j(\mathbf{x}, \mathbf{k})\rangle. \quad (1.42)$$

Equation (1.42) is called Bloch's equation and $E_j(\mathbf{k})$ defines the band structure of the solid. If we displace \mathbf{k} by reciprocal lattice vector $\mathbf{k} + \mathbf{G}$ in Bloch's Hamiltonian, the Hamiltonian does not change; because all unique \mathbf{k} lie in the first Brillouin zone

$$\begin{aligned} \hat{H}(\mathbf{k} + \mathbf{G}) &= e^{-i(\mathbf{k}+\mathbf{G})\cdot\mathbf{x}} \hat{H} e^{i(\mathbf{k}+\mathbf{G})\cdot\mathbf{x}}, \\ &= \frac{1}{2m}(\mathbf{p} + \hbar\mathbf{k} + \hbar\mathbf{G})^2 + V(\mathbf{x}), \\ \Rightarrow \hat{H}(\mathbf{k} + \mathbf{G}) &= \hat{H}(\mathbf{k}). \end{aligned} \quad (1.43)$$

It means, domain of crystal momentum is a d-dimensional torus. If we adiabatically change the crystal momentum in the Bloch Hamiltonian with out closing the band gap, we get non-zero Berry phase as discussed in section 1.2

$$\mathbf{A}_j(\mathbf{k}) = i \langle \phi_j(\mathbf{x}, \mathbf{k}) | \nabla_{\mathbf{k}} | \phi_j(\mathbf{x}, \mathbf{k}) \rangle, \quad (1.44)$$

Bloch's equation (1.42) is invariant under local phase shift in crystal momentum space

$$|\phi_j(\mathbf{x}, \mathbf{k})\rangle \rightarrow e^{i\beta(\mathbf{k})} |\phi_j(\mathbf{x}, \mathbf{k})\rangle.$$

Putting the new transformed eigenstate in equation (1.44),

$$\mathbf{A}'_j(\mathbf{k}) = \mathbf{A}_j(\mathbf{k}) + \nabla\beta(\mathbf{k}).$$

We see that Berry connection transforms like electromagnetic vector potential. Although $\mathbf{A}_j(\mathbf{k})$ is gauge dependent, since, Bloch's Hamiltonian is periodic in crystal momentum space $\hat{H}(\mathbf{k} + \mathbf{G}) = \hat{H}(\mathbf{k})$, so Berry phase is not arbitrary

$$\gamma_j = \oint \mathbf{A}_j \cdot d\mathbf{k} = \int_S \mathbf{F}_j \cdot d\mathbf{S}, \quad (1.45)$$

where $\mathbf{F}_j(\mathbf{k}) = \nabla_{\mathbf{k}} \times \mathbf{A}_j(\mathbf{k})$ is called Berry curvature.

For any two dimensional Brillouin zone which has torus topology, the value of the integral

$$\frac{1}{2\pi} \int_S \mathbf{F}_j(\mathbf{k}) \cdot d\mathbf{S} = C_j, \quad C_j \in \mathbb{Z}, \quad (1.46)$$

is an integer, and it is a topological invariant called the Chern number of the jth band. The Chern number of a band of an insulator is a topological invariant in a sense that we can continuously change the Hamiltonian of the electrons on the lattice while keeping energy gaps separating the jth band from the other bands open. In such a case, the Berry curvature continuously

deforms, but its integral over the BZ, which is the Chern number, cannot change. When we deform the electronic Hamiltonian on crystal lattice in such a way that some energy gaps separating the j th band from the other nearest bands are closed and reopened again, this deformation is not adiabatic, and the Chern number might change.

In the next section, we derive a general result of the Berry curvature for a two-level system. For a two-level system, we can calculate the Berry curvature without calculating the eigenstates.

1.4 Berry Curvature of Two-Level System in 2D \mathbf{k} -Space

Hamiltonian of a two-level system is

$$\hat{H} = \mathbf{d}(\mathbf{k}) \cdot \boldsymbol{\sigma},$$

where

$$\mathbf{d}(\mathbf{k}) = (d_x(\mathbf{k}), d_y(\mathbf{k}), d_z(\mathbf{k})), \quad \mathbf{k} = (k_x, k_y).$$

It has two energy bands: one having positive energy and other with negative energy, as solved in subsection (1.2.2). If we adiabatically change \mathbf{k} , we can define a Berry connection and a Berry curvature,

$$\mathbf{A}^\pm(\mathbf{k}) = i \langle \chi_\pm | \partial_{\mathbf{k}} \chi_\pm \rangle.$$

Where \pm represents positive and negative energy bands respectively.

$$\begin{aligned} A_j^\pm(\mathbf{k}) &= i \langle \chi_\pm | \partial_{k_j} \chi_\pm \rangle, \\ &= i \frac{\partial d_\alpha}{\partial k_j} \langle \chi_\pm | \partial_{d_\alpha} \chi_\pm \rangle, \\ &= \frac{\partial d_\alpha}{\partial k_j} A_\alpha^\pm(\mathbf{d}), \end{aligned}$$

where ∂_{d_α} is a component of the gradient operator and $A_\alpha^\pm(\mathbf{d})$ is the Berry connection in \mathbf{d} space. The Berry curvature in \mathbf{k} -space has only non-zero z -components,

$$\begin{aligned} F_z(\mathbf{k}) &= \frac{\partial A_y^\pm}{\partial k_x} - \frac{\partial A_x^\pm}{\partial k_y}, \\ &= \frac{\partial}{\partial k_x} \left(\frac{\partial d_\alpha}{\partial k_y} A_\alpha^\pm(\mathbf{d}) \right) - \frac{\partial}{\partial k_y} \left(\frac{\partial d_\beta}{\partial k_x} A_\beta^\pm(\mathbf{d}) \right), \\ &= \frac{\partial d_\alpha}{\partial k_x} \frac{\partial d_\beta}{\partial k_y} \left(\frac{\partial A_\alpha^\pm}{\partial d_\beta} - \frac{\partial A_\beta^\pm}{\partial d_\alpha} \right), \end{aligned}$$

the expressions in the parenthesis are equal to the Berry curvature in d-space

$$F_z(\mathbf{k}) = \frac{\partial d_\alpha}{\partial k_x} \frac{\partial d_\beta}{\partial k_y} F_\gamma(\mathbf{d}) \epsilon_{\alpha\beta\gamma},$$

where

$$F_\gamma(\mathbf{d}) = \mp \frac{d_\gamma}{2|\mathbf{d}|^3},$$

is a component of the Berry curvature for two level system in d-space. The above expression can be written in the following form

$$\boxed{F_z(\mathbf{k}) = \mp \frac{\mathbf{d}}{2|\mathbf{d}|^3} \cdot \frac{\partial \mathbf{d}}{\partial k_x} \times \frac{\partial \mathbf{d}}{\partial k_y}.} \quad (1.47)$$

The above expression is a general result for two-level system in 2D k-space, and it is independent of the eigenstates of a two level-system. In the next section, we introduce symmetries, especially time reversal symmetry. Considerations based on symmetries lead to the simplification of intricate problems in physics. In condensed matter systems, we can classify different types of Hamiltonians based on underlying symmetries and predict certain properties without knowing the exact form of Hamiltonian.

1.5 Time-Reversal Symmetry (TRS)

The time-reversal symmetry is an example of discrete symmetry. In classical mechanics, we can easily find the time reversed variables by inverting the sign of time. However, in quantum mechanics inverting sign of time like $|\psi(\mathbf{x}, -t)\rangle$ does not work; because it does not satisfy the Schrödinger equation [5]. In quantum mechanics, we need to define a time reversal operator that must be anti-unitary.

In this section, we study the operation of time-reversal operator on operators like position and momentum, which make us able to study time-reversal symmetry of the Schrödinger equation. Lastly, we study how symmetries restricts the Berry curvature of a band and what would be its consequences.

1.5.1 TRS in Classical Mechanics

In classical mechanics, motion of a classical particle in the presence of potential $V(\mathbf{x}, t)$, in six dimensional phase space (\mathbf{x}, \mathbf{p}) , is dictated by the Newton's equation of motion

$$m\ddot{\mathbf{x}} = -\nabla V(\mathbf{x}, t). \quad (1.48)$$

If V is independent of time then

$$m \frac{d^2 \mathbf{x}(-t)}{d(-t)^2} = -\nabla V(\mathbf{x}),$$

TRS exists in the Newton's law of motion. So, by reversing the time, a classical particle traverses the same trajectory as for the forward time. If, for example, a dissipative force acts on a classical particle, then this breaks the TRS, and as a result, forward time and reversed time trajectory will not be the same.

1.5.2 TRS in Quantum Mechanics

Let $\hat{\Theta}$ is the time reversal operator such that its action on any state is defined in the following way

$$\hat{\Theta}^\dagger \hat{U}(t) \hat{\Theta} |\alpha\rangle \equiv \hat{U}(-t) |\alpha\rangle. \quad (1.49)$$

$\hat{U}(t) = e^{-i\hat{H}t/\hbar} \hat{U}(0)$ is the unitary time evolution operator. Left multiplying equation (1.49) by $\hat{\Theta}$, and using the fact $\hat{\Theta}^\dagger \hat{\Theta} = \mathbb{1}$; because the time reversal operator should be either unitary or anti-unitary operator

$$\hat{U}(t) \hat{\Theta} |\alpha\rangle = \hat{\Theta} \hat{U}(-t) |\alpha\rangle,$$

Expanding upto linear order in time

$$\begin{aligned} \left(1 - \frac{i\hat{H}\delta t}{\hbar}\right) |\alpha\rangle &\approx \hat{\Theta} \left(\frac{1 + i\hat{H}\delta t}{\hbar}\right) |\alpha\rangle, \\ -i\hat{H}\hat{\Theta} &= \hat{\Theta}i\hat{H}. \end{aligned}$$

If $\hat{\Theta}$ is an anti-unitary operator, its action on a complex number results in complex conjugation of that number: $\hat{\Theta}i = -i\hat{\Theta}$, putting in the above equation

$$\begin{aligned} \hat{H}\hat{\Theta} &= \hat{\Theta}\hat{H}, \\ \Rightarrow [\hat{H}, \hat{\Theta}] &= 0, \end{aligned}$$

time reversal symmetry exists if we define time reversal operator as anti-unitary [5].

Example 01:

In classical mechanics, if a system has TRS then $x(t) = x(-t)$, by using this classical intuition, we can write

$$\hat{\Theta} |x\rangle = |x\rangle,$$

$$\hat{x}|x\rangle = x|x\rangle, \quad (1.50)$$

$$\begin{aligned} \hat{\Theta}\hat{x}\hat{\Theta}^\dagger\hat{\Theta}|x\rangle &= x\hat{\Theta}|x\rangle, \\ \Rightarrow \hat{\Theta}\hat{x}\hat{\Theta}^\dagger|x\rangle &= x|x\rangle, \end{aligned} \quad (1.51)$$

comparing equation (1.51) with (1.50)

$$\boxed{\hat{\Theta}\hat{x}\hat{\Theta}^\dagger = \hat{x}.}$$

Example 02:

The momentum operator picks minus sign by time reversal operation

$$\hat{\Theta}\hat{p}\hat{\Theta}^\dagger = -\hat{p}.$$

Proof:

As we know

$$\begin{aligned} [\hat{x}, \hat{p}] &= i\hbar, \\ (\hat{x}\hat{p} - \hat{p}\hat{x}) &= i\hbar, \\ \hat{\Theta}(\hat{x}\hat{p} - \hat{p}\hat{x})\hat{\Theta}^\dagger &= \hat{\Theta}i\hbar\hat{\Theta}^\dagger, \\ \hat{\Theta}\hat{x}\hat{\Theta}^\dagger\hat{\Theta}\hat{p}\hat{\Theta}^\dagger - \hat{\Theta}\hat{p}\hat{\Theta}^\dagger\hat{\Theta}\hat{x}\hat{\Theta}^\dagger &= -i\hbar, \end{aligned}$$

using

$$\hat{\Theta}\hat{x}\hat{\Theta}^\dagger = \hat{x},$$

in the above equation

$$\begin{aligned} x\hat{\Theta}\hat{p}\hat{\Theta}^\dagger - \hat{\Theta}\hat{p}\hat{\Theta}^\dagger x &= -i\hbar, \\ [x, \hat{\Theta}\hat{p}\hat{\Theta}^\dagger] &= -i\hbar, \end{aligned}$$

If

$$\hat{\Theta}\hat{p}\hat{\Theta}^{-1} = -\hat{p},$$

then

$$[\hat{x}, \hat{p}] = i\hbar.$$

1.5.3 TRS of Schrödinger Equation

Let us consider evolution of a state of a spin-less quantum particle under a general Hamiltonian $\hat{H}(\hat{\mathbf{x}}, \hat{\mathbf{p}})$

$$i\hbar \frac{d}{dt} |\psi_s(t)\rangle = \hat{H}(\hat{\mathbf{x}}, \hat{\mathbf{p}}) |\psi_s(t)\rangle.$$

Acting with the time reversal operator on both sides of the above equation

$$\begin{aligned}
\hat{\Theta} i\hbar \hat{\Theta}^\dagger \hat{\Theta} \frac{d|\psi_s(t)\rangle}{dt} &= \hat{\Theta} \hat{H}(\hat{\mathbf{x}}, \hat{\mathbf{p}}) \hat{\Theta}^\dagger \hat{\Theta} |\psi_s(t)\rangle, \\
-i\hbar \frac{d|\hat{\Theta}\psi_s(t)\rangle}{dt} &= \hat{H}(\hat{\mathbf{x}}, -\hat{\mathbf{p}}) |\hat{\Theta}\psi_s(t)\rangle, \\
i\hbar \frac{d|\hat{\Theta}\psi_s(t)\rangle}{d(-t)} &= \hat{H}(\hat{\mathbf{x}}, -\hat{\mathbf{p}}) |\hat{\Theta}\psi_s(t)\rangle,
\end{aligned} \tag{1.52}$$

if

$$\hat{H}(\hat{\mathbf{x}}, -\hat{\mathbf{p}}) = \hat{H}(\hat{\mathbf{x}}, \hat{\mathbf{p}}),$$

then the Schrödinger Equation is time reversal invariant [6]. What will be the form of time reversed wave functions in position representation?, to see this, taking inner product with $\langle \mathbf{x} |$ on the both sides of above equation (1.52)

$$i\hbar \frac{d\langle \mathbf{x} | \hat{\Theta}\psi_s(t)\rangle}{d(-t)} = \hat{H}(\hat{\mathbf{x}}, -\hat{\mathbf{p}}) \langle \mathbf{x} | \hat{\Theta}\psi_s(t)\rangle, \tag{1.53}$$

consider expansion

$$|\psi_s(t)\rangle = \int d\mathbf{x} |\mathbf{x}\rangle \langle \mathbf{x} | \psi_s(t)\rangle,$$

let

$$\langle \mathbf{x} | \psi_s(t)\rangle \equiv \psi_s(\mathbf{x}, t),$$

putting in the expansion

$$|\psi_s(t)\rangle = \int d\mathbf{x} \psi_s(\mathbf{x}) |\mathbf{x}\rangle,$$

operation time reversal operator on both sides

$$\begin{aligned}
\hat{\Theta} |\psi_s(t)\rangle &= \int d\mathbf{x} \hat{\Theta} \psi_s(\mathbf{x}, t) \hat{\Theta}^\dagger \hat{\Theta} |\mathbf{x}\rangle, \\
\hat{\Theta} |\psi_s(t)\rangle &= \int d\mathbf{x} \hat{\Theta} \psi_s(\mathbf{x}, t) \hat{\Theta}^\dagger |\mathbf{x}\rangle,
\end{aligned}$$

$\psi(\mathbf{x}, t)$ is a complex function, and when anti-unitary operator operates on it, as a result, it gets conjugated, so the above equation becomes

$$\hat{\Theta} |\psi_s(t)\rangle = \int d\mathbf{x} \psi_s^*(\mathbf{x}, t) |\mathbf{x}\rangle,$$

taking inner product with $\langle \mathbf{x}' |$ on the both sides of the above equation

$$\begin{aligned}\langle \mathbf{x}' | \hat{\Theta} \psi_s(t) \rangle &= \int d\mathbf{x} \psi_s^*(\mathbf{x}, t) \langle \mathbf{x}' | \mathbf{x} \rangle, \\ \langle \mathbf{x}' | \hat{\Theta} \psi_s(t) \rangle &= \int d\mathbf{x} \psi_s^*(\mathbf{x}, t) \delta(\mathbf{x} - \mathbf{x}'), \\ \Rightarrow \langle \mathbf{x} | \hat{\Theta} \psi_s(t) \rangle &= \psi_s^*(\mathbf{x}, t),\end{aligned}$$

for this case time-reversal operator acts like conjugation operator \hat{K} . Substituting this result in equation (1.53)

$$i\hbar \frac{\partial \psi_s^*(\mathbf{x})}{\partial(-t)} = \hat{H}(\hat{\mathbf{x}}, -\hat{\mathbf{p}}) \psi_s^*(\mathbf{x}, t),$$

if

$$\hat{H}(\hat{\mathbf{x}}, -\hat{\mathbf{p}}) = \hat{H}(\hat{\mathbf{x}}, \hat{\mathbf{p}}),$$

then $\psi_s^*(\mathbf{x}, t)$ is a solution of the time reversed Schrödinger Equation. Let us check the Hamiltonian of a charged particle in magnetic field

$$\hat{H}(\hat{\mathbf{x}}, \hat{\mathbf{p}}) = \frac{(\hat{\mathbf{p}} + q\mathbf{A})^2}{2m} + V(\hat{\mathbf{x}}), \quad (1.54)$$

for this case,

$$\hat{H}(\hat{\mathbf{x}}, -\hat{\mathbf{p}}) \neq \hat{H}(\hat{\mathbf{x}}, \hat{\mathbf{p}}),$$

so, TRS is broken for this case. Furthermore, above discussion is valid only for the case of spin-less particles, and for particles having spin, we need to modify the definition of time reversal operator.

For a particle having non-zero spin, TR operator is defined in $|\mathbf{x}, \sigma_z\rangle$ basis as [6]

$$\hat{\Theta} = i\sigma_y \hat{K}. \quad (1.55)$$

1.5.4 Kramers Degeneracy

In general, if a particle has an integer spin then applying the TR operator twice gives $\hat{\Theta}^2 = \mathbb{1}$. However, if a particle has half integer spin then $\hat{\Theta}^2 = -\mathbb{1}$. This fact $\hat{\Theta}^2 = -\mathbb{1}$ leads to the existence of the Kramers Degeneracy [6]. It states that when a system has TRS having a half integer spin, there exist [at](#) least two states which have same energy, and also the states are mutually orthogonal.

Proof:

Since due to time reversal symmetry $\hat{H}\hat{\Theta} = \hat{\Theta}\hat{H}$, let $|\phi\rangle$ be an eigenstate of

the Hamiltonian with energy E

$$\begin{aligned}
\hat{H}|\phi\rangle &= E|\phi\rangle, \\
\hat{H}|\hat{\Theta}\phi\rangle &= \hat{H}\hat{\Theta}|\phi\rangle, \\
&= \hat{\Theta}\hat{H}|\phi\rangle, \\
\hat{H}|\hat{\Theta}\phi\rangle &= E|\hat{\Theta}\phi\rangle,
\end{aligned} \tag{1.56}$$

so, $|\phi\rangle$ and $|\hat{\Theta}\phi\rangle$ states are degenerate having same energy E. Also,

$$\begin{aligned}
\langle\phi|\hat{\Theta}\phi\rangle &= \langle\hat{\Theta}(\hat{\Theta}\phi)|\phi\rangle, \\
&= \langle\hat{\Theta}^2\phi|\phi\rangle, \\
\langle\phi|\hat{\Theta}\phi\rangle &= -\langle\phi|\phi\rangle,
\end{aligned} \tag{1.57}$$

$$\Rightarrow \boxed{\langle\phi|\hat{\Theta}\phi\rangle = 0.} \tag{1.58}$$

Equation (1.58) shows that $|\phi\rangle$ and $|\hat{\Theta}\phi\rangle$ states are orthogonal to each other. The definition of time reversal operator $\hat{\Theta} = i\sigma_y\hat{K}$ and its consequence like Kramers degeneracy is valid for systems having real spins. However, for the systems having only pseudo spins, the time reversal operator is simply $\hat{\Theta} = \hat{K}$.

1.5.5 Symmetry Restrictions on Berry Phase

If crystal has inversion symmetry then

$$|\phi_j(\mathbf{x}, \mathbf{k})\rangle \rightarrow |\phi_j(-\mathbf{x}, -\mathbf{k})\rangle = |\phi_j(\mathbf{x}, \mathbf{k})\rangle,$$

Berry connection of the jth band implies

$$\begin{aligned}
\mathbf{A}_j(\mathbf{k}) &= i\langle\phi_j(\mathbf{x}, \mathbf{k})|\nabla_{\mathbf{k}}|\phi_j(\mathbf{x}, \mathbf{k})\rangle, \\
&= -i\langle\phi_j(-\mathbf{x}, -\mathbf{k})|\nabla_{-\mathbf{k}}|\phi_j(-\mathbf{x}, -\mathbf{k})\rangle, \\
&= -\mathbf{A}_j(-\mathbf{k}),
\end{aligned}$$

Berry curvature for the jth band becomes

$$\begin{aligned}
\mathbf{F}_j(\mathbf{k}) &= \nabla_{\mathbf{k}} \times \mathbf{A}_j(\mathbf{k}), \\
&= \nabla_{-\mathbf{k}} \times \mathbf{A}_j(-\mathbf{k}), \\
\Rightarrow \mathbf{F}_j(\mathbf{k}) &= \mathbf{F}_j(-\mathbf{k}).
\end{aligned} \tag{1.59}$$

However, if the system also has time reversal symmetry, then

$$\hat{\Theta}^\dagger |\phi_j(\mathbf{x}, \mathbf{k})\rangle \hat{\Theta} \rightarrow |\phi_j^*(\mathbf{x}, -\mathbf{k})\rangle = |\phi_j(\mathbf{x}, \mathbf{k})\rangle,$$

and Berry connection implies

$$\begin{aligned} \hat{\Theta}^\dagger \mathbf{A}_j(\mathbf{k}) \hat{\Theta} &= \hat{\Theta}^\dagger [i \langle \phi_j(\mathbf{x}, \mathbf{k}) | \nabla_{\mathbf{k}} | \phi_j(\mathbf{x}, \mathbf{k}) \rangle] \hat{\Theta}, \\ \mathbf{A}_j(-\mathbf{k}) &= -i \langle \phi_j(\mathbf{x}, -\mathbf{k}) | \nabla_{-\mathbf{k}} | \phi_j(\mathbf{x}, -\mathbf{k}) \rangle, \\ &= i \langle \phi_j(\mathbf{x}, \mathbf{k}) | \nabla_{\mathbf{k}} | \phi_j(\mathbf{x}, \mathbf{k}) \rangle, \\ &= \mathbf{A}_j(\mathbf{k}), \end{aligned}$$

and Berry connection becomes

$$\begin{aligned} \hat{\Theta}^\dagger \mathbf{F}_j(\mathbf{k}) \hat{\Theta} &= \hat{\Theta}^\dagger [\nabla_{\mathbf{k}} \times \mathbf{A}_j(\mathbf{k})] \hat{\Theta}, \\ \mathbf{F}_j(-\mathbf{k}) &= \nabla_{-\mathbf{k}} \times \mathbf{A}_j(-\mathbf{k}), \\ &= -\nabla_{\mathbf{k}} \times \mathbf{A}_j(\mathbf{k}) \\ \Rightarrow \mathbf{F}_j(-\mathbf{k}) &= -\mathbf{F}_j(\mathbf{k}). \end{aligned} \tag{1.60}$$

From equation (1.59) and (1.60), it implies that, if a system has both space inversion symmetry and time reversal symmetry, Berry curvature is equal to zero for all values of \mathbf{k} . If we only break the space inversion symmetry, we get non-zero Berry curvature. However, the integration over 2D Brillouin zone

$$\frac{1}{2\pi} \int_{BZ} \mathbf{F}_j(\mathbf{k}) \cdot d^2\mathbf{k} = C_j,$$

is called Chern number of the j th band, is still zero. Because due to TRS symmetry,

$$\mathbf{F}_j(-\mathbf{k}) = -\mathbf{F}_j(\mathbf{k}), \quad \Rightarrow C_j = 0.$$

However, if we break the time reversal symmetry of a Hamiltonian, C_j is always an integer [6].

Chapter 2

Su-Schrieffer-Heeger (SSH) Model

In this chapter, I discuss the SSH model, a 1D topological model. The salient features of topological insulators are that gapless states exist at the interface of two distinct topological phases, the existence of topological invariants, and fractionalization of electric charges. The SSH model manifests these features of a topological insulator. The topological invariant for this 1D case is the winding number, which plays the same role as the Chern number in 2D does. The winding number is the number of times \mathbf{d} wraps around the origin in d_x and d_y plane. We can distinguish different topological phases by the winding number. Also, due to the quantization of the winding number, we get quantized physical observables like electric polarization.

2.1 Polarization In 1D

At an elementary level, the electric polarization is defined as dipole moment in a unit volume. Due to this polarization, there is bulk and surface charge on an insulator. However, in 1D, polarization is equal to the end charge. For a 1D band structure, polarization is related with Berry phase of the occupied Bloch wave-functions around the 1D Brillouin zone,

$$P = \frac{e}{2\pi} \sum_n \oint_{BZ} A_n(k) dk. \quad (2.1)$$

Where

$$A_n(k) = i \langle \phi_n(x, k) | \partial_k \phi_n(x, k) \rangle, \quad (2.2)$$

and sum is over all occupied bands.

Proof:

We introduce Wannier functions: which are superposition of Bloch states, and these functions are normalizable,

$$\begin{aligned} |w_n(x - R_\alpha)\rangle &= \frac{\sqrt{NL}}{2\pi} \int_{BZ} dk e^{ik(x-R_\alpha)} |\phi_n(x, k)\rangle, \\ |\phi_n(x, k)\rangle &= \frac{1}{\sqrt{N}} \sum_\alpha e^{ik(x-R_\alpha)} |w_n(x - R_\alpha)\rangle, \end{aligned}$$

putting in equation (2.2),

$$\begin{aligned} A_n(k) &= \frac{i}{N} \sum_\alpha \sum_{\alpha'} \left\langle w_n(x - R_{\alpha'}) e^{ik(x-R_{\alpha'})} \left| \partial_k e^{ik(x-R_\alpha)} w_n(x - R_\alpha) \right\rangle, \\ &= \frac{i}{N} \sum_\alpha \sum_{\alpha'} \int dx e^{-ik(x-R_{\alpha'})} e^{ik(x-R_\alpha)} i(x - R_\alpha) w_n^*(x - R_{\alpha'}) w_n(x - R_\alpha), \\ &= \frac{i}{N} \sum_\alpha \sum_{\alpha'} \int dx e^{ik(R_{\alpha'}-R_\alpha)} i(x - R_\alpha) w_n^*(x - R_{\alpha'}) w_n(x - R_\alpha), \end{aligned}$$

putting in equation (2.1),

$$\begin{aligned} P &= \frac{e}{2\pi} \sum_n \oint_{BZ} dk \int dx \frac{i}{N} \sum_\alpha \sum_{\alpha'} \int dx e^{ik(R_{\alpha'}-R_\alpha)} i(x - R_\alpha) w_n^*(x - R_{\alpha'}) w_n(x - R_\alpha), \\ &= -\frac{e}{2\pi N} \sum_n \sum_\alpha \sum_{\alpha'} \int dx (x - R_\alpha) \left(\oint_{BZ} dk e^{ik(R_{\alpha'}-R_\alpha)} \right) w_n^*(x - R_{\alpha'}) w_n(x - R_\alpha), \end{aligned}$$

using,

$$\oint_{BZ} dk e^{ik(R_{\alpha'}-R_\alpha)} = \frac{2\pi}{a} \delta_{\alpha, \alpha'},$$

where a is length of the unit cell in 1D,

$$\begin{aligned} P &= -\frac{e}{2\pi Na} \sum_n \sum_\alpha \sum_{\alpha'} \int dx (x - R_\alpha) (2\pi \delta_{\alpha, \alpha'}) w_n^*(x - R_{\alpha'}) w_n(x - R_\alpha), \\ &= -\frac{e}{Na} \sum_n \sum_\alpha \int dx (x - R_\alpha) |w_n(x - R_\alpha)|^2, \\ &= -\frac{e}{L} \sum_n \int dx (x |w_n(x)|^2), \end{aligned}$$

where $L=Na$ is the length of the chain in 1D. The above equation is dipole moment per unit length, which is equal to polarization in 1D. The quantity $1/\pi \oint_{BZ} A_n(k) dk$ in equation (2.1) is the winding number. The goal of the next discussion is to introduce the SSH model, and by calculating the winding number, we will be able to calculate the polarization.

2.2 The SSH Model

The SSH model was developed as a basis for conducting poly-acetylene, which is subjected to a staggering of the hopping amplitude at half-filling. The staggering of the hopping amplitude stems naturally in many solid state systems known as Peierls instability. Due to the staggering, a band gap opens between two bands and the energy of the valence band is lowered. Thus, the staggering is energetically more propitious. Poly-acetylene has alternating single and double bonds, as shown in figure 2.1. It forms another staggered state, which is topologically distinct from the first if we interchange the position of the double bonds with the single bond, and considering that double bond has a larger hopping amplitude than single bond. If we change the staggering continuously, then we reach a critical point where band gap closes and further change in staggering causes again band gap opening. Such two topological phases are distinct in a way that: in one phase, the winding number is equal to one, but in another phase, it is equal to zero. As a result, 1D polarization is non-zero and quantized in one phase, but in the other phase it is equal to zero. Chiral symmetry plays a crucial role, forcing $d_z = 0$.

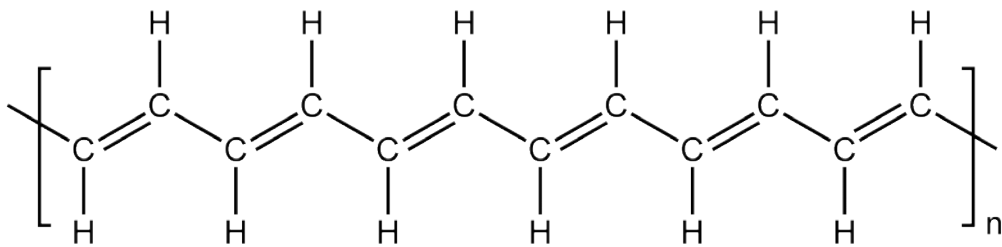


Figure 2.1: The polyacetylene chain has alternating single and double bonds that can be modelled with different hopping parameters for single and double bonds.

- Tight-binding Hamiltonian

A tight-binding Hamiltonian for hopping of spinless electrons on a one dimensional chain with staggered hopping amplitude can be written as,

$$\hat{H} = \sum_j \left[(t + \delta t) \hat{c}_{1j}^\dagger \hat{c}_{2j} + (t - \delta t) \hat{c}_{1j+1}^\dagger \hat{c}_{2j} + h.c \right], \quad (2.3)$$

here we arbitrarily defined a unit cell having length a with two atoms labelled by 1 and 2 with $\hat{c}_{1j}, \hat{c}_{2j}$ and $\hat{c}_{1j}^\dagger, \hat{c}_{2j}^\dagger$ are annihilation and creation operators at site 1 and 2 respectively. The staggering is defined by δt , and it acts as

band-gap parameter. By using Fourier transformation

$$\begin{aligned}\hat{c}_{1j} &= \frac{1}{\sqrt{N}} \sum_k e^{ikx_j} \hat{c}_{1k}, & \hat{c}_{2j} &= \frac{1}{\sqrt{N}} \sum_k e^{ikx_j} \hat{c}_{2k}, \\ \hat{c}_{1j}^\dagger &= \frac{1}{\sqrt{N}} \sum_k e^{-ikx_j} \hat{c}_{1k}^\dagger, & \hat{c}_{2j}^\dagger &= \frac{1}{\sqrt{N}} \sum_k e^{-ikx_j} \hat{c}_{2k}^\dagger,\end{aligned}$$

putting these expressions in equation (2.3)

$$\begin{aligned}\hat{H} &= \frac{1}{N} \sum_j \sum_k \sum_{k'} \left[(t + \delta t) e^{i(k'-k)x_j} \hat{c}_{1k}^\dagger \hat{c}_{2k'} + h.c. \right], \\ &\quad + \frac{1}{N} \sum_j \sum_k \sum_{k'} \left[(t - \delta t) e^{i(k'-k-a)x_j} \hat{c}_{1k}^\dagger \hat{c}_{2k'} + h.c. \right], \\ \hat{H} &= \frac{1}{N} \sum_k \sum_{k'} \left[(t + \delta t) \left(\sum_j e^{i(k'-k)x_j} \right) \hat{c}_{1k}^\dagger \hat{c}_{2k'} + h.c. \right], \\ &\quad + \frac{1}{N} \sum_k \sum_{k'} \left[(t - \delta t) e^{-ika} \left(\sum_j e^{i(k'-k)x_j} \right) \hat{c}_{1k}^\dagger \hat{c}_{2k'} + h.c. \right],\end{aligned}$$

using

$$\sum_j e^{i(k'-k)x_j} = N \delta_{k,k'},$$

$$\begin{aligned}\hat{H} &= \frac{1}{N} \sum_k \sum_{k'} \left[(t + \delta t) (N \delta_{k,k'}) \hat{c}_{1k}^\dagger \hat{c}_{2k'} + h.c. \right] \\ &\quad + \frac{1}{N} \sum_k \sum_{k'} \left[(t - \delta t) e^{-ika} (N \delta_{k,k'}) \hat{c}_{1k}^\dagger \hat{c}_{2k'} + h.c. \right], \\ \hat{H} &= \sum_k \left[(t + \delta t) \hat{c}_{1k}^\dagger \hat{c}_{2k} + h.c. \right] + \sum_k \left[(t - \delta t) e^{-ika} \hat{c}_{1k}^\dagger \hat{c}_{2k} + h.c. \right],\end{aligned}$$

finally, the Hamiltonian becomes

$$\begin{aligned}\hat{H} &= \sum_k \left[(t + \delta t) \hat{c}_{1k}^\dagger \hat{c}_{2k} + (t + \delta t) \hat{c}_{2k}^\dagger \hat{c}_{1k} \right] \\ &\quad + \left[(t - \delta t) e^{-ika} \hat{c}_{1k}^\dagger \hat{c}_{2k} + (t - \delta t) e^{ika} \hat{c}_{2k}^\dagger \hat{c}_{1k} \right], \\ \hat{H} &= \sum_k \left[(t + \delta t) + (t - \delta t) e^{-ika} \right] \hat{c}_{1k}^\dagger \hat{c}_{2k} \\ &\quad + \left[(t + \delta t) + (t - \delta t) e^{ika} \right] \hat{c}_{2k}^\dagger \hat{c}_{1k},\end{aligned}$$

above equation can be written as

$$\hat{H} = \sum_k \begin{pmatrix} \hat{c}_{1k}^\dagger & \hat{c}_{2k}^\dagger \end{pmatrix} \begin{pmatrix} 0 & (t + \delta t) + (t - \delta t)e^{-ika} \\ (t + \delta t) + (t - \delta t)e^{ika} & 0 \end{pmatrix} \begin{pmatrix} \hat{c}_{1k} \\ \hat{c}_{2k} \end{pmatrix},$$

where

$$H(k) = \begin{pmatrix} 0 & (t + \delta t) + (t - \delta t)e^{-ika} \\ (t + \delta t) + (t - \delta t)e^{ika} & 0 \end{pmatrix}, \quad (2.4)$$

by using Euler's identity $e^{ika} = \cos ka + i \sin ka$ in equation (2.4)

$$H(k) = \begin{pmatrix} 0 & (t + \delta t) + (t - \delta t) \cos ka \\ (t + \delta t) + (t - \delta t) \cos ka & -i(t - \delta t) \sin ka \\ + i(t - \delta t) \sin ka & 0 \end{pmatrix},$$

$$H(k) = (t + \delta t) + (t - \delta t) \cos ka \begin{pmatrix} 0 & 1 \\ 1 & 0 \end{pmatrix} + (t - \delta t) \sin ka \begin{pmatrix} 0 & -i \\ i & 0 \end{pmatrix},$$

$$H(k) = [(t + \delta t) + (t - \delta t) \cos ka] \sigma_x + [(t - \delta t) \sin ka] \sigma_y$$

where

$$d_x(k) = (t + \delta t) + (t - \delta t) \cos ka, \quad d_y(k) = (t - \delta t) \sin ka, \quad d_z = 0,$$

and

$$\sigma_x = \begin{pmatrix} 0 & 1 \\ 1 & 0 \end{pmatrix}, \quad \sigma_y = \begin{pmatrix} 0 & -i \\ i & 0 \end{pmatrix},$$

are the Pauli matrices in pseudo-spin basis. $H(k)$ can be written in the following form

$$\boxed{H(k) = \mathbf{d} \cdot \boldsymbol{\sigma}} \quad (2.5)$$

Let

$$t_1 \equiv t + \delta t, \quad t_2 \equiv t - \delta t,$$

then

$$d_x(k) = t_1 + t_2 \cos(ka), \quad d_y(k) = t_2 \sin(ka), \quad d_z = 0.$$

- Energy Spectrum:

$$E(k) = \pm \sqrt{\mathbf{d} \cdot \mathbf{d}},$$

$$= \pm \sqrt{(t_1 + t_2 \cos(ka))^2 + (t_2 \sin(ka))^2}$$

$$\Rightarrow E(k) = \pm \sqrt{t_1^2 + t_2^2 + 2t_1 t_2 \cos(ka)}. \quad (2.6)$$

Case 01:

When $\delta t > 0$ then from equation (2.6) we can write,

$$\begin{aligned}
 E(k) &= \pm \sqrt{t_1^2 + t_2^2 - 2t_1t_2 + 2t_1t_2 \cos(ka) + 2t_1t_2}, \\
 &= \pm \sqrt{(t_1 - t_2)^2 + 2t_1t_2(1 + \cos(ka))}, \\
 E(k) &= \pm \sqrt{(2\delta t)^2 + 4t_1t_2 \cos^2\left(\frac{ka}{2}\right)}, \tag{2.7}
 \end{aligned}$$

there is a band gap at the end of BZ, as shown in figure (2.2).

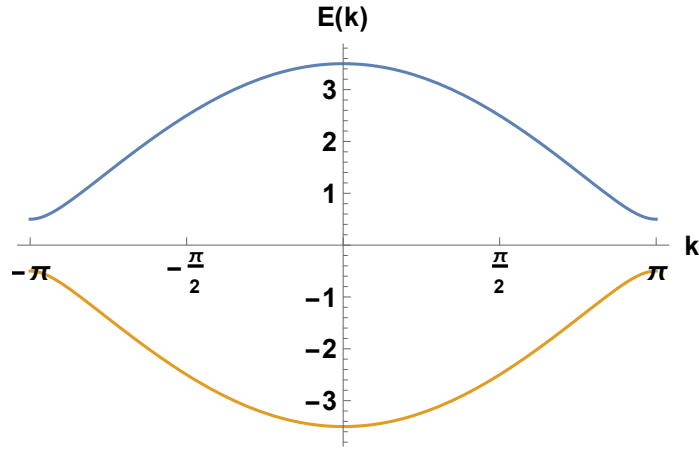


Figure 2.2: The plot of equation (2.7) when: $a = 1, t_1 = 2, t_2 = 1.5$.

For $\delta t > 0$, $d_x(k)$ is positive for all values of k , so $\hat{d}(k)$ does not sweep out any solid angle, as shown in figure (2.3), by using general result (1.32), the winding number is equal to zero for this case

$$\begin{aligned}
 \gamma &= \frac{1}{2}(\text{Solid angle swept by } \hat{d}(k)), \\
 &= 0, \\
 \Rightarrow P &= 0.
 \end{aligned}$$

Case 02:

When

$$\delta t = 0, \quad \Rightarrow t_1 = t_2 = t,$$

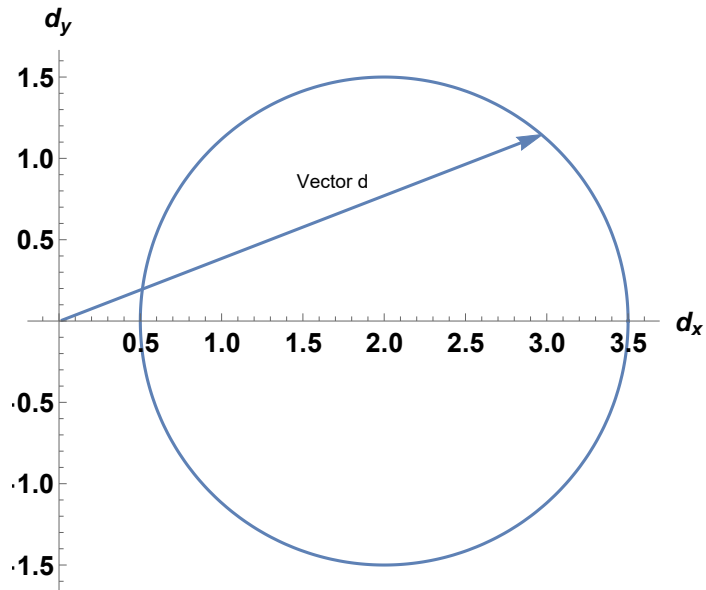


Figure 2.3: Parametric plot of $d_x(k), d_y(k)$: $a = 1, t_1 = 2, t_2 = 1.5$.

equation (2.7) implies

$$\begin{aligned}
 E(k) &= \pm \sqrt{t^2 + t^2 + 2t^2 \cos(ka)}, \\
 &= \pm \sqrt{2t^2 + 2t^2 \cos(ka)}, \\
 E(k) &= \pm 2t \left| \cos\left(\frac{ka}{2}\right) \right|, \tag{2.8}
 \end{aligned}$$

band gap closes at the end of BZ, as shown in figure 2.4, this point

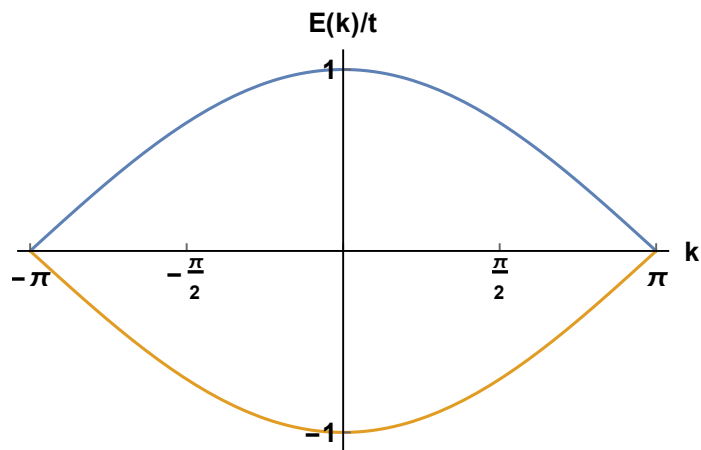


Figure 2.4: Plot of equation (2.8), taking $a=1$.

is quantum phase transition point. Plot of $d_x(k)$ shows that it passes

through the origin, as shown in figure 2.5,

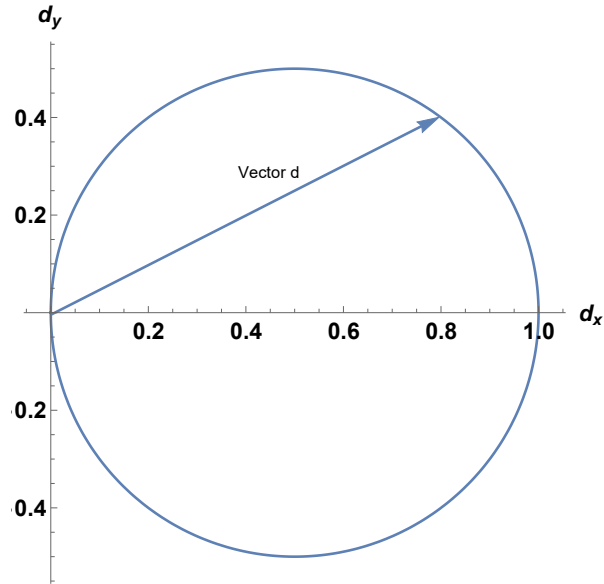


Figure 2.5: Parametric plot of $d_x(k), d_y(k)$: $a = 1, t_1 = 1, t_2 = 1$.

Case 03:

When $\delta t < 0$, band gap, which is equal to $|4\delta t|$, opens again at the end of the BZ, as shown in figure 2.6, but in this case $d_x(k)$ has both

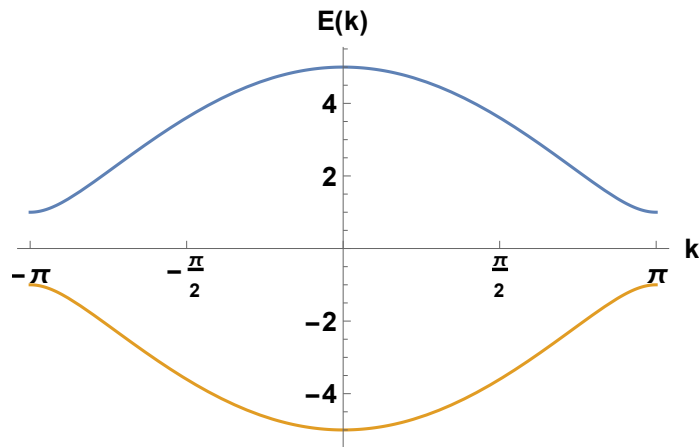


Figure 2.6: Plot of equation (2.7): $a = 1, t_1 = 2, t_2 = 3$.

positive and negative values, so that $\hat{d}(k)$ rotates by an angle of 2π , as shown in the figure (2.7),

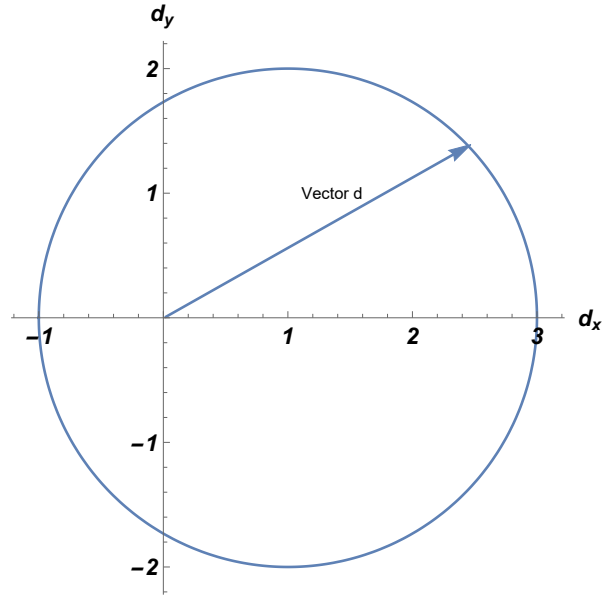


Figure 2.7: Parametric plot of $d_x(k), d_y(k)$: $a = 1, t_1 = 2, t_2 = 3$.

consequently,

$$\begin{aligned}\gamma &= \frac{1}{2}(\text{Solid angle swept by } \hat{d}(k)), \\ &= \frac{1}{2}(2\pi), \\ \Rightarrow P &= \frac{e}{2}.\end{aligned}$$

- Symmetry:

Only when $d_z = 0$, there exists the sharp distinction between two phases because of quantization of the winding number. If $d_z \neq 0$ polarization varies from $\delta t < 0$ to $\delta t > 0$ continuously.

The condition $d_z = 0$ is protected by chiral symmetry. If

$$\sigma_z \hat{H} \sigma_z = -\hat{H},$$

then chiral symmetry exists. Let us check the chiral symmetry of the SSH model,

$$\begin{aligned}\sigma_z \hat{H} \sigma_z &= \sigma_z (d_x \sigma_x + d_y \sigma_y) \sigma_z, \\ &= \sigma_z d_x (\sigma_x \sigma_z) + d_y (\sigma_y \sigma_z),\end{aligned}\tag{2.9}$$

by using the following property of Pauli matrices,

$$\{\sigma_x, \sigma_z\} = 0, \quad \Rightarrow \sigma_x \sigma_z = -\sigma_z \sigma_x,$$

$$\begin{aligned}
\{\sigma_y, \sigma_z\} &= 0, & \Rightarrow \sigma_y \sigma_z &= -\sigma_z \sigma_y, \\
\sigma_z \hat{H} \sigma_z &= \sigma_z d_x (-\sigma_z \sigma_x) + \sigma_z d_y (-\sigma_z \sigma_y), \\
&= -(\sigma_z \sigma_z) d_x \sigma_x - (\sigma_z \sigma_z) d_y \sigma_y, \\
&= -(\mathbb{1}) d_x \sigma_x - (\mathbb{1}) d_y \sigma_y, \\
\Rightarrow \sigma_z \hat{H} \sigma_z &= -\hat{H}.
\end{aligned}$$

This shows that the SSH model has chiral symmetry. Chiral symmetry leads to particle-hole symmetry.

2.2.1 Domain Wall States and the J-Rebba Model

The interface between polyacetylene's two ground states results in a soliton state with a $\pm e/2$ polarization on the boundary. In the presence of such a domain wall, the system has a zero-energy mid-gap state. This state is protected in a way that, without closing the bulk energy gap, it is impossible to get rid of it. The fact that it is on the interface of topologically distinct states can be traced back to its creation. J-Rebba first found these topological zero modes in the 1D field theory. The SSH model presents the J-Rebba modes with its functional understanding. Let $|\delta t| \ll t$ and $k = \frac{\pi}{a} + q$, $|q| \ll \frac{\pi}{a}$. We

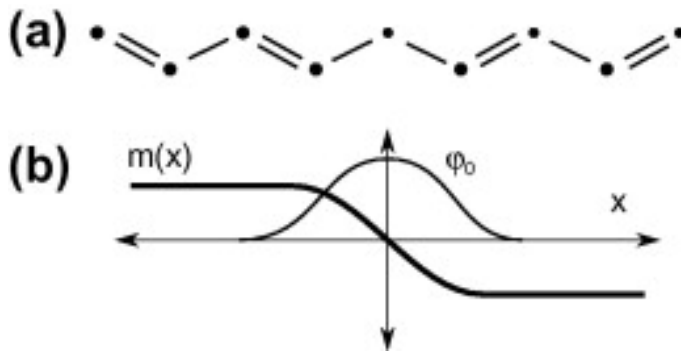


Figure 2.8: (a) An interface of the two distinct topological ground states in the SSH model. (b) A normalizable state at the interface.

can expand d_x and d_y about $\frac{\pi}{a}$,

$$\begin{aligned}
d_x(k) &= (t + \delta t) + (t - \delta t) \cos a\left(\frac{\pi}{a} + q\right), & d_y(k) &= (t - \delta t) \sin a\left(\frac{\pi}{a} + q\right), \\
d_x(k) &= (t + \delta t) + (t - \delta t) \cos(\pi + qa), & d_y(k) &= (t - \delta t) \sin(\pi + qa),
\end{aligned}$$

expanding cosine and sine terms, we get

$$\begin{aligned} d_x(k) &= (t + \delta t) + (t - \delta t) \cos(\pi + qa), & d_y &= (t - \delta t) \sin(\pi + qa), \\ d_x &\approx (t + \delta t) + (t - \delta t)(-1), & d_y &\approx (t - \delta t)(-qa), \\ d_x &\approx \delta t = m, & d_y &\approx -atq = vq, \end{aligned}$$

as a result, the Hamiltonian (2.5) becomes

$$H_{eff} \approx \sigma_x m + \sigma_y vq, \quad (2.10)$$

replacing $q \rightarrow -i \frac{\partial}{\partial x}$ in the above equation, and allowing m to vary spatially such that m changes sign about origin as show in figure (2.8b)

$$H_{eff} \approx \sigma_x m(x) + \sigma_y v(-i \frac{\partial}{\partial x}). \quad (2.11)$$

Equation (2.11) is a massive Dirac Hamiltonian having dispersion relation $E(q) = \pm \sqrt{v^2 q^2 + m^2}$. The given Hamiltonian has zero energy modes at the domain wall called J-Rabbi zero mode.

$$H_{eff} |\psi\rangle = 0,$$

where

$$H_{eff} = \begin{pmatrix} 0 & m - v \frac{\partial}{\partial x} \\ m + v \frac{\partial}{\partial x} & 0 \end{pmatrix}, \quad |\psi_1\rangle = \begin{pmatrix} 0 \\ \phi_0 \end{pmatrix}, \quad |\psi_2\rangle = \begin{pmatrix} 1 \\ 0 \end{pmatrix},$$

for 1st solution

$$\begin{aligned} H_{eff} |\psi_1\rangle &= 0, \\ \begin{pmatrix} 0 & m(x) - v \frac{\partial}{\partial x} \\ m(x) + v \frac{\partial}{\partial x} & 0 \end{pmatrix} \begin{pmatrix} 0 \\ \phi_0 \end{pmatrix} &= 0, \\ \Rightarrow (m - v \frac{\partial}{\partial x}) \chi &= 0, \end{aligned} \quad (2.12)$$

solution of the above equation is

$$\phi_0 = A e^{1/v \int_0^x m(x') dx'}. \quad (2.13)$$

ϕ_0 is normalizable if m varies spatially and there is a kink about the origin. This zero mode is topological because it does not depend on the precise form of $m(x')$. It depends only on the change of sign.

Chapter 3

Haldane Model

This model is an example of a topological insulator that goes beyond the integer quantum Hall effect. It reveals that a topological insulator is a general concept, and it can arise in any insulating system. It also demonstrates that as long as the topological index, the Chern number is non-zero, we observe all topological phenomena expected for the integer quantum Hall effect; for example, quantization of the Hall conductivity and existence of dissipation-less edge states.

Haldane model is a two-dimensional model lattice model that reveals quantization of the Hall conductivity in a zero magnetic field. In the usual quantum Hall effect, the gap at Fermi level arises because of the splitting of spectrum into Landau levels by the external magnetic field. However, this model involves a two-dimensional honeycomb lattice on which electrons have gapless linear dispersion relation at the end of the Brillouin zone (graphene spectrum). The gapless spectrum is protected by the following symmetries: inversion symmetry and time-reversal symmetry. If we break inversion symmetry, the system becomes a trivial insulator, but if we break the time reversal symmetry, the system behaves like integer quantum Hall system with Hall conductivity $\sigma_{xy} = \pm e^2/h$. However, if both symmetries are broken, they compete with each and their relative strength decides the state.

Between the Haldane model and the conventional quantum Hall system, there are two major differences.

- The net B field in the Haldane model is zero while the quantum Hall effect has a uniform B field.
- There is a strong lattice background in the Haldane Model; however, quantum Hall effect requires a weak lattice potential.

3.1 Model Hamiltonian

In this model, we consider honeycomb lattice having two sub-lattices, A and B, as shown in figure 3.1. We take real nearest hopping amplitude t_1 because it encloses zero net magnetic flux, but second nearest neighbours hopping is complex because it encloses non-zero magnetic flux. The complex hopping amplitude $t_2 e^{i\phi}$, where $e^{i\phi}$ is called the Ananabov phase, is responsible for breaking the time-reversal symmetry. We

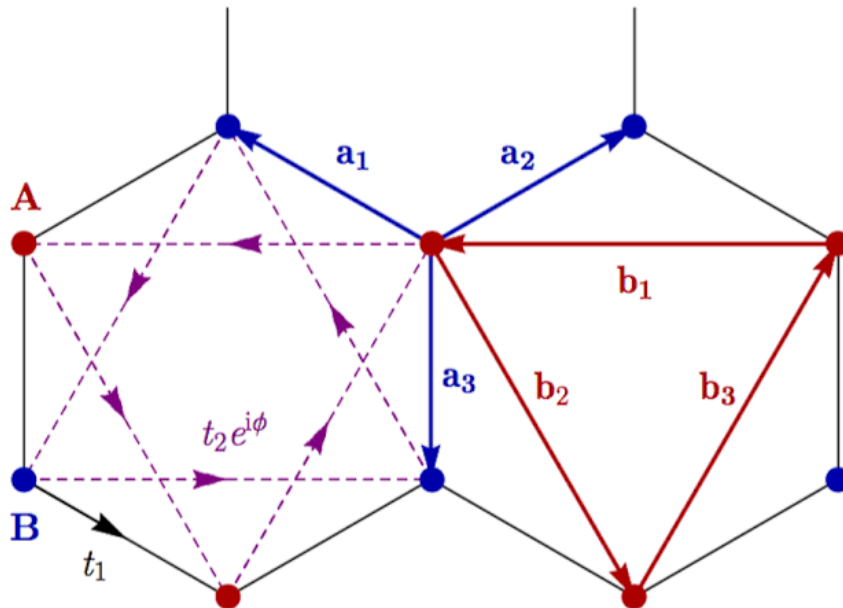


Figure 3.1: The honeycomb lattice with complex second hopping amplitudes. The arrows connecting lattice site A and B shows the direction of time: both have opposite arrows.

break the inversion symmetry by introducing on-site energy $+M$ for the lattice A and $-M$ for the lattice B. Including all these ingredients; the tight-binding Hamiltonian can be written as

$$\begin{aligned} \hat{H} = & -t_1 \sum_{\langle ij \rangle} (\hat{a}_i^\dagger \hat{b}_j + h.c) - t_2 \sum_{\langle\langle ij \rangle\rangle} (e^{i\phi} \hat{a}_i^\dagger \hat{a}_j + h.c) \\ & - t_2 \sum_{\langle\langle ij \rangle\rangle} (e^{-i\phi} \hat{b}_i^\dagger \hat{b}_j + h.c) + M \sum_i \hat{a}_i^\dagger \hat{a}_i - \sum_i \hat{b}_i^\dagger \hat{b}_i. \end{aligned} \quad (3.1)$$

Where \hat{a}_i^\dagger and \hat{b}_i^\dagger are creation operators, \hat{a}_j and \hat{b}_j are annihilation operators on lattice A and B at site i and j respectively, $\langle .. \rangle$ represents nearest neighbours hopping and $\langle\langle .. \rangle\rangle$ next nearest hopping in the lattice. The first term in the Hamiltonian represents

nearest hopping, the second term shows second nearest hopping along the arrows connecting lattice A sites, the third term includes second nearest hopping along the reversed arrows connecting B sites, the second last term is on-site energy M at A, and the last term is on-site energy $-M$ at site B.

We can diagonalize this Hamiltonian by transforming it into momentum space. By using the following Fourier transformation

$$\begin{aligned}\hat{a}_i &= \frac{1}{\sqrt{N/2}} \sum_{\mathbf{k}} e^{-i\mathbf{k}\cdot\mathbf{x}_i} \hat{a}_{\mathbf{k}}, & \hat{b}_i &= \frac{1}{\sqrt{N/2}} \sum_{\mathbf{k}} e^{-i\mathbf{k}\cdot\mathbf{x}_i} \hat{b}_{\mathbf{k}}, \\ \hat{a}_i^\dagger &= \frac{1}{\sqrt{N/2}} \sum_{\mathbf{k}} e^{i\mathbf{k}\cdot\mathbf{x}_i} \hat{a}_{\mathbf{k}}^\dagger, & \hat{b}_i^\dagger &= \frac{1}{\sqrt{N/2}} \sum_{\mathbf{k}} e^{i\mathbf{k}\cdot\mathbf{x}_i} \hat{b}_{\mathbf{k}}^\dagger,\end{aligned}$$

the first term of the Hamiltonian yields

$$\begin{aligned}\hat{H} &= -t_1 \frac{2}{N} \sum_i \sum_{\mathbf{k}, \mathbf{k}'} \sum_{\alpha=1}^3 \left(e^{i\mathbf{k}'\cdot\mathbf{x}_i} e^{-i\mathbf{k}\cdot(\mathbf{x}_i+\mathbf{a}_\alpha)} \hat{a}_{\mathbf{k}'}^\dagger \hat{b}_{\mathbf{k}} + h.c \right) \\ &\quad - t_2 \frac{2}{N} \sum_i \sum_{\mathbf{k}, \mathbf{k}'} \sum_{\alpha=1}^3 \left(e^{i\phi} e^{i\mathbf{k}'\cdot\mathbf{x}_i} e^{-i\mathbf{k}\cdot(\mathbf{x}_i+\mathbf{b}_\alpha)} \hat{a}_{\mathbf{k}'}^\dagger \hat{a}_{\mathbf{k}} + h.c \right) \\ &\quad - t_2 \frac{2}{N} \sum_i \sum_{\mathbf{k}, \mathbf{k}'} \sum_{\alpha=1}^3 \left(e^{-i\phi} e^{i\mathbf{k}'\cdot\mathbf{x}_i} e^{-i\mathbf{k}\cdot(\mathbf{x}_i+\mathbf{b}_\alpha)} \hat{b}_{\mathbf{k}'}^\dagger \hat{b}_{\mathbf{k}} + h.c \right) \\ &\quad + M \frac{2}{N} \sum_i \sum_{\mathbf{k}, \mathbf{k}'} \left(e^{i\mathbf{k}'\cdot\mathbf{x}_i} e^{-i\mathbf{k}\cdot\mathbf{x}_i} \hat{a}_{\mathbf{k}'}^\dagger \hat{a}_{\mathbf{k}} - e^{i\mathbf{k}'\cdot\mathbf{x}_i} e^{-i\mathbf{k}\cdot\mathbf{x}_i} \hat{b}_{\mathbf{k}'}^\dagger \hat{b}_{\mathbf{k}} \right),\end{aligned}$$

by using the identity $\sum_i e^{-i(\mathbf{k}-\mathbf{k}')\cdot\mathbf{x}_i} = N/2\delta_{\mathbf{k},\mathbf{k}'}$, the above Hamiltonian simplifies to

$$\begin{aligned}\hat{H} &= -t_1 \sum_{\mathbf{k}} \sum_{\alpha}^3 \left(e^{-i\mathbf{k}\cdot\mathbf{a}_\alpha} \hat{a}_{\mathbf{k}}^\dagger \hat{b}_{\mathbf{k}} + e^{i\mathbf{k}\cdot\mathbf{a}_\alpha} \hat{b}_{\mathbf{k}}^\dagger \hat{a}_{\mathbf{k}} \right) \\ &\quad - t_2 \sum_{\mathbf{k}} \sum_{\alpha}^3 \left(e^{i\phi} e^{-i\mathbf{k}\cdot\mathbf{b}_\alpha} \hat{a}_{\mathbf{k}}^\dagger \hat{a}_{\mathbf{k}} + e^{-i\phi} e^{i\mathbf{k}\cdot\mathbf{b}_\alpha} \hat{a}_{\mathbf{k}}^\dagger \hat{a}_{\mathbf{k}} \right) \\ &\quad - t_2 \sum_{\mathbf{k}} \sum_{\alpha}^3 \left(e^{-i\phi} e^{-i\mathbf{k}\cdot\mathbf{b}_\alpha} \hat{b}_{\mathbf{k}}^\dagger \hat{b}_{\mathbf{k}} + e^{i\phi} e^{i\mathbf{k}\cdot\mathbf{b}_\alpha} \hat{b}_{\mathbf{k}}^\dagger \hat{b}_{\mathbf{k}} \right) \\ &\quad + M \sum_{\mathbf{k}} \left(\hat{a}_{\mathbf{k}}^\dagger \hat{a}_{\mathbf{k}} - \hat{b}_{\mathbf{k}}^\dagger \hat{b}_{\mathbf{k}} \right).\end{aligned}$$

The above Hamiltonian can be written in matrix form as

$$\hat{H} = - \sum_{\mathbf{k}} \begin{pmatrix} \hat{a}_{\mathbf{k}}^\dagger & \hat{b}_{\mathbf{k}}^\dagger \end{pmatrix} \begin{pmatrix} t_2 \sum_{\alpha=1}^3 (e^{i(\mathbf{k} \cdot \mathbf{b}_\alpha - \phi)} + e^{-i(\mathbf{k} \cdot \mathbf{b}_\alpha - \phi)}) & \\ & + M \\ t_1 \sum_{\alpha=1}^3 e^{i\mathbf{k} \cdot \mathbf{a}_\alpha} & t_2 \sum_{\alpha=1}^3 (e^{i(\mathbf{k} \cdot \mathbf{b}_\alpha + \phi)} + e^{-i(\mathbf{k} \cdot \mathbf{b}_\alpha + \phi)}) - M \end{pmatrix} \begin{pmatrix} \hat{a}_{\mathbf{k}} \\ \hat{b}_{\mathbf{k}} \end{pmatrix}.$$

Let

$$H(\mathbf{k}) \equiv \begin{pmatrix} t_2 \sum_{\alpha=1}^3 (e^{i(\mathbf{k} \cdot \mathbf{b}_\alpha - \phi)} + e^{-i(\mathbf{k} \cdot \mathbf{b}_\alpha - \phi)}) + M & \\ & t_1 \sum_{\alpha=1}^3 e^{i\mathbf{k} \cdot \mathbf{a}_\alpha} \\ t_1 \sum_{\alpha=1}^3 e^{i\mathbf{k} \cdot \mathbf{a}_\alpha} & t_2 \sum_{\alpha=1}^3 (e^{i(\mathbf{k} \cdot \mathbf{b}_\alpha + \phi)} + e^{-i(\mathbf{k} \cdot \mathbf{b}_\alpha + \phi)}) - M \end{pmatrix},$$

then

$$\hat{H} = - \sum_{\mathbf{k}} \begin{pmatrix} \hat{a}_{\mathbf{k}}^\dagger & \hat{b}_{\mathbf{k}}^\dagger \end{pmatrix} H(\mathbf{k}) \begin{pmatrix} \hat{a}_{\mathbf{k}} \\ \hat{b}_{\mathbf{k}} \end{pmatrix}. \quad (3.2)$$

Let

$$H_{aa}(\mathbf{k}) = t_2 \sum_{\alpha=1}^3 (e^{i(\mathbf{k} \cdot \mathbf{b}_\alpha - \phi)} + e^{-i(\mathbf{k} \cdot \mathbf{b}_\alpha - \phi)}), \quad H_{ab}(\mathbf{k}) = t_1 \sum_{\alpha=1}^3 e^{-i\mathbf{k} \cdot \mathbf{a}_\alpha},$$

$$H_{bb}(\mathbf{k}) = t_2 \sum_{\alpha=1}^3 (e^{i(\mathbf{k} \cdot \mathbf{b}_\alpha + \phi)} + e^{-i(\mathbf{k} \cdot \mathbf{b}_\alpha + \phi)}), \quad H_{ba}(\mathbf{k}) = t_1 \sum_{\alpha=1}^3 e^{i\mathbf{k} \cdot \mathbf{a}_\alpha},$$

and by using Euler identity $e^{i\theta} = \cos \theta + i \sin \theta$, the above expressions become

$$H_{aa}(\mathbf{k}) = 2t_2 \sum_{\alpha=1}^3 \cos(\mathbf{k} \cdot \mathbf{b}_\alpha - \phi),$$

$$H_{bb}(\mathbf{k}) = 2t_2 \sum_{\alpha=1}^3 \cos(\mathbf{k} \cdot \mathbf{b}_\alpha + \phi),$$

$$H_{ab}(\mathbf{k}) = t_1 \sum_{\alpha=1}^3 [\cos(\mathbf{k} \cdot \mathbf{a}_\alpha) - i \sin(\mathbf{k} \cdot \mathbf{a}_\alpha)],$$

$$H_{ba}(\mathbf{k}) = t_1 \sum_{\alpha=1}^3 [\cos(\mathbf{k} \cdot \mathbf{a}_\alpha) + i \sin(\mathbf{k} \cdot \mathbf{a}_\alpha)],$$

then $H(\mathbf{k})$ becomes

$$H(\mathbf{k}) = \begin{pmatrix} H_{aa}(\mathbf{k}) + M & H_{ab}(\mathbf{k}) \\ H_{ba}(\mathbf{k}) & H_{bb}(\mathbf{k}) - M \end{pmatrix}.$$

The above Hamiltonian can be written in the pseudo-spin basis:

$$H(\mathbf{k}) = \frac{H_{aa}(\mathbf{k}) + H_{bb}(\mathbf{k})}{2} \mathbb{1} + t_1 \sum_{\alpha=1}^3 [\cos(\mathbf{k} \cdot \mathbf{a}_\alpha) \sigma_x + \sin(\mathbf{k} \cdot \mathbf{a}_\alpha) \sigma_y] + \frac{H_{aa}(\mathbf{k}) - H_{bb}(\mathbf{k})}{2} \sigma_z + M \sigma_z, \quad (3.3)$$

where

$$H_{aa}(\mathbf{k}) + H_{bb}(\mathbf{k}) = 4t_2 \cos \phi \sum_{\alpha=1}^3 \cos(\mathbf{k} \cdot \mathbf{b}_\alpha), \quad (3.4)$$

$$H_{aa}(\mathbf{k}) - H_{bb}(\mathbf{k}) = -4t_2 \sin \phi \sum_{\alpha=1}^3 \sin(\mathbf{k} \cdot \mathbf{b}_\alpha). \quad (3.5)$$

Substituting equation (3.4) and (3.5) in equation (3.3)

$$\begin{aligned} H(\mathbf{k}) = & 2t_2 \cos \phi \sum_{\alpha=1}^3 \cos(\mathbf{k} \cdot \mathbf{b}_\alpha) \mathbb{1} + t_1 \sum_{\alpha=1}^3 [\cos(\mathbf{k} \cdot \mathbf{a}_\alpha) \sigma_x + \sin(\mathbf{k} \cdot \mathbf{a}_\alpha) \sigma_y] \\ & + \left[M - 2t_2 \sin \phi \sum_{\alpha=1}^3 \sin(\mathbf{k} \cdot \mathbf{b}_\alpha) \right]. \end{aligned} \quad (3.6)$$

From the geometry of the honeycomb lattice in figure (3.1)

$$\begin{aligned} \mathbf{a}_1 &= (0, a), & \mathbf{b}_1 &= \left(-\frac{\sqrt{3}a}{2}, \frac{3a}{2} \right), \\ \mathbf{a}_2 &= \left(\frac{-\sqrt{3}}{2}, \frac{-a}{2} \right), & \mathbf{b}_2 &= \left(-\frac{\sqrt{3}a}{2}, \frac{-3a}{2} \right), \\ \mathbf{a}_3 &= \left(\frac{\sqrt{3}}{2}, \frac{-a}{2} \right), & \mathbf{b}_3 &= (-\sqrt{3}a, 0). \end{aligned}$$

It is evident that $H(\mathbf{k}) \neq H(-\mathbf{k})$, the last term in the Hamiltonian breaks the time reversal symmetry as long as $\phi \neq n\pi$. If we take $\phi = 0$ and $M=0$, Hamiltonian (3.6) reduces to tight-binding graphene Hamiltonian, which has gapless linear spectrum at $\mathbf{K}_0 = 4\pi/3\sqrt{3}a(1, 0)$ and $\mathbf{K}'_0 = 4\pi/3\sqrt{3}a(-1, 0)$ at the end of the BZ. The energy spectrum of Hamiltonian (3.6) is

$$\begin{aligned} E_{\pm}(\mathbf{k}) = & 2t_2 \cos \phi \sum_{\alpha=1}^3 \cos(\mathbf{k} \cdot \mathbf{b}_\alpha) \pm |t_1| \sqrt{\left[\sum_{\alpha=1}^3 \cos(\mathbf{k} \cdot \mathbf{a}_\alpha) \right]^2 + \left[\sum_{\alpha=1}^3 \sin(\mathbf{k} \cdot \mathbf{a}_\alpha) \right]^2} \\ & \sqrt{\left[M - 2t_2 \sin \phi \sum_{\alpha=1}^3 \sin(\mathbf{k} \cdot \mathbf{b}_\alpha) \right]^2}. \end{aligned}$$

At \mathbf{K}_0 point, the energy gap Δ is

$$\begin{aligned} \Delta &= E_+(\mathbf{K}_0) - E_-(\mathbf{K}_0), \\ &= 2 \left| M - 3\sqrt{3}t_2 \sin \phi \right|, \end{aligned} \quad (3.7)$$

and at \mathbf{K}'_0 point

$$\begin{aligned}\Delta &= E_+(\mathbf{K}'_0) - E_-(\mathbf{K}'_0), \\ &= 2 \left| M + 3\sqrt{3}t_2 \sin \phi \right|.\end{aligned}\quad (3.8)$$

Equations (3.7) and (3.8) show that the system remains gapless until both $M=0$ and $\phi = 0$. Let us expand Hamiltonian (3.6) in the vicinity of \mathbf{K}_0 and \mathbf{K}'_0 . To do this, putting $\mathbf{k} = \mathbf{K}_0 + \mathbf{q}$ and $\mathbf{k} = \mathbf{K}'_0 + \mathbf{q}$ in the Hamiltonian and keeping terms upto linear order in q_x and q_y . The Hamiltonian around \mathbf{K}_0 becomes

$$\hat{H}(\mathbf{q}) \approx v_F(q_x\sigma_x + q_y\sigma_y) + \left[M - 3\sqrt{3}t_2 \sin \phi \right] \sigma_z. \quad (3.9)$$

We can write equation (3.9) in the form of two-level Hamiltonian

$$\hat{H}(\mathbf{q}) \approx \mathbf{d}_{\mathbf{K}_0} \cdot \boldsymbol{\sigma}, \quad (3.10)$$

where $\mathbf{d}_{\mathbf{K}_0} = (v_Fq_x, v_Fq_y, M - 3\sqrt{3}t_2 \sin \phi)$ and $(\sigma_x, \sigma_y, \sigma_z)$ are Pauli matrices in pseudo-spin basis. Similarly in the proximity of \mathbf{K}'_0 point, the Hamiltonian becomes

$$\hat{H}(\mathbf{q}) \approx v_F(q_x\sigma_x - q_y\sigma_y) + \left[M + 3\sqrt{3}t_2 \sin \phi \right] \sigma_z. \quad (3.11)$$

The above Hamiltonian can also be written in two-level system Hamiltonian as

$$\hat{H}(\mathbf{q}) \approx \mathbf{d}_{\mathbf{K}'_0} \cdot \boldsymbol{\sigma}, \quad (3.12)$$

where $\mathbf{d}_{\mathbf{K}'_0} = (v_Fq_x, -v_Fq_y, M + 3\sqrt{3}t_2 \sin \phi)$ and $v_F = 3/2at_1$ is the Fermi velocity.

3.1.1 Berry Curvature and Chern number Calculation

Hamiltonian (3.9) and (3.10) are two-level Hamiltonian, so we can use equation (1.47) to calculate the Berry curvature around \mathbf{K}_0 and \mathbf{K}'_0 points

$$\begin{aligned}F_{\pm}(\mathbf{q}) &= \mp \frac{\mathbf{d}_{\mathbf{K}_0}}{2|\mathbf{d}_{\mathbf{K}_0}|^3} \cdot \frac{\partial \mathbf{d}_{\mathbf{K}_0}}{\partial q_x} \times \frac{\partial \mathbf{d}_{\mathbf{K}_0}}{\partial q_y}, \\ &= \mp \frac{1}{2|\mathbf{d}_{\mathbf{K}_0}|^3} \begin{vmatrix} v_Fq_x & v_Fq_y & M - 3\sqrt{3}t_2 \sin \phi \\ v_F & 0 & 0 \\ 0 & v_F & 0 \end{vmatrix},\end{aligned}$$

after simplification, it implies

$$\boxed{F_{\pm}(\mathbf{q}) = \mp \frac{v_F^2}{2|\mathbf{d}_{\mathbf{K}_0}|^3} \times \left(M - 3\sqrt{3}t_2 \sin \phi \right)}. \quad (3.13)$$

Similarly around \mathbf{K}'_0 , the Berry curvature becomes

$$F_{\pm}(\mathbf{q}) = \pm \frac{v_F^2}{2|\mathbf{d}_{\mathbf{K}_0}|^3} \times (M + 3\sqrt{3}t_2 \sin \phi). \quad (3.14)$$

Equations (3.13) and (3.14) show that the sign of Berry curvature around two Dirac points depends on relative strength of inversion symmetry breaking term M and the time-reversal breaking term $3\sqrt{3}t_2 \sin \phi$, and their relative strength determines the Chern number which is defined as

$$C_{\pm} = \frac{1}{2\pi} \int_S F_{\pm}(\mathbf{q}) d^2 \mathbf{q}. \quad (3.15)$$

For $M < |3\sqrt{3}t_2 \sin \phi|$, the Berry curvature has same sign, so each node contributes $\mp 1/2$ and $\mp 1/2$ to the Chern number ∓ 1 . However, for $M > |3\sqrt{3}t_2 \sin \phi|$, two nodes' Berry curvature has opposite sign, as a result, the Chern number vanishes in this regime. When $M = |3\sqrt{3}t_2 \sin \phi|$, it acts as phase transition point by making system gapless at one of two Dirac points. We can draw a phase diagram for Chern numbers as

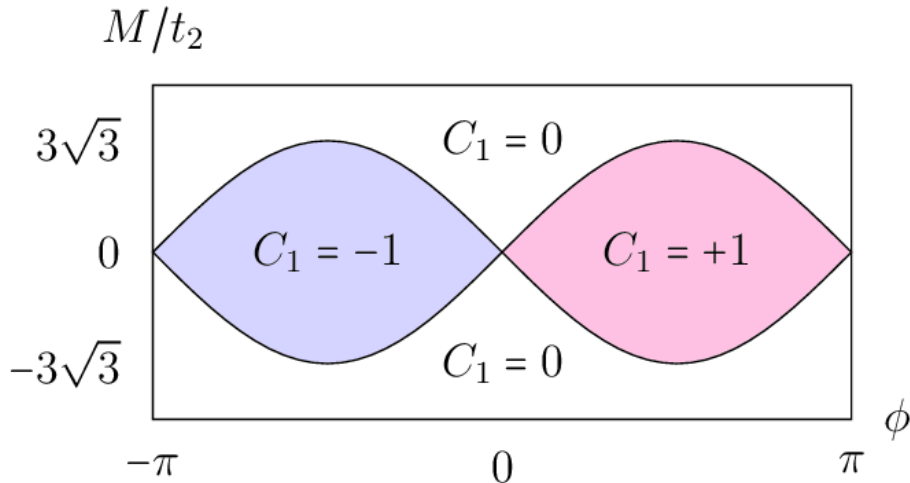


Figure 3.2: Phase diagram of the Chern insulator. Inside the coloured region the condition $M < |3\sqrt{3}t_2 \sin \phi|$ leads to non-zero Chern number. The points on curved boundary line acts as phase transition points. In the rest of the region $M > |3\sqrt{3}t_2 \sin \phi|$ implies zero Chern number.

Chapter 4

Floquet Theory and Semi-Dirac Hamiltonian

It has recently been shown that periodic perturbations can be used as a versatile experimental knob to access new phases that cannot be reachable in equilibrium systems; for example, synthetic matter and quantum motors, etc. This new arena of research is called “Floquet Engineering”, and it has revitalized interest in periodically driven systems [7].

In the simplest case, we consider a monochromatic external driving perturbation, defined by a driving amplitude and a single frequency. The dynamics of the periodically driven systems can be intricate, but it simplifies if we study it in two extreme cases, under the slow and fast driving perturbations. In the first case, the system closely follows the instantaneous Hamiltonian. However, in the second scenario, when the driving frequency is high compared with the non-driven model’s natural frequencies, the system effectively experiences a static potential that can be a function of the driving amplitude.

In this chapter, first of all, I introduce the Floquet theory, which is applicable for periodically driven systems far away from the adiabatic limit. Secondly, by using the Floquet theory, I study how new topological phases emerge in a semi-Dirac material by irradiating the material with electromagnetic waves.

4.1 Floquet Theorem

To study periodically driven systems far away from adiabatic limit, we use the Floquet theorem. It states that the evolution operator can be written as

$$\hat{U}_s(t_2, t_1) = e^{-i\hat{K}_s(t_2)} e^{-i\hat{H}_F(t_2-t_1)} e^{i\hat{K}_s(t_1)}. \quad (4.1)$$

$\hat{K}_s(t) = \hat{K}_s(t+T)$ is a periodic hermitian operator and \hat{H}_F is a time-independent Hamilton Floquet operator. In addition, we have no unique choice for the periodic operator $\hat{K}_s(t)$ and Floquet Hamiltonian \hat{H}_F , there

is some flexibility to describe them. There are different convenient gauge choices that depend on the details of the setup. Although these choices are equivalent, but they lead to different approximation schemes.

The Stroboscopic Floquet Hamiltonian and the P-Operator

The formalism of Floquet's theorem gets simplified if we observe the system stroboscopically, i.e. at times $t_2 = t_1 + NT$, where NT is the stroboscopic time measured in units of the driving period [7]. The time evolution operator of a time dependent Hamiltonian is

$$\hat{U}_s(t_2, t_1) = \hat{T}_r \exp\left(-i \int_{t_1}^{t_2} dt' \hat{H}(t')\right),$$

\hat{T}_r is the time-ordering operator. The evolution operator can be written as

$$\hat{U}_s(t_2, t_1) = \prod_{t_1 \leq t'_j \leq t_2} \exp\left[-i \hat{H}(t'_j)(t'_{j+1} - t'_j)\right],$$

it is invariant under discrete translation in time as

$$(t_1, t_2) \rightarrow (t_1 + NT, t_2 + NT),$$

where N is an integer. We can use the factorization property of the evolution operator: $\hat{U}_s(t_2, t_1) = \hat{U}_s(t_2, t')\hat{U}_s(t', t_1)$ for any arbitrary time t' , by using this

$$\begin{aligned} \hat{U}_s(t_0 + 2T, t_0) &= \hat{U}_s(t_0 + 2T, t_0 + T)\hat{U}_s(t_0 + T, t_0), \\ &= \hat{U}_s(t_0 + T, t_0)\hat{U}_s(t_0 + T, t_0), \\ &= \left[\hat{U}_s(t_0 + T, t_0)\right]^2, \end{aligned}$$

generalizing this

$$\hat{U}_s(t_0 + NT, t_0) = \left[\hat{U}_s(t_0 + T, t_0)\right]^N. \quad (4.2)$$

With the time-independent stroboscopic Floquet Hamiltonian $\hat{H}_F[t_0]$, we may describe evolution within one cycle as,

$$\hat{U}_s(t_0 + NT, t_0) = \exp\left(-i \hat{H}_F[t_0]NT\right), \quad (4.3)$$

where $\hat{H}_F[t_0]$ depends upon choice of t_0 , which is a gauge choice. The evolution operator implies

$$\begin{aligned} \hat{U}_s(t_2, t_1) &= \hat{U}_s(t_2, t_0 + NT)\hat{U}_s(t_0 + NT, t_0)\hat{U}_s(t_0, t_1), \\ &= \hat{U}_s(t_2, t_0 + NT)\left[\hat{U}_s(t_0 + T, t_0)\right]^N\hat{U}_s(t_0, t_1), \\ &= \hat{U}_s(t_2, t_0 + NT)\exp\left(-i \hat{H}_F[t_0]NT\right)\hat{U}_s(t_0, t_1), \end{aligned} \quad (4.4)$$

the above equation can be written as,

$$\begin{aligned}\hat{U}_s(t_2, t_1) &= \hat{U}_s(t_2, t_0 + NT) \exp\left(i\hat{H}_F[t_0](t_2 - t_0 - NT)\right) \\ &\quad \times \exp\left(-i\hat{H}_F[t_0](t_2 - t_1)\right) \exp\left(i\hat{H}_F[t_0](t_0 - t_1)\right) \hat{U}_s(t_0, t_1).\end{aligned}\quad (4.5)$$

Let us define

$$\begin{aligned}\hat{P}_s(t_2, t_0 + NT) &\equiv \hat{U}_s(t_2, t_0 + NT) \exp\left(i\hat{H}_F[t_0](t_2 - t_0 - NT)\right), \\ \hat{P}_s(t_1, t_0) &\equiv \hat{U}_s(t_1, t_0) \exp\left(i\hat{H}_F[t_0](t_1 - t_0)\right),\end{aligned}$$

Equation (4.5) can be expressed as

$$\Rightarrow \hat{U}_s(t_2, t_1) = \hat{P}_s(t_2, t_0 + NT) \exp\left(-i\hat{H}_F[t_0](t_2 - t_1)\right) \hat{P}_s^\dagger(t_1, t_0).\quad (4.6)$$

Let us further simplify $\hat{P}_s(t_2, t_0 + NT)$,

$$\hat{P}_s(t_2, t_0 + NT) = \hat{U}_s(t_2, t_0 + NT) \exp\left(i\hat{H}_F[t_0](t_2 - t_0 - NT)\right),$$

by using the factorization property of the evolution operator, we can write

$$\hat{P}_s(t_2, t_0 + NT) = \hat{U}_s(t_2, t_0) \hat{U}_s(t_0, t_0 + NT) \exp\left(i\hat{H}_F[t_0](t_2 - t_0 - NT)\right),$$

using equation (4.3)

$$\begin{aligned}\hat{P}_s(t_2, t_0 + NT) &= \hat{U}(t_2, t_0) \exp\left(i\hat{H}_F[t_0]T\right) \exp\left(i\hat{H}_F[t_0](t_2 - t_0 - NT)\right), \\ &= \hat{U}_s(t_2, t_0) \exp\left(i\hat{H}_F[t_0](t_2 - t_0)\right), \\ &= \hat{P}_s(t_2, t_0).\end{aligned}$$

Equation (4.6) becomes

$$\hat{U}_s(t_2, t_1) = \hat{P}_s(t_2, t_0) \exp\left(-i\hat{H}_F[t_0](t_2 - t_1)\right) \hat{P}_s^\dagger(t_1, t_0).\quad (4.7)$$

Let us define

$$\begin{aligned}\hat{P}_s(t_2, t_0) &= \hat{U}_s(t_2, t_0) \exp\left(i\hat{H}_F[t_0](t_2 - t_0)\right) \equiv \exp\left(-i\hat{K}_F[t_0](t_2)\right), \\ \hat{P}_s^\dagger(t_1, t_0) &= \exp\left(i\hat{H}_F[t_0](t_0 - t_1)\right) \hat{U}_s(t_0, t_1) \equiv \exp\left(i\hat{K}_F[t_0](t_1)\right).\end{aligned}$$

Equation (4.6) implies

$$\begin{aligned}\hat{U}_s(t_2, t_1) &= \exp\left(-i\hat{K}_F[t_0](t_2)\right) \exp\left(-i\hat{H}_F[t_0](t_2 - t_1)\right) \\ &\quad \times \exp\left(i\hat{K}_F[t_0](t_1)\right).\end{aligned}\quad (4.8)$$

The above result is the evolution operator written in the form of kick operator $\hat{K}_F[t_0]$, which explicitly depends on the gauge choice t_0 . Notice that, with the above definition, the operator \hat{P}_s is periodic $\hat{P}_s(t_2 + NT, t_0) = \hat{P}_s(t_2, t_0 + NT) = \hat{P}_s(t_2, t_0)$. Also $\hat{P}_s(t_0 + NT, t_0) = 0$, for an arbitrary integer N . It means at stroboscopic times kick operator vanishes.

In the next section, let us rewrite the Floquet's result in differential form.

4.1.1 Floquet Hamiltonian in differential Form

The evolution operator satisfies the following evolution equation

$$i \frac{\partial \hat{U}_s(t_2, t_1)}{\partial t_2} = \hat{H}(t_2) \hat{U}_s(t_2, t_1). \quad (4.9)$$

Differentiating equation (4.7) w.r.t t_2

$$\begin{aligned} i \frac{\partial \hat{U}_s(t_2, t_1)}{\partial t_2} &= i \frac{\partial \hat{P}_s(t_2, t_0)}{\partial t_2} \exp\left(-i \hat{H}_F[t_0](t_2 - t_1)\right) \hat{P}_s^\dagger(t_1, t_0) \\ &\quad + \hat{P}_s(t_2, t_0) \hat{H}_F[t_0] \exp\left(-i \hat{H}_F[t_0](t_2 - t_1)\right) \hat{P}_s^\dagger(t_1, t_0), \end{aligned} \quad (4.10)$$

comparing equation (4.10) with (4.9),

$$\begin{aligned} \hat{H}(t_2) \hat{U}_s(t_2, t_1) &= i \frac{\partial \hat{P}_s(t_2, t_0)}{\partial t_2} \exp\left(-i \hat{H}_F[t_0](t_2 - t_1)\right) \hat{P}_s^\dagger(t_1, t_0) \\ &\quad + \hat{P}_s(t_2, t_0) \hat{H}_F[t_0] \exp\left(-i \hat{H}_F[t_0](t_2 - t_1)\right) \hat{P}_s^\dagger(t_1, t_0). \end{aligned}$$

Right multiplying by $\hat{P}_s(t_1, t_0) \exp\left(i \hat{H}_F[t_0](t_2 - t_1)\right)$ on both sides of the above equation

$$\hat{H}(t_2) \hat{U}_s(t_2, t_1) \hat{P}_s(t_1, t_0) \exp\left(i \hat{H}_F[t_0](t_2 - t_1)\right) = i \frac{\partial \hat{P}_s(t_2, t_0)}{\partial t_2} + \hat{P}_s(t_2, t_0) \hat{H}_F[t_0].$$

Putting

$$\hat{P}_s(t_1, t_0) = \hat{U}_s(t_1, t_0) \exp\left(i \hat{H}_F[t_0](t_1 - t_0)\right)$$

in the previous equation

$$\begin{aligned} \hat{H}(t_2) \hat{U}_s(t_2, t_1, t_0) \hat{U}_s(t_1, t_0) \exp\left(i \hat{H}_F[t_0](t_1 - t_0)\right) \exp\left(i \hat{H}_F[t_0](t_2 - t_1)\right) \\ = i \frac{\partial \hat{P}_s(t_2, t_0)}{\partial t_2} + \hat{P}_s(t_2, t_0) \hat{H}_F[t_0], \end{aligned}$$

using the factorization property: $\hat{U}_s(t_2, t_1, t_0) \hat{U}_s(t_1, t_0) = \hat{U}_s(t_2, t_0)$,

$$\begin{aligned} \hat{H}(t_2) \hat{U}_s(t_2, t_0) \exp\left(i \hat{H}_F[t_0](t_2 - t_0)\right) &= i \frac{\partial \hat{P}_s(t_2, t_0)}{\partial t_2} + \hat{P}_s(t_2, t_0) \hat{H}_F[t_0], \\ \Rightarrow \hat{H}(t_2) \hat{P}_s(t_2, t_0) &= i \frac{\partial \hat{P}_s(t_2, t_0)}{\partial t_2} + \hat{P}_s(t_2, t_0) \hat{H}_F[t_0]. \end{aligned}$$

Left multiplying the above equation by $\hat{P}_s^\dagger(t_2, t_0)$,

$$\hat{H}_F[t_0] = \hat{P}_s^\dagger(t_2, t_0) \hat{H}(t_2) \hat{P}_s(t_2, t_0) - i \hat{P}_s^\dagger(t_2, t_0) \frac{\partial \hat{P}_s(t_2, t_0)}{\partial t_2}, \quad (4.11)$$

equation (4.11) gives us a relation between actual time-dependent Hamiltonian and the Floquet Hamiltonian, and it also shows that there exists a periodic operator \hat{P}_s such that left hand side of equation (4.11) is independent of time, allowing us to map actual time-dependent Hamiltonian $\hat{H}(t_2)$ to the time-independent Floquet Hamiltonian $\hat{H}_F[t_0]$.

Another possibility for application of equation (4.11) is it allows us to do reverse engineering. Once we choose a Floquet's Hamiltonian $\hat{H}_F[t_0]$ with a periodic operator \hat{P}_s having interesting properties, we can get actual time-dependent Hamiltonian $\hat{H}(t)$ by using equation (4.11), and by knowing the time-dependent protocol $\hat{H}(t)$, we can implement experimentally to realize those properties [7].

In the next section, we try to write the evolution operator in terms of a unique Floquet Hamiltonian, which is gauge independent.

4.1.2 The Non-Stroboscopic Floquet Hamiltonian and the Kick Operator

In the previous section, we showed that one can choose a family of stroboscopic Floquet Hamiltonian $\hat{H}_F[t_0]$, each of which gives evolution operator at stroboscopic times $\hat{U}_s(t_0 + NT, t_0) = \exp(-i\hat{H}_F[t_0]NT)$. There are different Floquet gauge choices t_0 , and these stroboscopic Floquet Hamiltonians choices are gauge equivalent [7].

On the other hand, because t_0 is a gauge choice, all these Hamiltonians are gauge equivalent to some fixed Floquet Hamiltonian \hat{H}_F , therefore there exists a family of hermitian operators $\hat{K}(t_0)$ called kick operators such that

$$\hat{H}_F = \exp(i\hat{K}_F(t_0))\hat{H}_F[t_0]\exp(-i\hat{K}_F(t_0)). \quad (4.12)$$

By construction, in this case, Floquet gauge dependence is carried by the kick operator \hat{K}_F , and it is periodic: $\hat{K}_F(t_0 + NT) = \hat{K}_F(t_0)$. We can write the \hat{P} in terms of the kick operator \hat{K} , and it is our next discussion.

4.1.3 Relation between the Kick Operator and the P-Operator

From equation (4.3)

$$\hat{U}_s(t_0 + NT, t_0) = \exp(-i\hat{H}_F[t_0]NT),$$

using the unitarity property of the evolution operator: $\hat{U}_s\hat{U}_s^\dagger = \mathbb{1}$,

$$\begin{aligned} \hat{U}_s(t_0 + NT, t_0) &= \hat{U}_s^\dagger(t_0 + \delta t, t_0)\hat{U}_s(t_0 + \delta t, t_0)\exp(-i\hat{H}_F[t_0]NT) \\ &\quad \times \hat{U}_s^\dagger(t_0 + \delta t, t_0)\hat{U}_s(t_0 + \delta t, t_0). \end{aligned}$$

If

$$\hat{U}_s(t_0 + \delta t, t_0) \hat{H}_F[t_0] \hat{U}_s^\dagger(t_0 + \delta t, t_0) = \hat{H}_F[t_0 + \delta t], \quad (4.13)$$

the evolution operator becomes

$$\begin{aligned} \hat{U}_s(t_0 + NT, t_0) &= \hat{U}_s^\dagger(t_0 + \delta t, t_0) \exp\left(-i\hat{H}_F[t_0 + \delta t]NT\right) \\ &\quad \times \hat{U}_s(t_0 + \delta t, t_0). \end{aligned} \quad (4.14)$$

By using the definition of P-operator

$$\hat{P}_s(t_0 + \delta t, t_0) = \hat{U}_s(t_0 + \delta t, t_0) \exp\left(i\hat{H}_F[t_0]\delta t\right),$$

if $\delta t \rightarrow 0$

$$\hat{P}_s(t_0 + \delta t, t_0) = \hat{U}_s(t_0 + \delta t, t_0),$$

substituting this result in equation (4.13)

$$\hat{H}_F[t_0 + \delta t] = \hat{P}_s(t_0 + \delta t, t_0) \hat{H}_F[t_0] \hat{P}_s^\dagger(t_0 + \delta t, t_0). \quad (4.15)$$

From equation (4.12) substituting the value of $\hat{H}_F[t_0]$

$$\begin{aligned} \hat{H}_F[t_0 + \delta t] &= \hat{P}_s(t_0 + \delta t, t_0) \exp\left(-i\hat{K}_F(t_0)\right) \hat{H}_F \exp\left(i\hat{K}_F(t_0)\right) \\ &\quad \times \hat{P}_s^\dagger(t_0 + \delta t, t_0), \end{aligned} \quad (4.16)$$

by definition

$$\hat{H}_F[t_0 + \delta t] = \exp\left(-i\hat{K}_F(t_0 + \delta t)\right) \hat{H}_F[t_0] \exp\left(i\hat{K}_F(t_0 + \delta t)\right), \quad (4.17)$$

comparing equation (4.17) with (4.16)

$$\boxed{\hat{P}_s(t, t_0) = \exp\left(-i\hat{K}_s(t)\right) \exp\left(i\hat{K}_s(t_0)\right)}. \quad (4.18)$$

substituting the result from equation (4.18) in equation (4.7)

$$\begin{aligned} \hat{U}_s(t_2, t_1) &= \exp\left(-i\hat{K}_s(t_2)\right) \exp\left(i\hat{K}_s(t_0)\right) \exp\left(-i\hat{H}_F[t_0](t_2 - t_1)\right) \\ &\quad \exp\left(-i\hat{K}_s(t_0)\right) \exp\left(i\hat{K}_s(t_1)\right), \end{aligned} \quad (4.19)$$

from equation (4.12)

$$\exp\left(i\hat{K}_s(t_0)\right) \hat{H}_F[t_0] \exp\left(-i\hat{K}_s(t_0)\right) = \hat{H}_F,$$

$$\hat{U}_s(t_2, t_1) = \exp\left(-i\hat{K}_s(t_2)\right) \exp\left(-i\hat{H}_F(t_2 - t_1)\right) \exp\left(i\hat{K}_s(t_1)\right). \quad (4.20)$$

Equation (4.20) is a Floquet theorem result. Equations (4.8) and (4.20) show that we can write the evolution operator in term of time-independent Floquet Hamiltonian $\hat{H}_F[t_0]$ or \hat{H}_F and the time dependence is carried by fast oscillating operators \hat{P} or \hat{K} , respectively. We can also simplify by expanding them. In the next section, we address how we can expand these operators.

4.1.4 Inverse Frequency Expansion for the Floquet Hamiltonian

A Floquet hamiltonian can not be obtained in a closed form, other than in a few exceptional cases. An important limit where one can define the Floquet Hamiltonian at least perturbatively applies to rapid driving situations where the driving frequency is much higher than all of the natural frequencies of the system. For instance, the driving period is small compared to the oscillation period for a pendulum. In this limit, the system has a hard time absorbing energy from the drive, resulting in a virtual process that dresses the low-energy Hamiltonian.

The Magnus Expansion for the stroboscopic Floquet Hamiltonian is a very efficient tool for calculating the Floquet Hamiltonian in the high-frequency limit [7], which is a perturbative method to find $\hat{H}_F[t_0]$,

$$\hat{U}_s(t_0 + T, t_0) = T_r \exp\left(\frac{-i}{\hbar} \int_{t_0}^{t_0+T} dt \hat{H}(t)\right),$$

using equation (4.3) we can write the above equation as

$$\hat{U}_s(t_0 + T, t_0) = \exp\left(\frac{-i}{\hbar} \hat{H}_F[t_0]T\right).$$

Taking natural log on the both sides of the above equation

$$\begin{aligned} \frac{-i}{\hbar} \hat{H}_F[t_0]T &= \ln \left[T_r \exp\left(\frac{-i}{\hbar} \int_{t_0}^{t_0+T} dt \hat{H}(t)\right) \right], \\ \hat{H}_F[t_0] &= \frac{i\hbar}{T} \ln \left[T_r \exp\left(\frac{-i}{\hbar} \int_{t_0}^{t_0+T} dt \hat{H}(t)\right) \right], \end{aligned}$$

expanding the exponential and taking care of time-ordering because generally $[\hat{H}(t), \hat{H}(t')] \neq 0$

$$\begin{aligned} \hat{H}_F[t_0] &= \frac{i\hbar}{T} \left[\frac{-i}{\hbar} \int_{t_0}^{t_0+T} dt \hat{H}(t) \right. \\ &+ \frac{(-i)^2}{2! \hbar^2} \int_{t_0}^{t_0+T} dt_1 \int_{t_0}^{t_1} dt_2 [\hat{H}(t_1), \hat{H}(t_2)] \\ &+ \frac{(-i)^3}{3! \hbar^3} \int_{t_0}^{t_0+T} dt_1 \int_{t_0}^{t_1} dt_2 \int_{t_0}^{t_2} dt_3 \\ &\quad \left. \times \left([\hat{H}(t_1), [\hat{H}(t_2), \hat{H}(t_3)]] + (1 \leftrightarrow 3) \right) + \dots \right]. \end{aligned} \tag{4.21}$$

We can represent $\hat{H}_F[t_0]$ in a perturbative series:

$$\hat{H}_F[t_0] = \sum_{n=0}^{\infty} \hat{H}_F^{(n)}[t_0], \tag{4.22}$$

comparing equation (3.21) with (3.20)

$$\hat{H}_F^{(0)}[t_0] = \frac{1}{T} \int_{t_0}^{t_0+T} dt \hat{H}(t), \quad (4.23)$$

and

$$\hat{H}_F^{(1)}[t_0] = \frac{1}{2i\hbar T} \int_{t_0}^{t_0+T} dt_1 \int_{t_0}^{t_1} dt_2 [\hat{H}(t_1), \hat{H}(t_2)], \quad (4.24)$$

as $T = \frac{2\pi}{\omega}$, the higher order terms in the expansion (4.21) are suppressed with increasing driving frequency, making this formalism valid.

4.2 Semi-Dirac Hamiltonian

We present a basic Hamiltonian to explain the movement and the merging of Dirac points in the two-dimensional electronic spectrum. This merging is a topological transition that separates a semi-metallic phase having two gapless Dirac nodes from an insulating phase with a gap. A tight-binding Hamiltonian, with three equal hopping parameters between nearest neighbours, describes the spectrum of graphene, which is a honeycomb lattice. The considerable development of research on graphene is partly because of its unusual spectrum, displaying linear spectrum at the corner of the Brillouin zone close to two special points \mathbf{K} and \mathbf{K}' called Dirac points. Dirac-like Hamiltonian describes its low-energy, massless quasi-particles

$$\hat{H} = -i\hbar v_F \boldsymbol{\sigma} \cdot \nabla,$$

where $v_F \approx 10^6 \text{ms}^{-1}$ is the Fermi velocity and $\boldsymbol{\sigma} = (\sigma_x, \sigma_y)$ are the Pauli matrices [8].

It has been realized that, by tuning the hopping parameters, new interesting physics can emerge, in particular, the presence of a topological transition dividing a semi-metallic phase with two Dirac points from the insulating phase when one of the three hopping amplitudes is modified [9]. In this case, low energy Hamiltonian becomes

$$H(\mathbf{q}) = \begin{pmatrix} 0 & -\Delta + \frac{q_x^2}{2m^*} - iv_F q_y \\ -\Delta + \frac{q_x^2}{2m^*} + iv_F q_y & 0 \end{pmatrix},$$

where $\Delta = 2t - t'$. This Hamiltonian has the following properties:

- We can move the Dirac points inside the BZ by varying one of the hopping parameters t' , and two Dirac points can merge with each other. So, we can change the topology of BZ by varying t' .

- It is a combination of two different types of dispersion relations: Linear spectrum in one crystal momentum direction and quadratic spectrum in the other direction.

Although such variations in hopping parameters in graphene may not be possible; a staggered hopping parameter could be found in other systems such as VO_2/TiO_2 nano-structures or an artificial lattice of cold atoms where the movement of Dirac points can be intrigued by adjusting the intensity of laser fields.

First, we take a honeycomb lattice with three different hopping parameters, as shown in figure 4.1, and write tight-binding Hamiltonian to develop the semi-Dirac Hamiltonian,

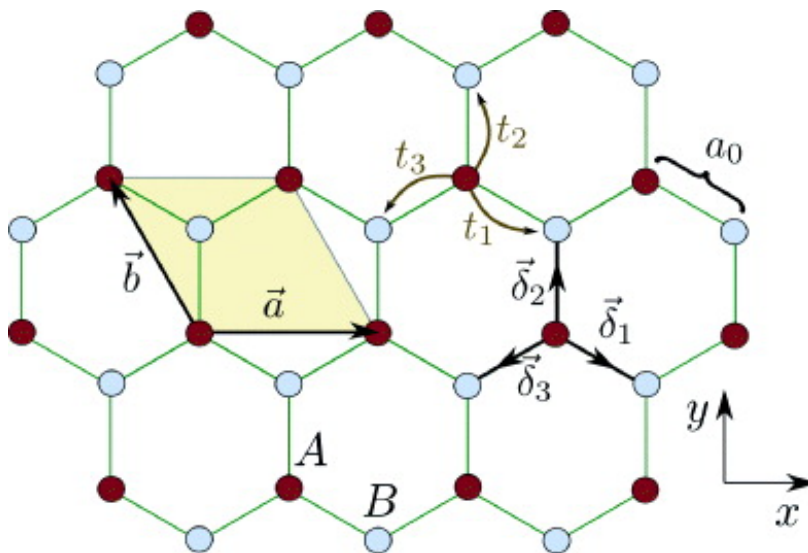


Figure 4.1: A honeycomb lattice with different nearest hopping parameter t_1 , t_2 , and t_3 .

Tight-Binding Hamiltonian:

$$\hat{H} = - \sum_{\langle ij \rangle} t_{ij} (\hat{a}_i^\dagger \hat{b}_j + h.c.),$$

taking different hopping parameters for three nearest directions

$$\begin{aligned} \hat{H} = & - \sum_{i \in A} t_1 (\hat{a}_i^\dagger \hat{b}_{i+\delta_1} + h.c.) - \sum_{i \in A} t_2 (\hat{a}_i^\dagger \hat{b}_{i+\delta_2} + h.c.) \\ & - \sum_{i \in A} t_3 (\hat{a}_i^\dagger \hat{b}_{i+\delta_3} + h.c.). \end{aligned} \quad (4.25)$$

To diagonalize the Hamiltonian, we use Fourier transformation to convert it

into k-space

$$\begin{aligned}\hat{a}_i &= \frac{1}{\sqrt{N/2}} \sum_{\mathbf{k}} e^{i\mathbf{k}\cdot\mathbf{r}_i} \hat{a}_{\mathbf{k}}, & \hat{b}_{i+\delta_1} &= \frac{1}{\sqrt{N/2}} \sum_{\mathbf{k}} e^{i\mathbf{k}\cdot(\mathbf{r}_i+\delta_1)} \hat{b}_{\mathbf{k}}, \\ \hat{a}_i^\dagger &= \frac{1}{\sqrt{N/2}} \sum_{\mathbf{k}} e^{-i\mathbf{k}\cdot\mathbf{r}_i} \hat{a}_{\mathbf{k}}^\dagger, & \hat{b}_{i+\delta_1}^\dagger &= \frac{1}{\sqrt{N/2}} \sum_{\mathbf{k}} e^{-i\mathbf{k}\cdot(\mathbf{r}_i+\delta_1)} \hat{b}_{\mathbf{k}}^\dagger,\end{aligned}$$

1st term of equation (4.25) becomes

$$\begin{aligned}-\sum_{i \in A} t_1 \hat{a}_i^\dagger \hat{b}_{i+\delta_1} &= -t_1 \frac{2}{N} \sum_{i \in A} \sum_{\mathbf{k}} \sum_{\mathbf{k}'} e^{-i(\mathbf{k}'-\mathbf{k})\cdot\mathbf{r}} e^{i\mathbf{k}\cdot\delta_1} \hat{a}_{\mathbf{k}'}^\dagger \hat{b}_{\mathbf{k}}, \\ &= -t_1 \frac{2}{N} \sum_{\mathbf{k}} \sum_{\mathbf{k}'} e^{i\mathbf{k}\cdot\delta_1} \left[\sum_{i \in A} e^{-i(\mathbf{k}'-\mathbf{k})\cdot\mathbf{r}} \right] \hat{a}_{\mathbf{k}'}^\dagger \hat{b}_{\mathbf{k}}.\end{aligned}\quad (4.26)$$

By using the following identity,

$$\sum_{i \in A} e^{-i(\mathbf{k}'-\mathbf{k})\cdot\mathbf{r}} = \delta_{\mathbf{k},\mathbf{k}'} \frac{N}{2},$$

substituting it in equation (4.26)

$$\begin{aligned}-\sum_{i \in A} t_1 \hat{a}_i^\dagger \hat{b}_{i+\delta_1} &= -t_1 \frac{2}{N} \sum_{\mathbf{k}} \sum_{\mathbf{k}'} e^{i\mathbf{k}\cdot\delta_1} \left[\delta_{\mathbf{k},\mathbf{k}'} \frac{N}{2} \right] \hat{a}_{\mathbf{k}'}^\dagger \hat{b}_{\mathbf{k}}, \\ &= -t_1 \sum_{\mathbf{k}} e^{i\mathbf{k}\cdot\delta_1} \hat{a}_{\mathbf{k}}^\dagger \hat{b}_{\mathbf{k}}.\end{aligned}$$

Finally, the first term in k-space becomes

$$\Rightarrow \boxed{-\sum_{i \in A} t_1 \left(\hat{a}_i^\dagger \hat{b}_{i+\delta_1} + h.c \right) = -t_1 \sum_{\mathbf{k}} \left(e^{i\mathbf{k}\cdot\delta_1} \hat{a}_{\mathbf{k}}^\dagger \hat{b}_{\mathbf{k}} + h.c \right)},\quad (4.27)$$

similarly 2nd and 3rd term of Hamiltonian (4.25) in k-space can be written as

$$\boxed{-\sum_{i \in A} t_2 \left(\hat{a}_i^\dagger \hat{b}_{i+\delta_2} + h.c \right) = -t_2 \sum_{\mathbf{k}} \left(e^{i\mathbf{k}\cdot\delta_2} \hat{a}_{\mathbf{k}}^\dagger \hat{b}_{\mathbf{k}} + h.c \right)},\quad (4.28)$$

and

$$\boxed{-\sum_{i \in A} t_3 \left(\hat{a}_i^\dagger \hat{b}_{i+\delta_3} + h.c \right) = -t_3 \sum_{\mathbf{k}} \left(e^{i\mathbf{k}\cdot\delta_3} \hat{a}_{\mathbf{k}}^\dagger \hat{b}_{\mathbf{k}} + h.c \right)}.\quad (4.29)$$

Substituting results from equation (4.27), (4.28), and (4.29) in equation (4.25), the Hamiltonian in k-space becomes

$$\begin{aligned}\hat{H} &= -t_1 \sum_{\mathbf{k}} \left(e^{i\mathbf{k}\cdot\delta_1} \hat{a}_{\mathbf{k}}^\dagger \hat{b}_{\mathbf{k}} + e^{-i\mathbf{k}\cdot\delta_1} \hat{b}_{\mathbf{k}}^\dagger \hat{a}_{\mathbf{k}} \right) \\ &\quad - t_2 \sum_{\mathbf{k}} \left(e^{i\mathbf{k}\cdot\delta_2} \hat{a}_{\mathbf{k}}^\dagger \hat{b}_{\mathbf{k}} + e^{-i\mathbf{k}\cdot\delta_2} \hat{b}_{\mathbf{k}}^\dagger \hat{a}_{\mathbf{k}} \right) \\ &\quad - t_3 \sum_{\mathbf{k}} \left(e^{i\mathbf{k}\cdot\delta_3} \hat{a}_{\mathbf{k}}^\dagger \hat{b}_{\mathbf{k}} + e^{-i\mathbf{k}\cdot\delta_3} \hat{b}_{\mathbf{k}}^\dagger \hat{a}_{\mathbf{k}} \right).\end{aligned}\quad (4.30)$$

The right-hand side of equation (4.30) can be written in matrix form as

$$\hat{H} = \begin{pmatrix} \hat{a}_{\mathbf{k}}^\dagger & \hat{b}_{\mathbf{k}}^\dagger \end{pmatrix} \begin{pmatrix} 0 & t_1 e^{i\mathbf{k}\cdot\delta_1} + t_2 e^{i\mathbf{k}\cdot\delta_2} + t_3 e^{i\mathbf{k}\cdot\delta_3} \\ t_1 e^{-i\mathbf{k}\cdot\delta_1} + t_2 e^{-i\mathbf{k}\cdot\delta_2} + t_3 e^{-i\mathbf{k}\cdot\delta_3} & 0 \end{pmatrix} \begin{pmatrix} \hat{a}_{\mathbf{k}} \\ \hat{b}_{\mathbf{k}} \end{pmatrix}.$$

Let

$$\begin{aligned} f(\mathbf{k}) &= t_1 e^{i\mathbf{k}\cdot\delta_1} + t_2 e^{i\mathbf{k}\cdot\delta_2} + t_3 e^{i\mathbf{k}\cdot\delta_3}, \\ &= \sum_{\alpha=1}^3 t_\alpha e^{i\mathbf{k}\cdot\delta_\alpha}, \end{aligned}$$

$$\begin{aligned} \hat{H} &= \begin{pmatrix} \hat{a}_{\mathbf{k}}^\dagger & \hat{b}_{\mathbf{k}}^\dagger \end{pmatrix} \begin{pmatrix} 0 & f(\mathbf{k}) \\ f^*(\mathbf{k}) & 0 \end{pmatrix} \begin{pmatrix} \hat{a}_{\mathbf{k}} \\ \hat{b}_{\mathbf{k}} \end{pmatrix}, \\ &= \begin{pmatrix} \hat{a}_{\mathbf{k}}^\dagger & \hat{b}_{\mathbf{k}}^\dagger \end{pmatrix} H(\mathbf{k}) \begin{pmatrix} \hat{a}_{\mathbf{k}} \\ \hat{b}_{\mathbf{k}} \end{pmatrix}, \end{aligned}$$

where

$$H(\mathbf{k}) \equiv \begin{pmatrix} 0 & f(\mathbf{k}) \\ f^*(\mathbf{k}) & 0 \end{pmatrix}. \quad (4.31)$$

We can simplify $f(\mathbf{k})$ by writing exponential factors in terms of Bravais lattice vectors, \mathbf{a} and \mathbf{b}

$$\begin{aligned} f(\mathbf{k}) &= t_1 e^{i\mathbf{k}\cdot\delta_1} + t_2 e^{i\mathbf{k}\cdot\delta_2} + t_3 e^{i\mathbf{k}\cdot\delta_3}, \\ &= e^{i\mathbf{k}\cdot\delta_3} (t_1 e^{i\mathbf{k}\cdot(\delta_1-\delta_3)} + t_2 e^{i\mathbf{k}\cdot(\delta_2-\delta_3)} + t_3), \end{aligned} \quad (4.32)$$

from geometry of figure (4.1), we can write as

$$\delta_1 - \delta_3 = \mathbf{a}, \quad \delta_2 - \delta_3 = \mathbf{b}.$$

Equation (4.32) becomes

$$\begin{aligned} f(\mathbf{k}) &= e^{i\mathbf{k}\cdot\delta_3} (t_1 e^{i\mathbf{k}\cdot\mathbf{a}} + t_2 e^{i\mathbf{k}\cdot\mathbf{b}} + t_3), \\ &= e^{i\mathbf{k}\cdot\delta_3} g(\mathbf{k}). \end{aligned}$$

Substituting the value of $f(\mathbf{k})$ in equation (4.31)

$$H(\mathbf{k}) = \begin{pmatrix} 0 & e^{i\mathbf{k}\cdot\delta_3} g(\mathbf{k}) \\ e^{-i\mathbf{k}\cdot\delta_3} g^*(\mathbf{k}) & 0 \end{pmatrix}. \quad (4.33)$$

For the dispersion relation, using following eigenvalue equation.

$$\begin{aligned} |H(\mathbf{k}) - E(\mathbf{k})\mathbb{1}| &= 0, \\ \begin{vmatrix} -E(\mathbf{k}) & e^{i\mathbf{k}\cdot\delta_3} g(\mathbf{k}) \\ e^{-i\mathbf{k}\cdot\delta_3} g^*(\mathbf{k}) & -E(\mathbf{k}) \end{vmatrix} &= 0, \\ E^2(\mathbf{k}) &= e^{-i\mathbf{k}\cdot\delta_3} g(\mathbf{k}) e^{i\mathbf{k}\cdot\delta_3} g^*(\mathbf{k}), \\ &= |g(\mathbf{k})|^2, \\ \Rightarrow E(\mathbf{k}) &= \pm |g(\mathbf{k})|, \end{aligned}$$

the phase factors $e^{-i\mathbf{k}\cdot\delta_3}$ and $e^{i\mathbf{k}\cdot\delta_3}$ play no role in the dispersion relation of the above Hamiltonian. So, these factors can be ignored.

Let us simplify the problem by taking two hopping parameter equal

$$t_1 = t_2 = t, \quad t_3 = t',$$

$$g(\mathbf{k}) = t(e^{i\mathbf{k}\cdot\mathbf{a}} + e^{i\mathbf{k}\cdot\mathbf{b}}) + t', \quad (4.34)$$

where $\mathbf{a} = a_0(\frac{\sqrt{3}}{2}, \frac{3}{2})$, $\mathbf{b} = a_0(\frac{-\sqrt{3}}{2}, \frac{3}{2})$ are elementary vectors of Bravais lattice, a_0 is the inter-atomic distance as shown in figure 4.1. When $t = t'$ gap closes at the two points \mathbf{K}_0 and \mathbf{K}'_0 which are located at the of the Brillouin zone, so when $t = t'$

$$\mathbf{K}_0 = \frac{2\pi}{3\sqrt{3}a_0}(1, \sqrt{3}), \quad \mathbf{K}'_0 = \frac{2\pi}{3\sqrt{3}a_0}(-1, \sqrt{3}).$$

As t' increases, the two point \mathbf{K} and \mathbf{K}' come towards each other, their relative position is given by

$$K/K' = \left(\pm \frac{2}{3a_0} \arctan \sqrt{\frac{4t^2}{t'} - 1}, \frac{2\pi}{3a_0} \right).$$

When $t' = 2t$, these points merge into a single point $\mathbf{D}_0 = (0, \frac{2\pi}{3a_0})$, and for $t' > 2t$ a band gap opens between the two bands. Putting the value of a and b in equation (4.34)

$$g(\mathbf{k}) = t \exp\left(\frac{3ia_0k_y}{2}\right) \left[\exp\left(\frac{\sqrt{3}ia_0k_x}{2}\right) + \exp\left(\frac{-\sqrt{3}ia_0k_x}{2}\right) \right] + t',$$

$$\Rightarrow g(\mathbf{k}) = 2t \exp\left(\frac{3ia_0k_y}{2}\right) \cos\left(\frac{\sqrt{3}a_0k_x}{2}\right) + t'. \quad (4.35)$$

Expanding equation (4.35) about \mathbf{D}_0 : let $k_y = \frac{2\pi}{3a_0} + q_y$, $k_x = 0 + q_x$

$$g(\mathbf{q}) = 2t \exp\left(\frac{3ia_0}{2}\left(\frac{2\pi}{3a_0} + q_y\right)\right) \cos\left(\frac{\sqrt{3}a_0q_x}{2}\right) + t'$$

$$g(\mathbf{q}) \approx -2t \left(1 + \frac{3ia_0}{2}q_y\right) \left(1 - \frac{3}{4}a_0^2q_x^2\right) + t',$$

keeping q_x and q_y upto lowest order,

$$g(\mathbf{q}) \approx t' - 2t + \frac{3}{2}ta_0^2q_y^2 - 3ia_0tq_x.$$

Let

$$\Delta \equiv 2t - t', \quad m^* \equiv \frac{1}{3a_0^2 t}, \quad v_F \equiv 3a_0 t,$$

$$\Rightarrow g(\mathbf{q}) \approx -\Delta + \frac{q_x^2}{2m^*} - iv_F q_y. \quad (4.36)$$

The low energy effective Hamiltonian becomes

$$H(\mathbf{q}) \approx \begin{pmatrix} 0 & -\Delta + \frac{q_x^2}{2m^*} - iv_F q_y \\ -\Delta + \frac{q_x^2}{2m^*} + iv_F q_y & 0 \end{pmatrix}, \quad (4.37)$$

the dispersion relation is

$$E(\mathbf{q}) = \pm \sqrt{\left(\frac{q_x^2}{2m^*} - \Delta\right)^2 + v_F^2 q_y^2}.$$

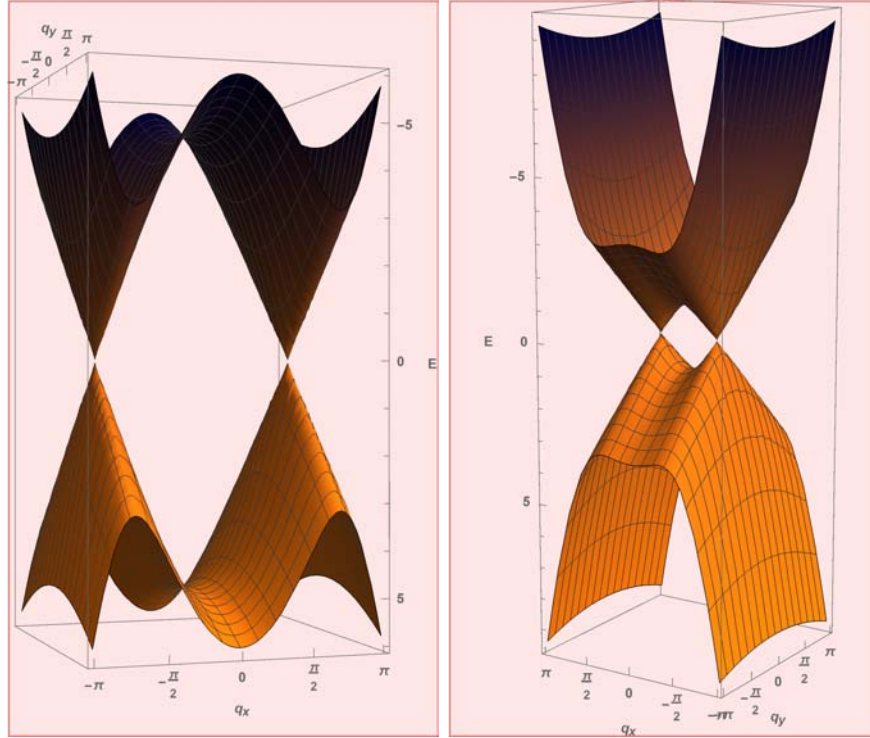


Figure 4.2: Left: plot of the dispersion relation taking $a=1$, $c=1$, $\Delta= -5$. Right: plot of the dispersion relation when $a=1$, $c=1$, $\Delta= -1$. These plot manifest that increasing the value of $\Delta= -5$ to $\Delta = -1$ the Dirac point move in BZ and come closer to each other.

Results:

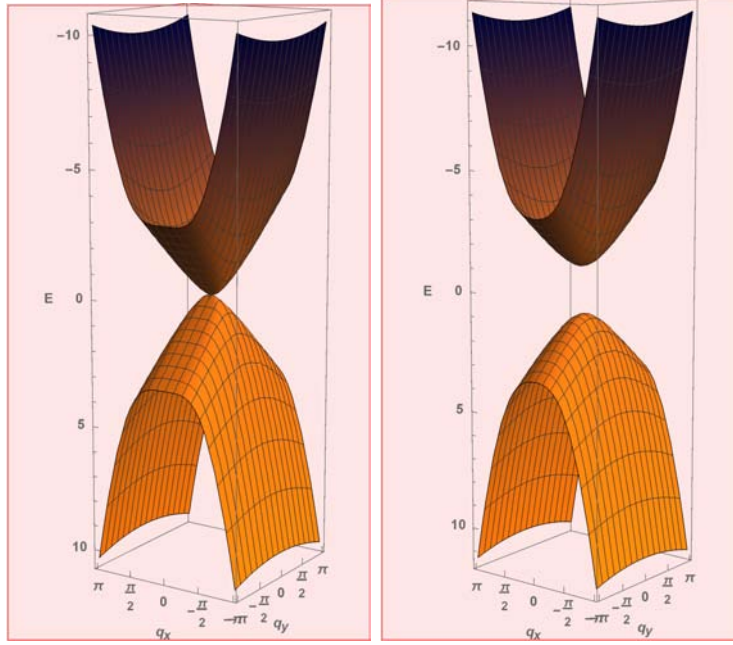


Figure 4.3: Left: Inside the BZ, the two Dirac points merges when $\Delta = 0$. Right: Further increasing Δ causes the a band gap opening. Plot is for the case when: $\Delta = 1$, $a=1$, and $c=1$.

- For $\Delta > 0$, we have two gapless Dirac points at points $(\pm\sqrt{2m^*\Delta}, 0)$. Furthermore, these points move close to each other by increasing the value of Δ from negative towards zero, as shown in figure 4.2.
- For $\Delta = 0 = t' - 2t$, two Dirac points merge into each other, as shown in the left figure 4.3.
- For $\Delta > 0$, a band gap opens as shown in the right figure 4.3.

Time Reversal Symmetry:

The effective Hamiltonian in equation (4.37) can be written in the form of two level Hamiltonian,

$$\hat{H}_0(\mathbf{q}) = \mathbf{d}(\mathbf{q}) \cdot \boldsymbol{\sigma}$$

where $\mathbf{d}(\mathbf{q}) = (aq_x^2 - \Delta, v_F q_y, 0)$, $\mathbf{q} = (q_x, q_y)$ is the crystal momentum in 2D, $\boldsymbol{\sigma} = (\sigma_1, \sigma_2, \sigma_3)$ are the Pauli matrices in the pseudo-spin basis, a is related with inverse of quasi-particle mass along x-axis, v_F is the Dirac velocity along y-axis, and Δ is the gap parameter.

Let us check the time reversal symmetry of the semi-Dirac Hamiltonian

$$\begin{aligned}
\hat{\Theta}H_0(\mathbf{q})\hat{\Theta}^\dagger &= \hat{K}H_0(\mathbf{q})\hat{K}^*, \\
&= \hat{K}(d_x\sigma_x + d_y\sigma_y)\hat{K}^*, \\
&= (d_x^*\sigma_x^* + d_y^*\sigma_y^*)\hat{K}\hat{K}^*, \\
&= (d_x\sigma_x - d_y\sigma_y),
\end{aligned}$$

because of $\mathbf{q} \rightarrow -\mathbf{q}$, $d_y \rightarrow -d_y$,

$$\Rightarrow \boxed{\hat{\Theta}\hat{H}_0(\mathbf{q})\hat{\Theta}^\dagger = \hat{H}_0(-\mathbf{q})}.$$

The Hamiltonian has time-reversal symmetry. If we add a perturbation like $\delta H = m\sigma_z$ in the semi-Dirac Hamiltonian, it opens a band gap. It leads to a non-zero Berry curvature, but the system is still time-reversal invariant. As a result, the Chern number will be zero. So, this perturbation cannot change the band's topology. We need to break the time-reversal symmetry of the semi-Dirac Hamiltonian if we want to change the band topology. In the next step, we apply a periodic time-dependent perturbation in the form of electromagnetic radiations. This perturbation breaks the time reversal-symmetry of the Hamiltonian, and we can expect a change in the band topology.

4.3 Floquet Theory

Now we investigate the effect of time-dependent perturbation in the form of radiations having vector potential $\mathbf{A}(t) = A_0(\sin \omega t, \sin(\omega t + \phi))$, where ω is angular frequency and ϕ is the polarization of the incident light. Here, we have ignored the spatial dependence of vector potential; because the wavelength of the incident light is larger than the sample size. The vector potential breaks the time-reversal symmetry of the Hamiltonian, so we can expect a topological phase transition, having a non-zero Chern number in this scenario [10]. By using minimal coupling

$$q_x \rightarrow q_x + eA_x \qquad q_y \rightarrow q_y + eA_y$$

$$\begin{aligned}
\hat{H}(\mathbf{q}, t) &= \left[a(q_x + eA_x)^2 - \Delta \right] \sigma_x + [v_F(q_y + eA_y)] \sigma_y \\
&= \left[a(q_x + eA_0 \sin \omega t)^2 - \Delta \right] \sigma_x + [v_F q_y + ev_F A_0 \sin(\omega t + \phi)] \sigma_y \\
&= (aq_x^2 + e^2 A_0^2 \sin^2(\omega t) + 2eaq_x A_0 \sin \omega t - \Delta) \sigma_x \\
&\quad + [cq_y + ecA_0 \sin(\omega t + \phi)] \sigma_y \\
&= (aq_x^2 - \Delta) \sigma_x + v_F q_y \sigma_y + (e^2 A_0^2 \sin^2(\omega t) + 2eaq_x A_0 \sin \omega t) \sigma_x \\
&\quad + (ev_F A_0 \sin(\omega t + \phi)) \sigma_y, \\
\hat{H}(\mathbf{q}, t) &= \hat{H}_0(\mathbf{q}) + H_1(\mathbf{q}, t) \sigma_x + H_2(\mathbf{q}, t) \sigma_y, \tag{4.38}
\end{aligned}$$

where

$$\begin{aligned}
H_1(\mathbf{q}, t) &\equiv \frac{ae^2 A_0^2}{2} (1 - \cos 2\omega t) + 2aeA_0 q_x \sin \omega t, \\
H_2(\mathbf{q}, t) &\equiv v_F e A_0 \sin(\omega t + \phi).
\end{aligned}$$

Because the frequency of the impinged light is much higher than the natural frequencies, such as the oscillation frequencies of atoms in the system, we can use the Floquet principle to obtain an effective time-independent Hamiltonian. By using the Magnus expansion developed in section 4.1.4 and taking $t_0 = 0$ initial time,

$$\hat{H}_F(\mathbf{q}) \approx \hat{H}_F^{(0)} + \hat{H}_F^{(1)}, \tag{4.39}$$

where

$$\hat{H}_F^{(0)}(\mathbf{q}) = \frac{1}{T} \int_0^T \hat{H}(\mathbf{q}, t) dt, \tag{4.40}$$

$$\hat{H}_F^{(1)}(\mathbf{q}) = \frac{1}{2i\hbar T} \int_0^T dt_1 \int_0^{t_1} dt_2 [\hat{H}(\mathbf{q}, t_1), \hat{H}(\mathbf{q}, t_2)]. \tag{4.41}$$

Substituting the value of $\hat{H}(\mathbf{q}, t)$ from equation (4.38) in equation (4.40)

$$\begin{aligned}
\hat{H}_F^{(0)}(\mathbf{q}) &= \frac{1}{T} \int_0^T \hat{H}(\mathbf{q}, t) dt, \\
&= \frac{1}{T} \int_0^T (\hat{H}_0(\mathbf{q}) + \hat{H}_1(\mathbf{q}, t) \sigma_x + \hat{H}_2(\mathbf{q}, t) \sigma_y) dt, \\
&= \frac{1}{T} \int_0^T \left(\hat{H}_0(\mathbf{q}) + \frac{ae^2 A_0^2}{2} (1 - \cos 2\omega t) + (2aeA_0 q_x \sin \omega t) \sigma_x \right. \\
&\quad \left. + (v_F e A_0 \sin(\omega t + \phi)) \sigma_y \right) dt,
\end{aligned}$$

Using $1/T \int_0^T dt(\sin \omega t) = 0$ and $1/T \int_0^T dt(\cos 2\omega t) = 0$

$$\Rightarrow \boxed{\hat{H}_F^{(0)}(\mathbf{q}) = \hat{H}_0(\mathbf{q}) + \frac{ae^2 A_0^2}{2} \sigma_x.} \tag{4.42}$$

Substituting the value of time dependent Hamiltonian in equation (4.41)

$$\begin{aligned}\hat{H}_F^{(1)}(\mathbf{q}) &= \frac{1}{2i\hbar T} \int_0^T dt_1 \int_0^{t_1} dt_2 \left[\hat{H}(\mathbf{q}, t_1), \hat{H}(\mathbf{q}, t_2) \right], \\ &= \frac{1}{2i\hbar T} \int_0^T dt_1 \int_0^{t_1} dt_2 \left[\hat{H}_0(\mathbf{q}) + H_1(\mathbf{q}, t_1)\sigma_x + H_2(\mathbf{q}, t_1)\sigma_y \right. \\ &\quad \left. , \hat{H}_0(\mathbf{q}) + H_1(\mathbf{q}, t_2)\sigma_x + H_2(\mathbf{q}, t_2)\sigma_y \right],\end{aligned}\tag{4.43}$$

the integrand of above the equation contains commutation relations of the time-dependent Hamiltonian at different times, which are solved in the appendix B. From equation (B.15) in the appendix

$$\boxed{\hat{H}_F^{(1)} = [m_0 + \beta q_x^2 + \gamma q_x + \eta q_x q_y] \sigma_z.}\tag{4.44}$$

Summing $H_F^{(0)}$ and $H_F^{(1)}$, equation (4.39) yields

$$\begin{aligned}\hat{H}_F &= \hat{H}_0(\mathbf{q}) + \frac{ae^2 A_0^2}{2} \sigma_x + [m_0 + \beta q_x^2 + \gamma q_x + \eta q_x q_y] \sigma_z, \\ &= (ak_x^2 - \Delta) \sigma_x + v_F q_y \sigma_y + \frac{ae^2 A_0^2}{2} \sigma_x + [m_0 + \beta q_x^2 + \gamma q_x + \eta q_x q_y] \sigma_z, \\ &= \left(ak_x^2 + \frac{ae^2 A_0^2}{2} - \Delta \right) \sigma_x + v_F q_y \sigma_y + [m_0 + \beta q_x^2 + \gamma q_x + \eta q_x q_y] \sigma_z,\end{aligned}\tag{4.45}$$

let $\delta \equiv \frac{ae^2 A_0^2}{2} - \Delta$ and $m_{eff} \equiv m_0 + \beta q_x^2 + \gamma q_x + \eta q_x q_y$, equation (4.45) becomes

$$\begin{aligned}\hat{H}_F(\mathbf{q}) &= (ak_x^2 + \delta) \sigma_x + v_F q_y \sigma_y + m_{eff} \sigma_z, \\ &= \mathbf{h}(\mathbf{q}) \cdot \boldsymbol{\sigma},\end{aligned}$$

with $\mathbf{h}(\mathbf{q}) = (ak_x^2 + \delta, v_F q_y, m_{eff})$ and the dispersion relation is: $E(q_x, q_y) = \pm \sqrt{(ak_x^2 + \delta)^2 + v_F^2 q_y^2 + m_{eff}^2}$. Note that due to incident light a band gap opens between Dirac nodes. Also, the term m_{eff} responsible for band gap opening, breaks the time reversal symmetry of the Hamiltonian: $\hat{\Theta} m_{eff} \hat{\Theta}^\dagger \neq m_{eff}$. We need to calculate the Berry curvature to determine the Chern numbers. By using the definition of the Berry curvature for two level system

from equation (1.46)

$$\begin{aligned}
F(q_x, q_y) &= \mp \frac{\mathbf{h}}{2|\mathbf{h}|^3} \cdot \frac{\partial \mathbf{h}}{\partial q_x} \times \frac{\partial \mathbf{h}}{\partial q_y}, \\
&= \mp \frac{1}{2|\mathbf{h}|^3} \begin{vmatrix} ak_x^2 + \delta & v_F q_y & m_{eff} \\ 2aq_x & 0 & 2\beta q_x + \gamma + \eta q_y \\ 0 & v_F & \eta q_x \end{vmatrix}, \\
&= \mp \frac{1}{2|\mathbf{h}|^3} [\gamma(aq_x^2 - \delta) - \eta q_y(aq_x^2 + \delta) + 2am_0 q_x - 2\delta\beta q_x].
\end{aligned} \tag{4.46}$$

It is evident that $F(q_x, q_y) \neq -F(-q_x, -q_y)$, as a result of broken time-reversal symmetry.

4.3.1 Chern number calculation for gape-less Semi-Dirac system

For circularly polarized ($\phi = \pm\pi/2$) light: $m_0 = 0$ and $\beta = 0$, the Berry curvature implies

$$F(q_x, q_y) = \mp \frac{1}{2|\mathbf{h}|^3} [\gamma(aq_x^2 - \delta) - \eta q_y(aq_x^2 + \delta)]. \tag{4.47}$$

Case 01:

For $\delta > 0$ with circularly polarized light, there are two Dirac nodes with band gap, as shown in the left figure 4.4. In the proximity of band minima we can approximate \mathbf{h} by keeping lowest order terms in q_x and q_y

$$\hat{h}(\mathbf{q}) \approx (\delta, v_F q_y, \gamma q_x). \tag{4.48}$$

The dispersion relation becomes $E_{\pm}(q_x, q_y) \approx \pm \sqrt{\delta^2 + v_F^2 q_y^2 + \gamma^2 q_x^2}$, which is a gapped Dirac spectrum. The total Berry flux for this gapped system in $\mp 2\pi \text{sgn}(\gamma)$, where \mp corresponds to positive and negative energy bands. the polarization of light determines the sign of γ . Consequently, two Dirac nodes contribute $\mp(1/2 + 1/2) = \mp 1$ to the Chern number.

Case 02:

When $\delta = 0$, plotted on the right side of figure 4.4, the two Dirac nodes merge into each other with band gap closing. This point acts as critical point, which separates Chern insulating phase from the topologically trivial phase.

Case 03:

For $\delta < 0$, the spectrum becomes gapped again, as shown in figure 4.5. In this case, the Chern number turns out to be zero. Thus, varying the intensity of light, we can drive the topological phase transition in the system

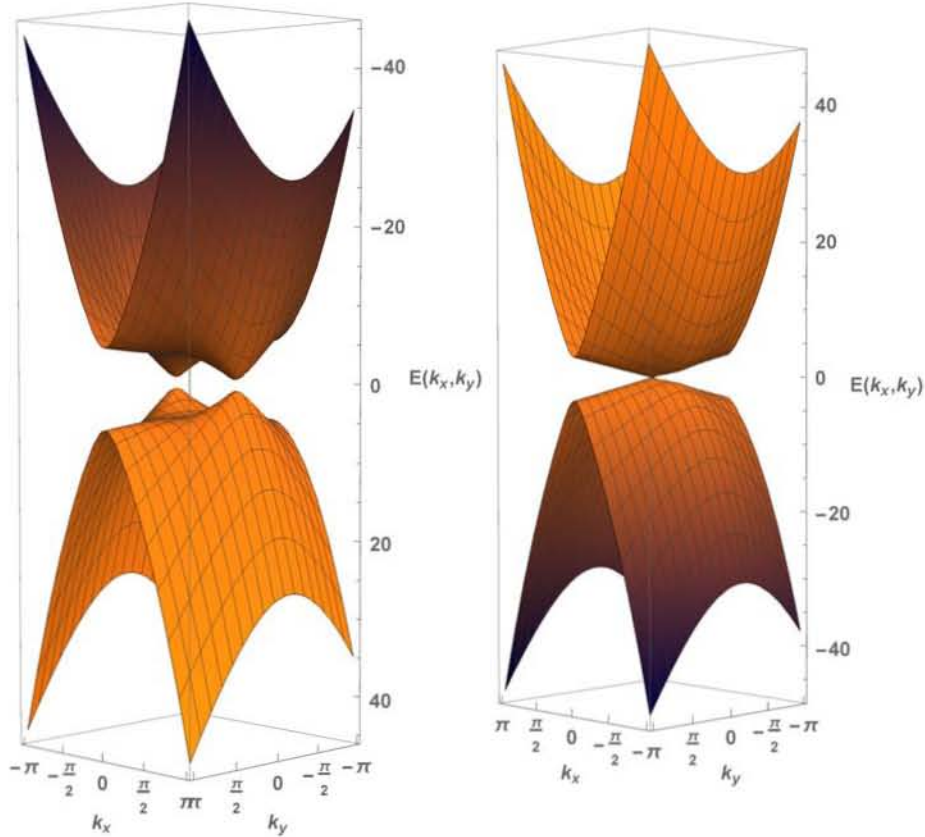


Figure 4.4: Left: Plot of the dispersion relation when $\delta > 0$. For this case, we have two gapped Dirac nodes inside BZ. Right: Plot of the energy spectrum when $\delta = 0$. Both plots show that the topology of band structure changes by varying the intensity of circularly polarized light.

4.3.2 Chern Insulating States in Gapped Semi-Dirac System

If we break both the inversion symmetry, by introducing perturbation term $\delta H = m\sigma_z$, and time-reversal symmetry, by shining polarized light on the surface of the semi-Dirac system, we expect that the system would mimic the phase diagram of Haldane model. The gapped semi-Dirac Hamiltonian is given as

$$\hat{H}_g(\mathbf{q}) = \hat{H}_0(\mathbf{q}) + m\sigma_z, \quad (4.49)$$

this Hamiltonian has broken inversion symmetry. Due to the asymmetric Berry curvature, its Chern number is zero representing a trivial insulator. When we shine a light on the Semi-Dirac material, light field $\mathbf{A}(t)$ couples with the momentum as discussed in the previous subsection, the Hamiltonian

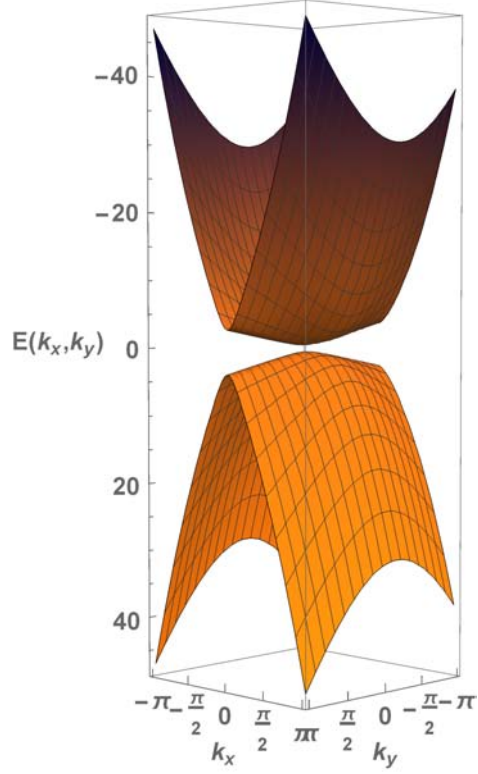


Figure 4.5: Plot of the dispersion relation when $\delta = -0.5$. In this case, two Dirac points merge into each other with a band gap. This phase acts as a trivial insulating phase.

becomes

$$\hat{H}_g(\mathbf{q}, t) = \hat{H}_0(\mathbf{q}) + H_1(\mathbf{q}, t)\sigma_x + H_2(\mathbf{q}, t)\sigma_y + m\sigma_z. \quad (4.50)$$

Following the same procedure to calculate the Floquet Hamiltonian it becomes

$$\begin{aligned} \hat{H}_F^{(0)}(\mathbf{q}) &= \hat{H}_0(\mathbf{q}) + \frac{ae^2 A_0^2}{2}\sigma_x + m\sigma_z, \\ \hat{H}_F^{(1)}(\mathbf{q}) &= [m_0 + \beta q_x^2 + \gamma q_x + \eta q_x q_y]\sigma_z + \delta \hat{H}_F. \end{aligned} \quad (4.51)$$

The extra term $\delta\hat{H}_F$ comes because of non-zero $\delta\hat{H}$ term in Hamiltonian (4.49), and it is calculated in the appendix C. From equation (C.2), substituting the value of $\delta\hat{H}_F^{(1)}(\mathbf{q})$ in equation (4.51)

$$\hat{H}_F^{(1)}(\mathbf{q}) = [m_0 + \beta q_x^2 + \gamma q_x + \eta q_x q_y] \sigma_z - \frac{2v_F e A_0 \cos \phi}{\hbar \omega} \sigma_x + \frac{4ea A_0 q_x}{\hbar \omega} \sigma_y,$$

by adding $\hat{H}_F^{(0)}(\mathbf{q})$ and $\hat{H}_F^{(1)}(\mathbf{q})$, which is equal to required Floquet Hamiltonian

$$\begin{aligned} \hat{H}_F(\mathbf{q}) &= \hat{H}_0(\mathbf{q}) + \frac{ae^2 A_0^2}{2} \sigma_x + m \sigma_z + [m_0 + \beta q_x^2 + \gamma q_x + \eta q_x q_y] \sigma_z \\ &\quad - \frac{2v_F e A_0 \cos \phi}{\hbar \omega} \sigma_x + \frac{4ea A_0 q_x}{\hbar \omega} \sigma_y, \end{aligned}$$

where

$$\hat{H}_0(\mathbf{q}) = (aq_x^2 - \Delta) \sigma_x + v_F q_y \sigma_y.$$

Let

$$\Lambda \equiv \frac{2v_F e A_0 \cos \phi}{\hbar \omega}, \quad \chi \equiv \frac{4ea A_0}{\hbar \omega},$$

the Floquet Hamiltonian can be written in the form of two level Hamiltonian as

$$\hat{H}_F(\mathbf{q}) = \mathbf{h}_g(\mathbf{q}) \cdot \boldsymbol{\sigma}.$$

where

$$\mathbf{h}_g(\mathbf{q}) = (aq_x^2 + \delta - m\Lambda, v_F q_y + m\chi q_x, m + m_{eff}), \quad (4.52)$$

and $\boldsymbol{\sigma} = (\sigma_x, \sigma_y, \sigma_z)$ are Pauli matrices in pseudo-spin basis.

Berry Curvature Calculation:

We can use the definition (1.47) to calculate the Berry curvature

$$\begin{aligned} F(q_x, q_y) &= \mp \frac{\mathbf{h}_g}{2|\mathbf{h}_g|^3} \cdot \frac{\partial \mathbf{h}_g}{\partial q_x} \times \frac{\partial \mathbf{h}_g}{\partial q_y}, \\ &= \mp \frac{1}{2|\mathbf{h}_g|^3} \begin{vmatrix} aq_x^2 + \delta - m\Lambda & v_F q_y + m\chi q_x & m + m_{eff} \\ 2aq_x & m\chi & 2\beta q_x + \gamma + \eta q_y \\ 0 & v_F & \eta q_x \end{vmatrix}, \\ &= \mp \frac{v_F}{2|\mathbf{h}_g|^3} \left[\gamma(aq_x^2 - \delta) - \eta q_y(aq_x^2 + \delta) + m\Lambda(q_y \eta + \gamma + 2mq_x) \right. \\ &\quad \left. (a + \beta\Lambda - \eta\chi(aq_x^2 - \delta)/v_F) - m^2 q_x \eta \Lambda \chi / v_F \right]. \end{aligned}$$

Again $F(q_x, q_y) \neq F(-q_x, -q_y)$, as a consequence of broken time reversal symmetry.

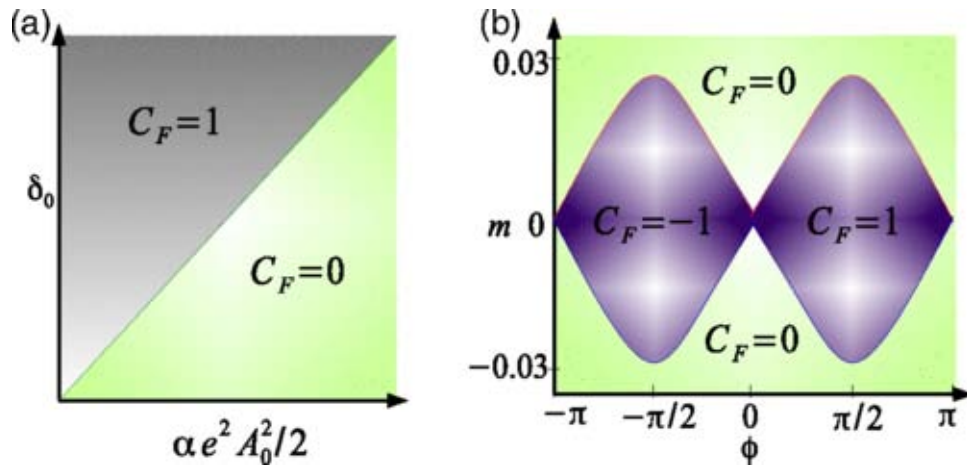


Figure 4.6: (a) Phase diagram of photo-induced Chern insulating states in gapless semi-Dirac system. (b) Phase diagram of Chern numbers in gapped semi-Dirac system as function of m and ϕ .

4.3.3 Chern number calculation for gapped Semi-Dirac system

The Berry curvature in this case is a function of mass m and polarization ϕ . As a result, if we fix the intensity A_0 and the frequency ω of the incident light, by varying m and polarization ϕ , the gapped semi-Dirac system imitates the phase diagram of the Haldane model as shown in the figure. In figure 4.6(b) the boundaries of blue region represent m_0 case when one of the Dirac nodes become gapless, and they act like critical points for phase transition. When $|m| < |m_0|$ two Dirac nodes have opposite sign, and they contribute $1/2, 1/2$ or $-1/2, -1/2$, to the Chern number, where sign depends on the polarization. However, when $|m| > |m_0|$, two Dirac nodes contribute with opposite signs, as a result, the Chern number vanishes in this region.

Conclusions

The crux of my thesis is summarized as:

- Topological insulator is a generic concept that can arise in different materials in one and two dimensional systems.
- Non-zero Berry phase of electronic wave function can lead to non-trivial topological phenomena in gapped systems.
- We can deform a topological Hamiltonian without changing topological index as long as system remains an insulator. This is one of the defining properties of topological insulators and it leads to quantization of physical properties like 1D polarization and Hall conductivity etc.
- In case of electronic Hamiltonian on a honeycomb lattice, low-energy spectrum is gapless because of time-reversal symmetry and space inversion symmetry, and we need to break time-reversal symmetry of the Hamiltonian to get topological non-trivial Chern insulating states.
- We can move Dirac nodes inside BZ by varying nearest neighbour hopping parameters, and they can even merge into each other. If we take one out of the three nearest hopping parameter different from rest of the two, we get semi-Dirac Hamiltonian in the vicinity of two Dirac nodes.
- Semi-Dirac Hamiltonian is time-reversal invariant. We can break the TRS by introducing time-dependent perturbations like shining of electromagnetic radiations on the material. As a result, Chern insulating states arise.
- In a gapless semi-Dirac system, by using circular polarized light we can induce Chern insulating states by varying the intensity of incident light. Hence, the intensity acts as experimental knob.
- In a gapped semi-Dirac material, by fixing the intensity and frequency of the incident light we can induce topological transition obtaining a phase diagram which is similar to Haldane's model phase diagram.

Appendix A

Gauge Transformation in Quantum Mechanics

$$\begin{aligned}
 (\hat{\mathbf{p}} - q\mathbf{A}'_{em}(\mathbf{x}, t)) |\psi'_s(\mathbf{x}, t)\rangle &= (-i\hbar\nabla - q\mathbf{A}_{em}(\mathbf{x}, t) - q\nabla\eta(\mathbf{x}, t)) \exp\{iq\eta(\mathbf{x}, t)/\hbar\} \\
 &\quad \times |\psi_s(\mathbf{x}, t)\rangle, \\
 &= \cancel{q \exp\{iq\eta(\mathbf{x}, t)/\hbar\}(\nabla\chi) |\psi_s(\mathbf{x}, t)\rangle} \\
 &\quad - i\hbar \exp\{iq\eta(\mathbf{x}, t)/\hbar\} |\nabla\psi_s(\mathbf{x}, t)\rangle \\
 &\quad - q\mathbf{A}_{em} \exp\{\eta(\mathbf{x}, t)/\hbar\} |\psi_s(\mathbf{x}, t)\rangle \\
 &\quad - \cancel{q \exp\{iq\chi(\mathbf{x}, t)/\hbar\}(\nabla\eta) |\psi_s(\mathbf{x}, t)\rangle}, \\
 &= -i\hbar \exp\{iq\eta(\mathbf{x}, t)/\hbar\} |\nabla\psi_s(\mathbf{x}, t)\rangle \\
 &\quad - q\mathbf{A}_{em} \exp\{iq\eta(\mathbf{x}, t)/\hbar\} |\psi_s(\mathbf{x}, t)\rangle, \\
 (\hat{\mathbf{p}} - q\mathbf{A}'_{em}(\mathbf{x}, t)) |\psi'_s(\mathbf{x}, t)\rangle &= -i\hbar \exp\{iq\eta(\mathbf{x}, t)/\hbar\} |\nabla\psi_s(\mathbf{x}, t)\rangle \\
 &\quad - q\mathbf{A}_{em} \exp\{iq\chi(\mathbf{x}, t)/\hbar\} |\psi_s(\mathbf{x}, t)\rangle, \tag{A.1}
 \end{aligned}$$

taking dot product between $(\hat{\mathbf{p}} - q\mathbf{A}'_{em}(\mathbf{x}, t))$ and equation (A.1),

$$\begin{aligned}
(\hat{\mathbf{p}} - q\mathbf{A}'_{em}(\mathbf{x}, t))^2 |\psi'_s(\mathbf{x}, t)\rangle &= (\hat{\mathbf{p}} - q\mathbf{A}'_{em}(\mathbf{x}, t)) \cdot (\hat{\mathbf{p}} - q\mathbf{A}'_{em}(\mathbf{x}, t)) |\psi'_s(\mathbf{x}, t)\rangle \\
&= (-i\hbar\nabla - q\mathbf{A}_{em}(\mathbf{x}, t) - q\nabla\eta(\mathbf{x}, t)) \cdot \\
&\quad (-i\hbar \exp\{iq\eta(\mathbf{x}, t)/\hbar\} |\nabla\psi_s(\mathbf{x}, t)\rangle - q\mathbf{A}_{em} \exp\{iq\eta(\mathbf{x}, t)/\hbar\} |\psi_s(\mathbf{x}, t)\rangle) \\
&= \cancel{-i\hbar q \exp\{iq\eta(\mathbf{x}, t)/\hbar\} \nabla\eta(\mathbf{x}, t) \cdot |\nabla\psi_s(\mathbf{x}, t)\rangle} \\
&\quad \cancel{-\hbar^2 \exp\{iq\chi(\mathbf{x}, t)/\hbar\} |\nabla^2\psi_s(\mathbf{x}, t)\rangle} \\
&\quad + i\hbar q \exp\{iq\eta(\mathbf{x}, t)/\hbar\} (\nabla \cdot \mathbf{A}_{em}) |\psi_s(\mathbf{x}, t)\rangle \\
&\quad \cancel{-q^2 \exp\{iq\chi(\mathbf{x}, t)/\hbar\} (\mathbf{A}_{em} \cdot \nabla\chi) |\psi_s(\mathbf{x}, t)\rangle} \\
&\quad + \cancel{i\hbar q \exp\{iq\eta(\mathbf{x}, t)/\hbar\} \mathbf{A}_{em} \cdot |\nabla\psi_s(\mathbf{x}, t)\rangle} \\
&\quad + i\hbar q \exp\{iq\eta(\mathbf{x}, t)/\hbar\} \mathbf{A}_{em} \cdot |\nabla\psi_s(\mathbf{x}, t)\rangle \\
&\quad + q^2 A_{em}^2 \exp\{iq\eta(\mathbf{x}, t)/\hbar\} |\psi_s(\mathbf{x}, t)\rangle \\
&\quad \cancel{+ i\hbar q \exp\{iq\eta(\mathbf{x}, t)/\hbar\} \nabla\eta(\mathbf{x}, t) \cdot |\nabla\psi_s(\mathbf{x}, t)\rangle} \\
&\quad \cancel{+ q^2 \exp\{iq\eta(\mathbf{x}, t)/\hbar\} (\mathbf{A}_{em} \cdot \nabla\eta) |\psi_s(\mathbf{x}, t)\rangle}, \\
&= \exp\{iq\eta(\mathbf{x}, t)/\hbar\} [-\hbar^2 \nabla^2 |\psi_s(\mathbf{x}, t)\rangle \\
&\quad + i\hbar q (\nabla \cdot \mathbf{A}_{em}) |\psi_s(\mathbf{x}, t)\rangle \\
&\quad + 2i\hbar q \mathbf{A}_{em} \cdot \nabla |\psi_s(\mathbf{x}, t)\rangle + q^2 A_{em}^2 \psi_s(\mathbf{x}, t)],
\end{aligned}$$

$$\begin{aligned}
(\hat{\mathbf{p}} - q\mathbf{A}'_{em}(\mathbf{x}, t))^2 |\psi'_s(\mathbf{x}, t)\rangle &= \exp\{iq\eta(\mathbf{x}, t)/\hbar\} \left[(-i\hbar\nabla - q\mathbf{A}_{em}(\mathbf{x}, t))^2 \right. \\
&\quad \left. \times |\psi_s(\mathbf{x}, t)\rangle \right]. \quad (\text{A.2})
\end{aligned}$$

Appendix B

Floquet Theory

$$\begin{aligned}
I &\equiv \left[\hat{H}_0(\mathbf{q}) + H_1(\mathbf{q}, t_1)\sigma_x + H_2(\mathbf{q}, t_1)\sigma_y \right. \\
&\quad \left. , \hat{H}_0(\mathbf{q}) + H_1(\mathbf{q}, t_2)\sigma_x + H_2(\mathbf{q}, t_2)\sigma_y \right], \\
&= \left[\hat{H}_0(\mathbf{q}), \hat{H}_0(\mathbf{q}) \right] + \left[\hat{H}_0(\mathbf{q}), \hat{H}_1(\mathbf{q}, t_2)\sigma_x \right] + \left[\hat{H}_0(\mathbf{q}), H_2(\mathbf{q}, t_2)\sigma_y \right] \\
&\quad + \left[H_1(\mathbf{q}, t_1)\sigma_x, \hat{H}_0(\mathbf{q}) \right] + [H_1(\mathbf{q}, t_1)\sigma_x, H_1(\mathbf{q}, t_1)\sigma_x] \\
&\quad + [H_1(\mathbf{q}, t_1)\sigma_x, H_2(\mathbf{q}, t_2)\sigma_y] + \left[H_2(\mathbf{q}, t_1)\sigma_y, \hat{H}_0(\mathbf{q}) \right] \\
&\quad + [H_2(\mathbf{q}, t_1)\sigma_y, H_1(\mathbf{q}, t_2)\sigma_x] \\
&\quad + [H_2(\mathbf{q}, t_1)\sigma_y, H_2(\mathbf{q}, t_2)\sigma_y],
\end{aligned} \tag{B.1}$$

1st commutators becomes

$$\boxed{\left[\hat{H}_0(\mathbf{q}), \hat{H}_0(\mathbf{q}) \right] = 0,}$$

2nd commutation relation in equation (B.1) implies

$$\begin{aligned}
\left[\hat{H}(\mathbf{q}), H_1(\mathbf{q}, t_2)\sigma_x \right] &= [(d_x\sigma_x + d_y\sigma_y), H_1(\mathbf{q}, t_2)\sigma_x], \\
&= d_x H_1(\mathbf{q}, t_2)[\sigma_x, \sigma_x] + d_y H_1(\mathbf{q}, t_2)[\sigma_y, \sigma_x], \\
&= d_y H_1(\mathbf{q}, t_2)(-2i\sigma_z),
\end{aligned}$$

$$\Rightarrow \boxed{\left[\hat{H}(\mathbf{q}), H_1(\mathbf{q}, t_2)\sigma_x \right] = -2iH_1(\mathbf{q}, t_2)d_y\sigma_z,} \tag{B.2}$$

3rd commutation relation implies

$$\begin{aligned}
\left[\hat{H}_0(\mathbf{q}), H_2(\mathbf{q}, t_2)\sigma_y \right] &= [(d_x\sigma_x + d_y\sigma_y), H_2(\mathbf{q}, t_2)\sigma_y], \\
&= d_x H_2(\mathbf{q}, t_2)[\sigma_x, \sigma_y] + d_y H_2(\mathbf{q}, t_2)[\sigma_x, \sigma_x], \\
&= d_x H_2(\mathbf{q}, t_2)(2i\sigma_z),
\end{aligned}$$

$$\Rightarrow \boxed{[\hat{H}(\mathbf{q}), H_2(\mathbf{q}, t_2)\sigma_y] = 2iH_2(\mathbf{q}, t_2)d_x\sigma_z}, \quad (\text{B.3})$$

$$\begin{aligned} [H_1(\mathbf{q}, t_1)\sigma_x, \hat{H}_0(\mathbf{q})] &= H_1(\mathbf{q}, t_1)[\sigma_x, (d_x\sigma_x + d_y\sigma_y)], \\ &= d_xH_1(\mathbf{q}, t_1)[\sigma_x, \sigma_x] + d_yH_1(\mathbf{q}, t_1)[\sigma_x, \sigma_y], \\ &= d_yH_1(\mathbf{q}, t_1)(2i\sigma_z), \end{aligned}$$

$$\Rightarrow \boxed{[H_1(\mathbf{q}, t_1)\sigma_x, \hat{H}_0(\mathbf{q})] = 2iH_1(\mathbf{q}, t_1)d_y\sigma_z}, \quad (\text{B.4})$$

the 4th term in equation (B.1) vanishes

$$\begin{aligned} [H_1(\mathbf{q}, t_1)\sigma_x, H_1(\mathbf{q}, t_2)\sigma_x] &= H_1(\mathbf{q}, t_1)H_1(\mathbf{q}, t_2)[\sigma_x, \sigma_x], \\ &= 0, \end{aligned}$$

$$\boxed{[H_1(\mathbf{q}, t_1)\sigma_x, H_1(\mathbf{q}, t_2)\sigma_x] = 0}, \quad (\text{B.5})$$

similarly

$$\boxed{[H_2(\mathbf{q}, t_1)\sigma_y, H_2(\mathbf{q}, t_2)\sigma_y] = 0}. \quad (\text{B.6})$$

The 7th term implies

$$\begin{aligned} [H_2(\mathbf{q}, t_1)\sigma_y, \hat{H}_0(\mathbf{q})] &= H_2(\mathbf{q}, t_1)[\sigma_y, (d_x\sigma_x + d_y\sigma_y)], \\ &= d_xH_2(\mathbf{q}, t_1)[\sigma_y, \sigma_x] + d_yH_2(\mathbf{q}, t_1)[\sigma_y, \sigma_y], \\ &= d_xH_2(\mathbf{q}, t_1)(-2i\sigma_z), \end{aligned}$$

$$\Rightarrow \boxed{[H_2(\mathbf{q}, t_1)\sigma_y, \hat{H}_0(\mathbf{q})] = -2iH_2(\mathbf{q}, t_1)d_x\sigma_z}, \quad (\text{B.7})$$

the second last term implies

$$\begin{aligned} [H_2(\mathbf{q}, t_1)\sigma_y, H_1(\mathbf{q}, t_2)\sigma_x] &= H_1(\mathbf{q}, t_2)H_2(\mathbf{q}, t_1)[\sigma_y, \sigma_x], \\ &= H_1(\mathbf{q}, t_2)H_2(\mathbf{q}, t_1)(-2i\sigma_z), \end{aligned}$$

$$\Rightarrow \boxed{[H_2(\mathbf{q}, t_1)\sigma_y, H_1(\mathbf{q}, t_2)\sigma_x] = -2iH_1(\mathbf{q}, t_2)H_2(\mathbf{q}, t_1)\sigma_z} \quad (\text{B.8})$$

the last term becomes

$$\begin{aligned} [H_1(\mathbf{q}, t_1)\sigma_x, H_2(\mathbf{q}, t_2)\sigma_y] &= H_1(\mathbf{q}, t_1)H_2(\mathbf{q}, t_2)[\sigma_x, \sigma_y], \\ &= H_1(\mathbf{q}, t_2)H_2(\mathbf{q}, t_1)(2i\sigma_z), \end{aligned}$$

$$\Rightarrow \boxed{[H_1(\mathbf{q}, t_1)\sigma_x, H_2(\mathbf{q}, t_2)\sigma_y] = 2iH_1(\mathbf{q}, t_1)H_2(\mathbf{q}, t_2)\sigma_z}. \quad (\text{B.9})$$

Putting the results from equation (B.2) to (B.9) in equation (B.1), the integrand simplifies to

$$\begin{aligned}
I &= -2iH_1(\mathbf{q}, t_2)d_y\sigma_z + 2iH_2(\mathbf{q}, t_2)d_x\sigma_z + 2iH_1(\mathbf{q}, t_1)d_y\sigma_z \\
&\quad - 2iH_2(\mathbf{q}, t_1)d_x\sigma_z - 2iH_1(\mathbf{q}, t_2)H_2(\mathbf{q}, t_1)\sigma_z \\
&\quad + 2iH_1(\mathbf{q}, t_1)H_2(\mathbf{q}, t_2)\sigma_z, \\
&= \{H_1(\mathbf{q}, t_1) - H_1(\mathbf{q}, t_2)\}d_y(2i\sigma_z) \\
&\quad + \{H_2(\mathbf{q}, t_1) - H_2(\mathbf{q}, t_2)\}d_x(2i\sigma_z) \\
&\quad + \{H_1(\mathbf{q}, t_1)H_2(\mathbf{q}, t_2) - H_1(\mathbf{q}, t_2)H_2(\mathbf{q}, t_1)\}(2i\sigma_z),
\end{aligned} \tag{B.10}$$

substituting the value of I in equation (4.43)

$$\begin{aligned}
\hat{H}_F^{[1]}(\mathbf{q}) &= \frac{\sigma_z}{\hbar T} \int_0^T dt_1 \int_0^{t_1} dt_2 \{H_1(\mathbf{q}, t_1) - H_1(\mathbf{q}, t_2)\}d_y \\
&\quad + \frac{\sigma_z}{\hbar T} \int_0^T dt_1 \int_0^{t_1} dt_2 \{H_2(\mathbf{q}, t_1) - H_2(\mathbf{q}, t_2)\}d_x \\
&\quad + \frac{\sigma_z}{\hbar T} \int_0^T dt_1 \int_0^{t_1} dt_2 \left[H_1(\mathbf{q}, t_1)H_2(\mathbf{q}, t_2) \right. \\
&\quad \quad \quad \left. - H_1(\mathbf{q}, t_2)H_2(\mathbf{q}, t_1) \right].
\end{aligned} \tag{B.11}$$

1st integral in equation (B.11)

$$\begin{aligned}
&\int_0^T dt_1 \int_0^{t_1} dt_2 \{H_1(\mathbf{q}, t_1) - H_1(\mathbf{q}, t_2)\}d_y \\
&= \frac{ae^2 A_0^2}{2} \int_0^T dt_1 \int_0^{t_1} dt_2 \{\cos 2\omega t_2 - \cos 2\omega t_1\} \\
&\quad + 2eaA_0q_x \int_0^T dt_1 \int_0^{t_1} dt_2 \{\sin \omega t_1 - \sin \omega t_2\}, \\
&= \frac{ae^2 A_0^2}{2} \int_0^T dt_1 \left\{ \left(\int_0^{t_1} dt_2 \cos 2\omega t_2 \right) - t_1 \cos 2\omega t_1 \right\} \\
&\quad + 2eaA_0q_x \int_0^T dt_1 \left\{ t_1 \sin \omega t_1 - \left(\int_0^{t_1} dt_2 \sin \omega t_2 \right) \right\}, \\
&= \frac{ae^2 A_0^2}{2} \int_0^T dt_1 \left\{ \frac{\sin 2\omega t_1}{2\omega} - t_1 \cos 2\omega t_1 \right\} \\
&\quad + 2eaA_0q_x \int_0^T dt_1 \left\{ t_1 \sin \omega t_1 - \frac{1}{\omega}(1 - \cos \omega t_1) \right\}, \\
&= 2eaA_0q_x \left\{ -\frac{T}{\omega} - \frac{T}{\omega} \right\}. \\
&= \frac{-4eaA_0q_x T}{\omega},
\end{aligned}$$

The following results were used in the above integral

$$\int_0^T dt_1 \sin 2\omega t_1 = 0, \quad \int_0^T dt_1 (t_1 \cos 2\omega t_1) = 0,$$

$$\int_0^T dt_1 (t_1 \sin 2\omega t_1) = -\frac{T}{\omega},$$

$$\int_0^T dt_1 \int_0^{t_1} dt_2 \{H_1(\mathbf{q}, t_1) - H_1(\mathbf{q}, t_2)\} d_y = \frac{-4eaA_0q_x T}{\omega} \quad (\text{B.12})$$

The second integral in equation (B.11) implies

$$\int_0^T dt_1 \int_0^{t_1} dt_2 \{H_2(\mathbf{q}, t_1) - H_2(\mathbf{q}, t_2)\},$$

$$= v_F e A_0 \int_0^T dt_1 \int_0^{t_1} dt_2 \{\sin(\omega t_2 + \phi) - \sin(\omega t_1 + \phi)\},$$

$$= v_F e A_0 \int_0^T dt_1 \left\{ \left(\int_0^{t_1} dt_2 \sin(\omega t_2 + \phi) \right) - t_1 \sin(\omega t_1 + \phi) \right\},$$

$$= v_F e A_0 \int_0^T dt_1 \left\{ \frac{1}{\omega} (\cos \phi - \cos(\omega t_1 + \phi)) - t_1 \sin(\omega t_1 + \phi) \right\},$$

$$= v_F e A_0 \left\{ \frac{T \cos \phi}{\omega} + \frac{T \cos \phi}{\omega} \right\},$$

$$= \frac{2v_F e A_0 T \cos \phi}{\omega},$$

$$\int_0^T dt_1 \int_0^{t_1} dt_2 \{H_2(\mathbf{q}, t_1) - H_2(\mathbf{q}, t_2)\} = \frac{2v_F e A_0 T \cos \phi}{\omega} \quad (\text{B.13})$$

The third integral in equation (B.11) implies

$$\begin{aligned}
& \int_0^T dt_1 \int_0^{t_1} dt_2 \{H_1(\mathbf{q}, t_1)H_2(\mathbf{q}, t_2) - H_1(\mathbf{q}, t_2)H_2(\mathbf{q}, t_1)\} \\
&= \int_0^T dt_1 H_1(\mathbf{q}, t_1) \left(\int_0^{t_1} dt_2 H_2(\mathbf{q}, t_2) \right) \\
&\quad - \int_0^T dt_1 H_2(\mathbf{q}, t_1) \left(\int_0^{t_1} dt_2 H_1(\mathbf{q}, t_2) \right), \\
&= v_F e A_0 \int_0^T dt_1 H_1(\mathbf{q}, t_1) \left(\int_0^{t_1} dt_2 \sin(\omega t_2 + \phi) \right) \\
&\quad - \int_0^T dt_1 H_2(\mathbf{q}, t_1) \left(\int_0^{t_1} dt_2 \frac{ae^2 A_0^2}{2} (1 - \cos 2\omega t_2) \right. \\
&\quad\quad\quad \left. + 2ae A_0 q_x \int_0^{t_1} dt_2 \sin \omega t_2 \right), \\
&= \frac{v_F e A_0}{\omega} \int_0^T dt_1 H_1(\mathbf{q}, t_1) (\cos \phi - \cos(\omega t_1 + \phi)) \\
&\quad - \int_0^T dt_1 H_2(\mathbf{q}, t_1) \left\{ \frac{ae^2 A_0^2}{2} \left(t_1 - \frac{\cos 2\omega t_2}{2\omega} \right) + \frac{2ae A_0 q_x}{\omega} (1 - \cos \omega t_1) \right\} \\
&= \frac{v_F e A_0 \cos \phi}{\omega} \int_0^T dt_1 H_1(\mathbf{q}, t_1) - \frac{v_F e A_0}{\omega} \int_0^T dt_1 H_1(\mathbf{q}, t_1) \cos(\omega t_1 + \phi) \\
&\quad - \frac{ae^2 A_0^2}{2} \int_0^T dt_1 H_2(\mathbf{q}, t_1) t_1 + \frac{ae^2 A_0^2}{4\omega} \int_0^T dt_1 H_2(\mathbf{q}, t_1) \cos 2\omega t_1 \\
&\quad - \frac{2ae A_0 q_x}{\omega} \int_0^T dt_1 H_2(\mathbf{q}, t_1) + \frac{2ae A_0 q_x}{\omega} \int_0^T dt_1 H_2(\mathbf{q}, t_1) \cos \omega t_1 \\
&= \frac{v_F e A_0 \cos \phi}{\omega} \int_0^T dt_1 \left\{ \frac{ae^2 A_0^2}{2} (1 - \cos 2\omega t_1) + 2ae A_0 q_x \sin \omega t_1 \right\} \\
&\quad - \frac{v_F e A_0}{\omega} \int_0^T dt_1 \left\{ \frac{ae^2 A_0^2}{2} (1 - \cos 2\omega t_1) + 2ae A_0 q_x \sin \omega t_1 \right\} \cos(\omega t_1 + \phi) \\
&\quad - \frac{av_F e^3 A_0^3}{2} \int_0^T dt_1 (t_1 \sin(\omega t + \phi)) + \frac{av_F e^3 A_0^3}{4\omega} \int_0^T dt_1 \sin(\omega t_1 + \phi) \cos 2\omega t_1 \\
&\quad - \frac{2av_F q_x e^2 A_0^2}{\omega} \int_0^T dt_1 \sin(\omega t_1 + \phi) + \frac{2av_F q_x e^2 A_0^2}{\omega} \int_0^T dt_1 \sin(\omega t_1 + \phi) \cos \omega t_1,
\end{aligned}$$

the following results are used in the above integral

$$\begin{aligned}
& \int_0^T dt_1 \cos(\omega t_1 + \phi) \sin \omega t_1 = \frac{-1}{2} \sin \phi, & \int_0^T dt_1 \cos 2\omega t_1 = 0, \\
& \int_0^T dt_1 \cos(\omega t_1 + \phi) \cos 2\omega t_1 = 0, & \int_0^T dt_1 \sin \omega t_1 = 0, \\
& \int_0^T dt_1 \sin(\omega t_1 + \phi) \cos \omega t_1 = \frac{1}{2} \sin \phi, \\
& \int_0^T dt_1 \int_0^{t_1} dt_2 \{H_1(\mathbf{q}, t_1)H_2(\mathbf{q}, t_2) - H_1(\mathbf{q}, t_2)H_2(\mathbf{q}, t_1)\} \\
& = \frac{v_F e A_0 \cos \phi}{\omega} \times \frac{a e^2 A_0^2}{2} \times T \cos \phi + \frac{a q_x v_F e^2 A_0^2}{\omega} \times T \sin \phi, \\
& + \frac{v_F e A_0 \cos \phi}{\omega} \times \frac{a e^2 A_0^2}{2} \times T \cos \phi + \frac{a q_x v_F e^2 A_0^2}{\omega} \times T \sin \phi, \\
& = \frac{v_F e A_0 \cos \phi}{\omega} \times \frac{a e^2 A_0^2}{2} \times 2T \cos \phi + \frac{a q_x v_F e^2 A_0^2}{\omega} \times 2T \sin \phi,
\end{aligned} \tag{B.14}$$

substituting above results in equation (B.11)

$$\begin{aligned}
\hat{H}_F^{[1]}(\mathbf{q}) &= \frac{\sigma_z}{\hbar T} \times \frac{-4eaA_0q_xT}{\omega} \times v_F k_y \\
&+ \frac{\sigma_z}{\hbar T} \times \frac{2v_F e A_0 T \cos \phi}{\omega} \times (aq_x^2 - \Delta) \\
&+ \frac{\sigma_z}{\hbar T} \times \frac{v_F e A_0 \cos \phi}{\omega} \times \frac{a e^2 A_0^2}{2} \times 2T \cos \phi \\
&+ \frac{\sigma_z}{\hbar T} \times \frac{a q_x v_F e^2 A_0^2}{\omega} \times 2T \sin \phi.
\end{aligned}$$

Let

$$\begin{aligned}
\eta &\equiv \frac{-4aeA_0v_F}{\hbar\omega}, & \beta &\equiv \frac{2aeA_0v_F}{\hbar\omega} \cos \phi, \\
m_0 &\equiv \frac{v_F e A_0}{\hbar\omega} (ae^2 A_0^2 - 2\Delta), & \gamma &\equiv \frac{2av_F e^2 A_0^2}{\hbar\omega} \sin \phi,
\end{aligned}$$

$$\boxed{\hat{H}_F^{(1)} = [m_0 + \beta q_x^2 + \gamma q_x + \eta q_x q_y] \sigma_z.} \tag{B.15}$$

Appendix C

Gapped semi-Dirac Hamiltonian

From the subsection

$$\delta\hat{H}_F^{(1)}(\mathbf{q}) = \frac{1}{2i\hbar T} \int_0^T dt_1 \int_0^{t_1} dt_2 \left\{ \left[\hat{H}(\mathbf{q}, t_1), m\sigma_z \right] + \left[m\sigma_z, \hat{H}(\mathbf{q}, t_2) \right] \right\}. \quad (\text{C.1})$$

Let

$$B \equiv \left[\hat{H}(\mathbf{q}, t_1), m\sigma_z \right] + \left[m\sigma_z, \hat{H}(\mathbf{q}, t_2) \right],$$

putting the value of $\hat{H}(\mathbf{q}, t_1)$ and $\hat{H}(\mathbf{q}, t_2)$ from section (4.3) and evaluating the commutator

$$B = 2im\sigma_x(H_2(\mathbf{q}, t_1) - H_2(\mathbf{q}, t_2)) + 2im\sigma_y(H_1(\mathbf{q}, t_2) - H_1(\mathbf{q}, t_1)).$$

Putting the value of B in equation (C.1)

$$\begin{aligned} \delta\hat{H}_F^{(1)}(\mathbf{q}) &= \frac{1}{2i\hbar T} \int_0^T dt_1 \int_0^{t_1} dt_2 \{ 2im\sigma_x(H_2(\mathbf{q}, t_1) - H_2(\mathbf{q}, t_2)) \} \\ &\quad + \frac{1}{2i\hbar T} \int_0^T dt_1 \int_0^{t_1} dt_2 \{ 2im\sigma_y(H_1(\mathbf{q}, t_2) - H_1(\mathbf{q}, t_1)) \}, \\ &= \frac{m\sigma_x}{\hbar T} \int_0^T dt_1 \int_0^{t_1} dt_2 \{ (H_2(\mathbf{q}, t_1) - H_2(\mathbf{q}, t_2)) \} \\ &\quad + \frac{m\sigma_y}{\hbar T} \int_0^T dt_1 \int_0^{t_1} dt_2 \{ (H_1(\mathbf{q}, t_2) - H_1(\mathbf{q}, t_1)) \}. \end{aligned}$$

The integrand in the above equation has been already evaluated in equation (B.12) and (B.13),

$$\delta\hat{H}_F^{(1)}(\mathbf{q}) = -\frac{m\sigma_x}{\hbar T} \times \frac{2v_F e A_0 T \cos \phi}{\omega} + \frac{m\sigma_y}{\hbar T} \times \frac{4ea A_0 q_x T}{\omega},$$

after simplification

$$\Rightarrow \delta \hat{H}_F^{(1)}(\mathbf{q}) = -\frac{2v_F e A_0 \cos \phi}{\hbar \omega} \sigma_x + \frac{4e a A_0 q_x}{\hbar \omega} \sigma_y. \quad (\text{C.2})$$

Bibliography

- [1] J. E. Moore, “The birth of topological insulators,” *Nature*, vol. 464, no. 7286, pp. 194–198, 2010.
- [2] D. Tong, “Lectures on the quantum hall effect,” *arXiv preprint arXiv:1606.06687*, 2016.
- [3] D. J. Griffiths, “Introduction to electrodynamics,” 2005.
- [4] D. J. Griffiths and D. F. Schroeter, *Introduction to quantum mechanics*. Cambridge University Press, 2018.
- [5] J. J. Sakurai, J. Napolitano, *et al.*, *Modern quantum mechanics*, vol. 185. Pearson Harlow, 2014.
- [6] R. Shankar, “Topological insulators—a review,” *arXiv preprint arXiv:1804.06471*, 2018.
- [7] M. Bukov, L. D’Alessio, and A. Polkovnikov, “Universal high-frequency behavior of periodically driven systems: from dynamical stabilization to floquet engineering,” *Advances in Physics*, vol. 64, no. 2, pp. 139–226, 2015.
- [8] M. Katsnelson, K. Novoselov, and A. Geim, “Chiral tunnelling and the klein paradox in graphene,” *Nature physics*, vol. 2, no. 9, pp. 620–625, 2006.
- [9] G. Montambaux, F. Piéchon, J.-N. Fuchs, and M. Goerbig, “A universal hamiltonian for motion and merging of dirac points in a two-dimensional crystal,” *The European Physical Journal B*, vol. 72, no. 4, p. 509, 2009.
- [10] K. Saha, “Photoinduced chern insulating states in semi-dirac materials,” *Physical Review B*, vol. 94, no. 8, p. 081103, 2016.